A STUDY OF THE LATERAL YARDING FORCES IN A CABLE THINNING

by

Gary Dale Falk

A THESIS

submitted to

Oregon State University

in partial fulfillment of
the requirements for the
degree of

Master of Science

June 1980

APPROVED:

John G. O'Leary

Professor of Forest Engineering in charge of major

John G. O'Leary, Acting Dept Head

Head of Department of Forest Engineering

Dean of Graduate School

Date thesis is presented May 25, 1979

Typed by Loui Hecht for Gary Dale Falk

AN ABSTRACT OF THE PAPER OF

Gary Dale Falk for the degree of Master of Science

in Forest Engineering presented on May 25, 1979

Title: A Study of the Lateral Yarding Forces in a Cable Thinning

Abstract approved: John O'Leary

This paper describes the results of a project conducted to determine the magnitude of and the parameters affecting the magnitude of the cable tensions generated during lateral yarding operations in a cable thinning. Specific emphasis was placed on measuring mainline tensions as a function of turn weight, turn length, mainline vertical angle, mainline to log lead angle, ground slope, distance from carriage, number of logs per turn and thinning intensity.

The results show that the force resisting initial movement, exclusive of the gravitational component, is independent of the variables studied except number of logs per turn and thinning intensity. The average resistive force for two log turns was twice the magnitude of the resistive force for one log turns. The resistive forces encountered in heavier thinnings were higher than those encountered in lighter thinnings.

An upper limit of the magnitude of the mainline tensions necessary to cause initial log movement can be predicted by determining the resistive force such that an arbitrary percentage of the turns will result in a resistive force that will be less. The mathematical expression is:

$$P = \frac{R + W\cos\Theta}{\cos(\alpha - \Theta)}$$

where P = tension necessary to cause initial movement

R = resistive force

W = turn weight

α = mainline angle

Θ = ground slope

The tensions developed during lateral inhaul, that is, after the turn has broken loose, can be predicted by the equation:

$$T = \frac{W(\mu\cos\Theta + \sin\Theta)}{\cos(\alpha - \Theta) + \mu\sin(\alpha - \Theta)}$$

where T = tension developed during lateral inhaul

μ = frictional coefficient

The frictional coefficient for this study was determined to be 0.64.

TABLE OF CONTENTS

LIST OF FIGURES

LIST OF FIGURES (CONT)

LIST OF TABLES

A STUDY OF THE LATERAL YARDING FORCES IN A CABLE THINNING

INTRODUCTION

Since the trend in forest management policy is moving toward intensive management practices, and the practical utilization of smaller diameter logs is increasing, and the amount of large, old growth timber that is left to be harvested is rapidly decreasing, the logging industry has begun to consider the need for efficient smallwood yarders to be used in harvesting and thinning operations. The efficient design and development of these yarders depends to a great extent on the magnitude of the forces resulting from lateral yarding since it is now recognized that the maximum cable tensions, and thus, power requirements, can occur during these operations. Yarder design is currently a trial and error procedure due primarily to the limited availability of design criteria.

Furthermore, current methods of analyzing the capability of cable systems for payload are done with the payload in the skyline corridor and assume full suspension, although some consideration is given to the effect of partial suspension of the log payload (1, 2). Since the maximum tensions occur during the lateral yarding operation, this type of analysis may not be entirely adequate. No formal attempt has been made to verify its adequacy either with respect to partial suspension or with respect to lateral yarding. This is partly due to the unavailability of data indicating what these forces are.

With a knowledge of the magnitude of and the factors affecting the forces experienced during lateral yarding, efficient design and development of yarders with respect to power, line size, and transmission requirements can be greatly accelerated. In addition, progress towards verifying the adequacy of current methods of payload analyses can be made. Since yarder design and payload analyses are intimately related, the end result of knowledge of the lateral yarding forces will make it possible for the timber sale planner to select the best system and equipment that will meet his desired objectives.

OBJECTIVES

The major emphasis of this study focuses on the tensions in the mainline. Skyline tensions are dependent on mainline tensions and topography and can be examined analytically when the magnitude and direction of the mainline tensions are known. The mainline tensions of particular concern are: the tensions necessary to cause initial movement of the log turn towards the carriage (the break-out force), and the tensions while the turn is moving toward the carriage. The effect of thinning intensity on these tensions is also investigated.

Besides thinning intensity, the other parameters that are investigated are as follows:

1. turn weight (W), total weight of all the logs in the turn
2. turn length (l), total length of all the logs in the turn
3. vertical angle of the mainline (α)
4. lead angle (mainline to log) (β)
5. ground slope (Θ), slope of ground in line with the mainline
6. distance from carriage
7. number of logs per turn

It was also important that the yarding operations be conducted in such a way that the project itself did not introduce any independent variables. In this way tensions and forces representative of the actual yarding conditions would be observed. However, this also meant that less attention could be given to detail that might help to empirically substantiate fundamental relationships.

It should also be noted that the objectives stated above were only part of the entire project. There were other objectives, not any less important, involved in the project that are not considered in this paper. The project was planned in anticipation of collecting data that would support the analyses of these other objectives as well.

PREVIOUS WORK

Several studies have been performed that investigate the resistance of log turns to movement (3-9). These studies, were conducted to provide data for comparing alternative skidding techniques and to determine tractive effort requirements. Because of the nature of the studies, ground based equipment was used and the studies were conducted on either specially treated or previously disturbed surfaces (roads and/or skid trails). These studies, because of their emphasis, were not particularly concerned with the break-out force, although Gibson (9) did some monitoring of these forces in his study. Also, because lateral yarding with cable systems does not take place on specially treated surfaces, but on undisturbed or only slightly disturbed surfaces, the results of these studies are not directly applicable to the forces involved in lateral yarding with cable systems. However, these studies do give some insight into the factors that affect resistive forces, and under certain conditions, provide a basis for comparison of results.

SITE DESCRIPTION AND LAYOUT

The area selected for the study was on the McDonald Forest, just off the Poison Oak Rd. (Figure 2). The area had been previously clear-cut and the residual stand was approximately 40 years old. The stand was predominately Douglas-fir (Pseudotsuga menziesii [mirb.] Franco) with mixed hardwood consisting of madrone (Madrona pacifica [Pursh]), big leaf maple (Acer macrophyllum [Pursh]), and red alder (Alnus rubra [Bong]). Figure 1 shows the relative proportions of types according to stems per acre and basal area, as well as average diameters.

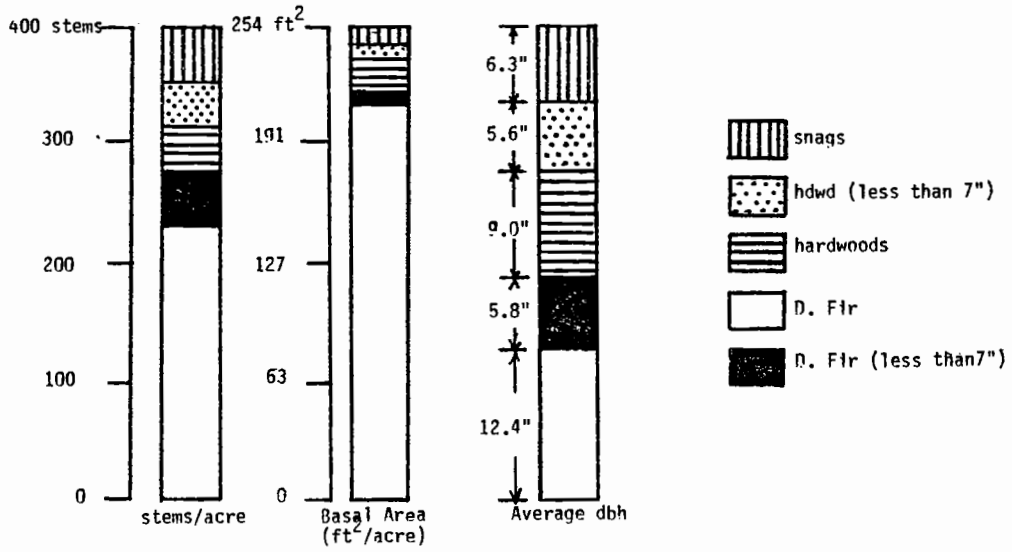

FIGURE 1. Stand composition according to type, size and number.

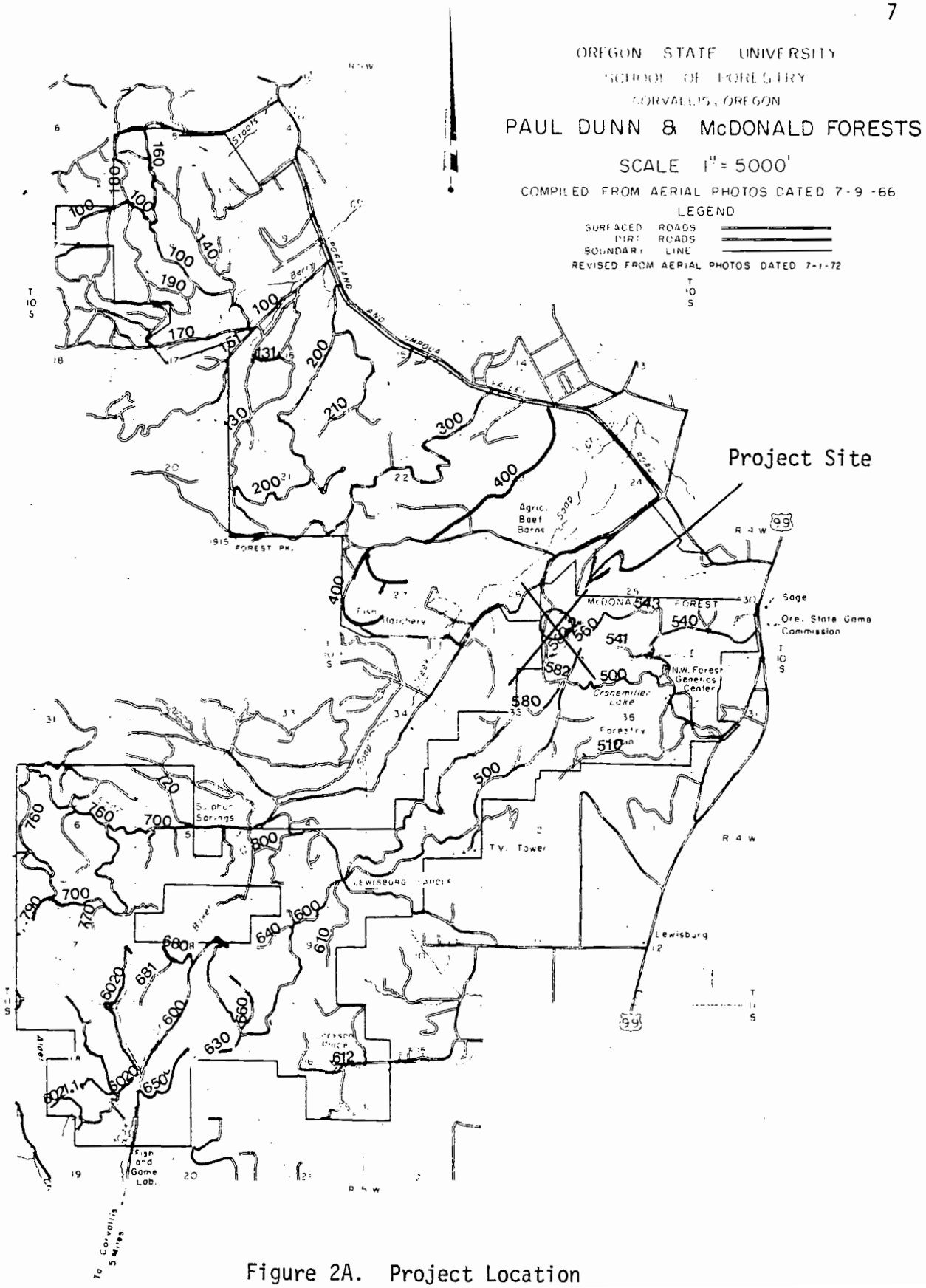

Figure 2A. Project Location

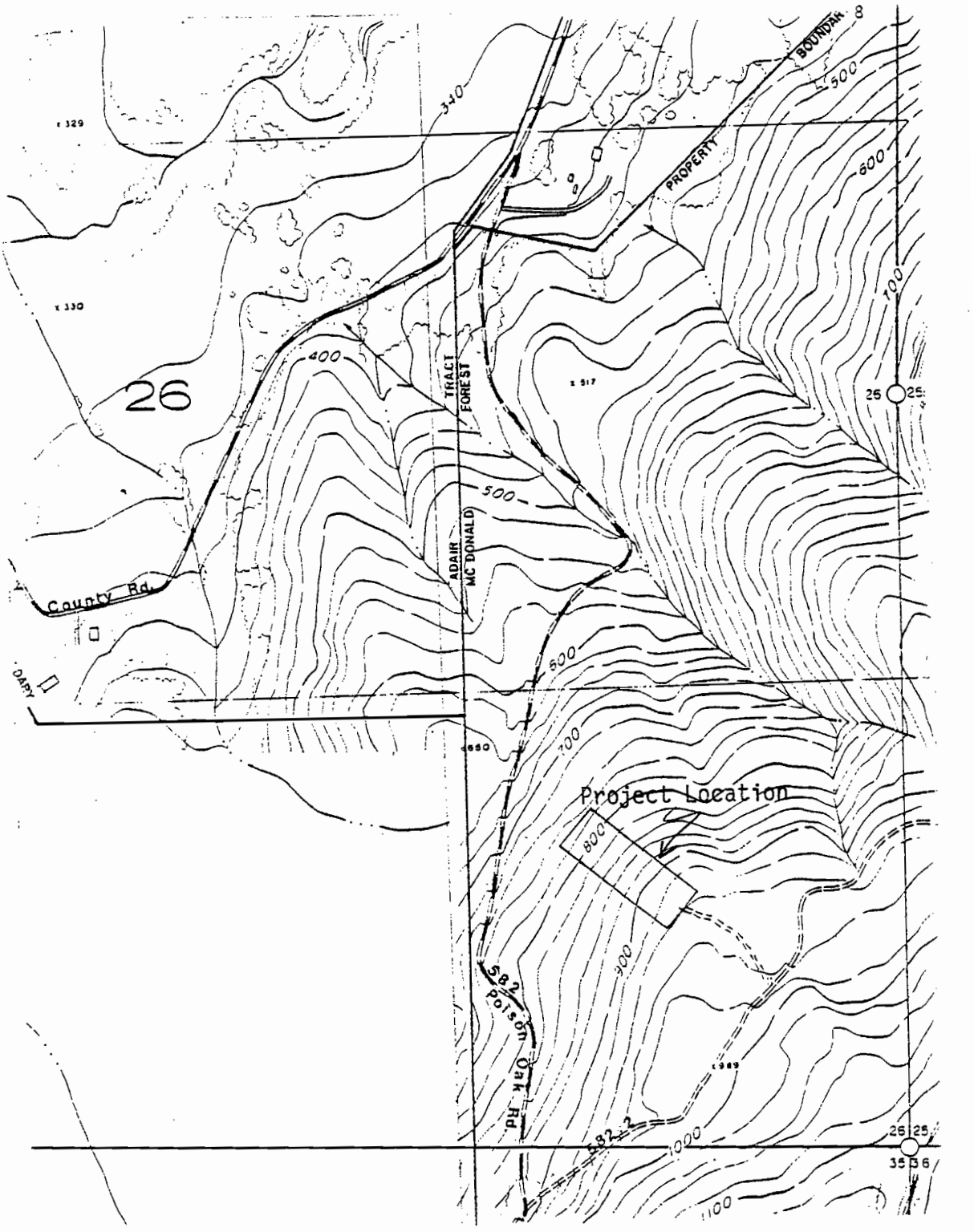

Figure 2A. Project Location

Slopes were moderate, averaging about 35%, (Appendix B) with a northerly aspect. Soils were clay with rock fragments, GC, according to the Unified Soil Classification. See Appendix A for a more complete soils description.

In order to determine the effect of thinning intensity, the area was divided into 8 units with the dimensions as shown in Figure 4. Each unit was approximately 1/3 acre, and the total area slightly less than 3 acres. Figure 3 shows the variation in stems per acre and basal area, respectively, among the units. Table 1 tabulates these values as well as the variation in average dbh.

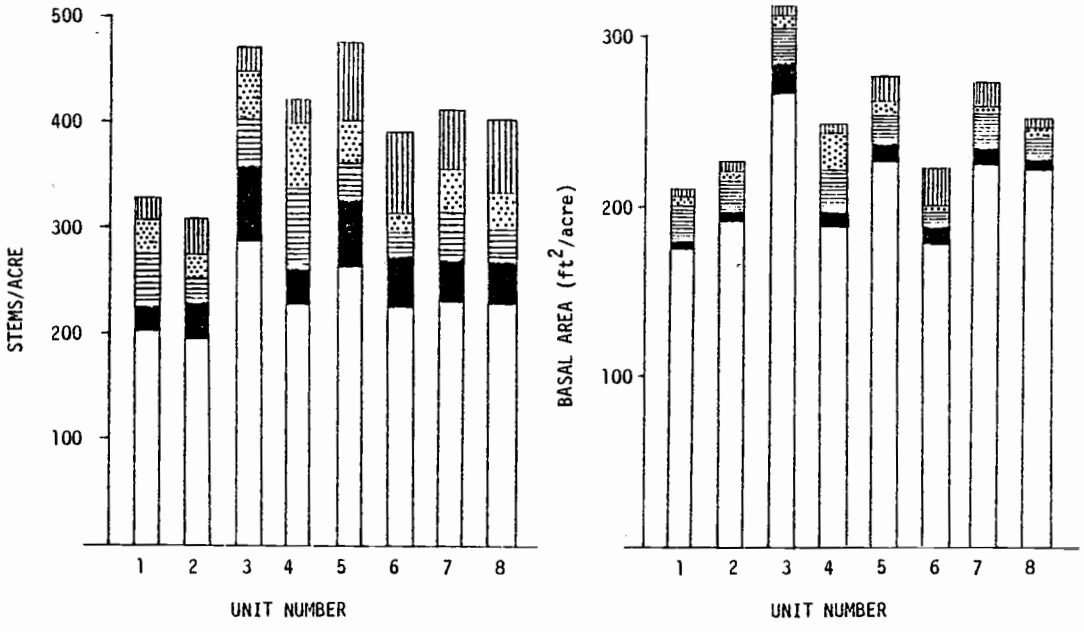

Figure 3. Variation in volume for each thinning unit.

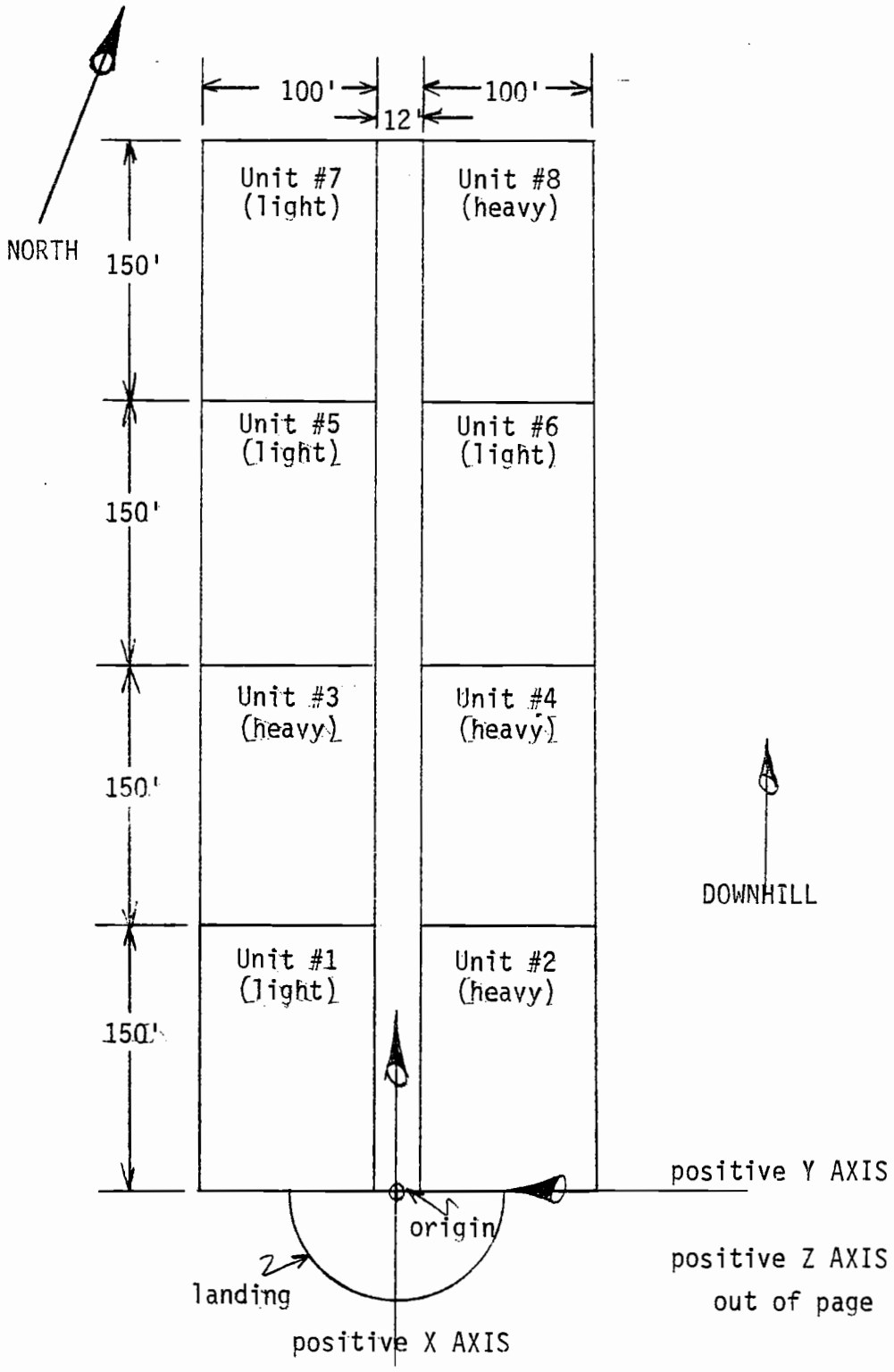

Figure 4. Plot layout showing dimensions, coordinate axis and unit numbers.

UNIT	CONIFER >7"	CONIFER <7"	HARDWOOD >7"	HARDWOOD <7"	SNAG	TOTAL
1 1	203	23	49	32	17	325
2	195	26	29	26	32	308
3	285	73	44	44	26	470
4	227	32	76	61	23	418
5	264	61	35	41	73	473
6	226	47	23	17	76	389
7	229	41	44	41	55	409
8	229	35	32	35	70	400
Total	232	42	41	37	47	400

A. Stems per acre

UNIT	CONIFER >7"	CONIFER <7"	HARDWOOD >7"	HARDWOOD <7"	SNAG	TOTAL
1	175	4	21	6	4	210
2	191	5	19	5	6	226
3	268	14	23	7	6	318
4	189	7	36	12	4	248
5	228	11	15	9	14	277
6	179	9	9	3	23	223
7	227	8	19	7	13	274
8	222	6	13	6	18	265
Total	210	8	19	7	11	254

B. Basal area (ft^2/acre)

UNIT	CONIFER >7"	CONIFER <7"	HARDWOOD >7"	HARDWOOD <7"	SNAG	TOTAL
1	12.2	5.4	8.7	5.8	6.2	11.2
2	13.0	5.9	10.2	5.6	5.5	10.7
3	12.6	5.8	9.4	5.5	5.9	10.2
4	12.0	6.4	9.1	6.0	5.4	9.8
5	11.5	5.8	8.5	5.5	7.0	9.5
6	13.0	5.9	8.8	5.4	6.2	10.2
7	12.9	5.7	8.6	5.5	6.7	9.5
8	11.5	5.8	8.5	5.5	7.0	9.5
Total	12.4	5.8	9.0	5.6	6.3	10.0

C. Average diameter (dbh-inches)

Table I. Volumes and average diameters (dbh) for each thinning unit.

Each unit was randomly assigned to one of two different thinning intensities; light or heavy. The heavily thinned units were cut to a residual stand of 128 stems/acre, and the lightly thinned units to 192 stems/acre. Intensities were based on stems 7" and larger dbh. Marking priorities were in accordance with the forest manager's policy of taking hardwoods first, defective or suppressed trees second, and then marking in order to achieve desired spacing.

The number of trees cut from each unit are shown in Figure 5. These cuts represent an average of 55% and 29% for heavy and light thinning respectively.

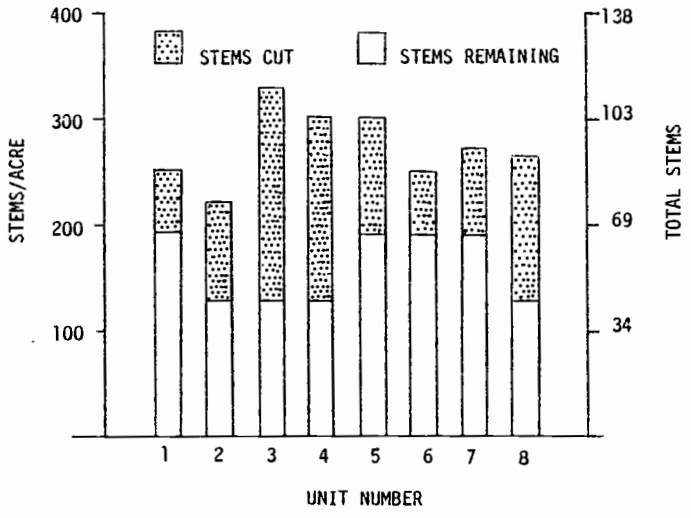

Figure 5. Number of trees cut from each unit.

DATA COLLECTION

Before Yarding

In order to determine distance measurements for the log turns and to develop a topographic map with which to determine elevations and ground slopes, the location of about 50% of the trees in the stand was determined with respect to lateral, longitudinal and vertical distances from a common reference point. Each tree located was numbered according to the unit it was in. Trees in the skyline corridor began with #0001, trees in Unit 1 began with #1001, trees in Unit 2 began with #2001, etc. After these trees were located, the remainder of the trees were numbered according to the same system. Appendix C shows a plot of and lists the coordinates of the trees located. Figure 4 shows the coordinate system chosen. It was during this part of data collection that the cruise data was obtained. .

During felling, the small and large end diameter and the length of each log was recorded. Each log was numbered according to the tree from which it came. For example, the logs from tree #2041 were numbered 2041.1, beginning with the butt log, and numbered consecutively (2041.2, 2041.3) for each log after the butt log. The stump was also numbered with the tree number so that the logs could be traced back to their original location in the stand.

During Yarding

Continuous measurements and recordings were made of both mainline tension and speed from initial turn movement until the turn was in the skyline corridor. The tension and line speed was measured with a

moving line tensiometer with integral line speed indicator made by Tri-Coastal Industries, Inc., and continuously recorded on a TEAC-R70A four channel tape recorder. The initial study plan was to also measure and record the mainline vertical angle as well as the skyline tensions during lateral yarding. The force balance inclinometer, Model SE-701FD made by Columbia Research Laboratories, Inc., which was to be used to measure mainline vertical angle was not adequately protected to withstand the rugged treatment it received. It, or the coaxial cable used to send the signal to the recorder, broke on several occasions resulting in erratic and inadequate recordings, so its use was discontinued. Skyline tensions were measured and recorded for many of the turns, but the static line tensiometer, also made by Tri-Coastal Industries, Inc., broke on three occasions, so its use was also discontinued.

Figure 6 shows a fairly typical oscillograph of the recordings. The graphs from upper to lower are: mainline tension, mainline vertical angle, mainline speed. The fourth channel, which is not shown, was reserved for skyline tension and wasn't recorded for this turn. Although the vertical mainline angle was not used, the oscillograph was useful in helping to interpret the recorded measurements. Since the skyline tensions were not always recorded, the use of that particular channel was sometimes used to record the sounds of the yarder and the whistle signals between the yarder operator and the choker setter. These signals were also useful in interpreting the graphs.

The number, location of the leading end of each log and the horizontal

DATA ANALYSIS

The analysis of the data will begin with how the regression of log weights was done, followed by the analysis of the break-out force, a discussion of the results, the analysis of the tensions generated after break-out, and finally a discussion of those results.

Log Weights

The recorded weights of 16 logs ranging from 190 to 1250 pounds was regressed using a volume estimated by $V=\frac{(d_1^2+d_2^2)l\pi}{576}$

V = estimated volume (ft^3)

d_1 = small end diameter (inches)

d_2 = large end diameter (inches)

l = log length (ft),

as the independent variable. The results of the regression yielded the equation $W=102+(34.4)V$, where

W = weight (lbs)

V = volume (ft^3)

with a coefficient of determination of 0.98. These results indicated that one could be 90% confident that the true value of a single observation would be within 110 lbs of the value estimated by the regression equation for the mean volume and within 120 lbs of the estimated value for volumes at the extremes. The regression line along with the observed data points are shown in Figure 7. This regression equation was used to determine the log weights used in all subsequent calculations.

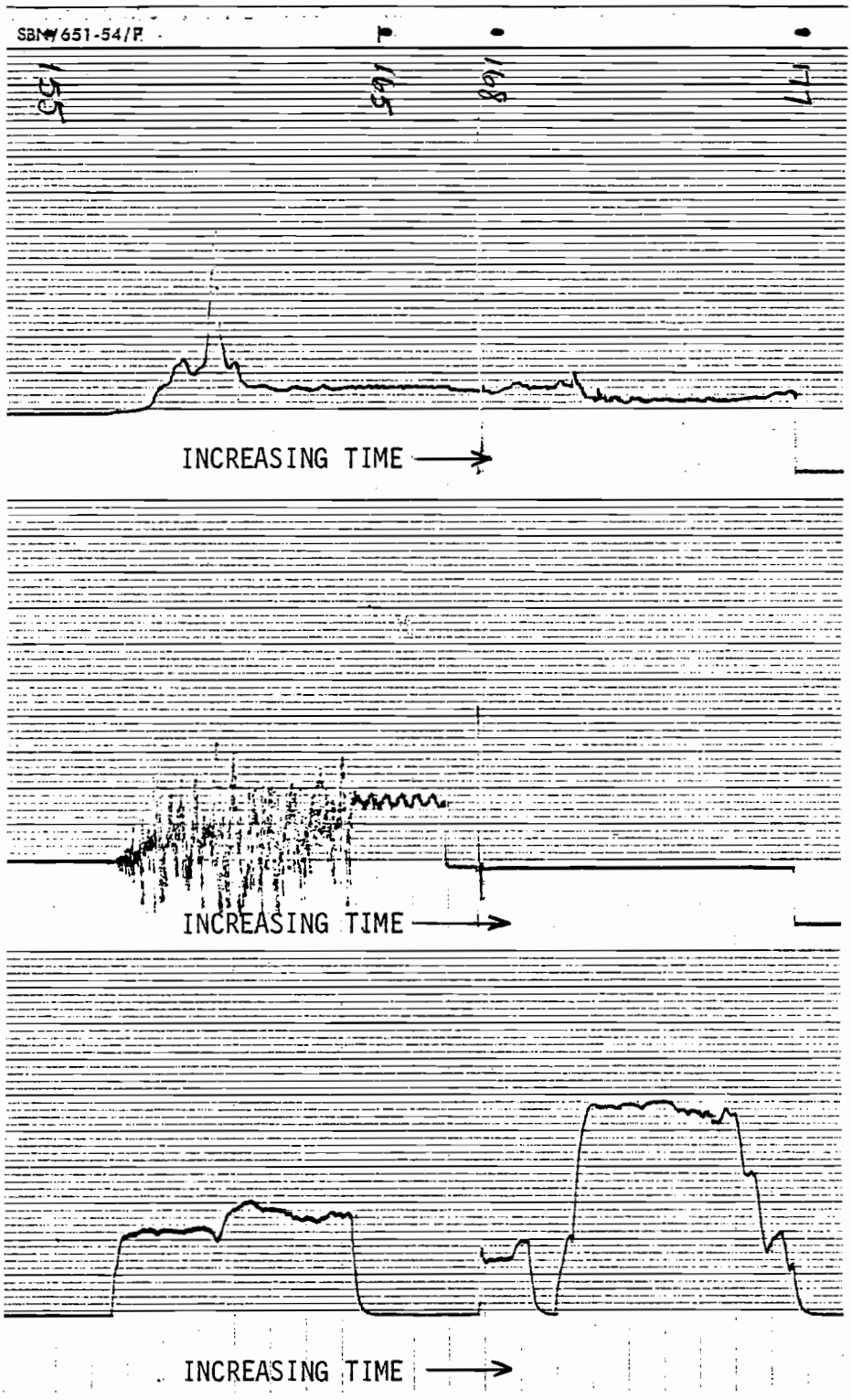

Figure 6. Typical oscillograph of tensions, speed and inclinometer recordings.

angle between the extension of the mainline and each log (the lead angle) was recorded for each turn. Because it was anticipated that the force balance inclinometer might not be reliable, the vertical angle from the leading end of the log to the carriage was measured with a clinometer and recorded. Carriage location was also noted. The turns were numbered in succession at the yarder and in the woods so the field notes and the recorded measurements at the yarder could be correlated.

To determine log weights, several logs were weighed by suspending them from a scale attached to the loader. From this a regression equation for log weight as a function of log volume was derived, the results of which are shown and explained further in the analysis.

Yarding was accomplished using a Shield-Bantam, 2 drum, 27' swing boom yarder with 3/4" skyline, 5/8" mainline, and 1/2" chokers and a Maki carriage. Weather conditions were consistent throughout the time of yarding, which took place during October 16-20, 1978. It was cloudy and overcast every day with some rain almost each day so that ground conditions were consistently wet.

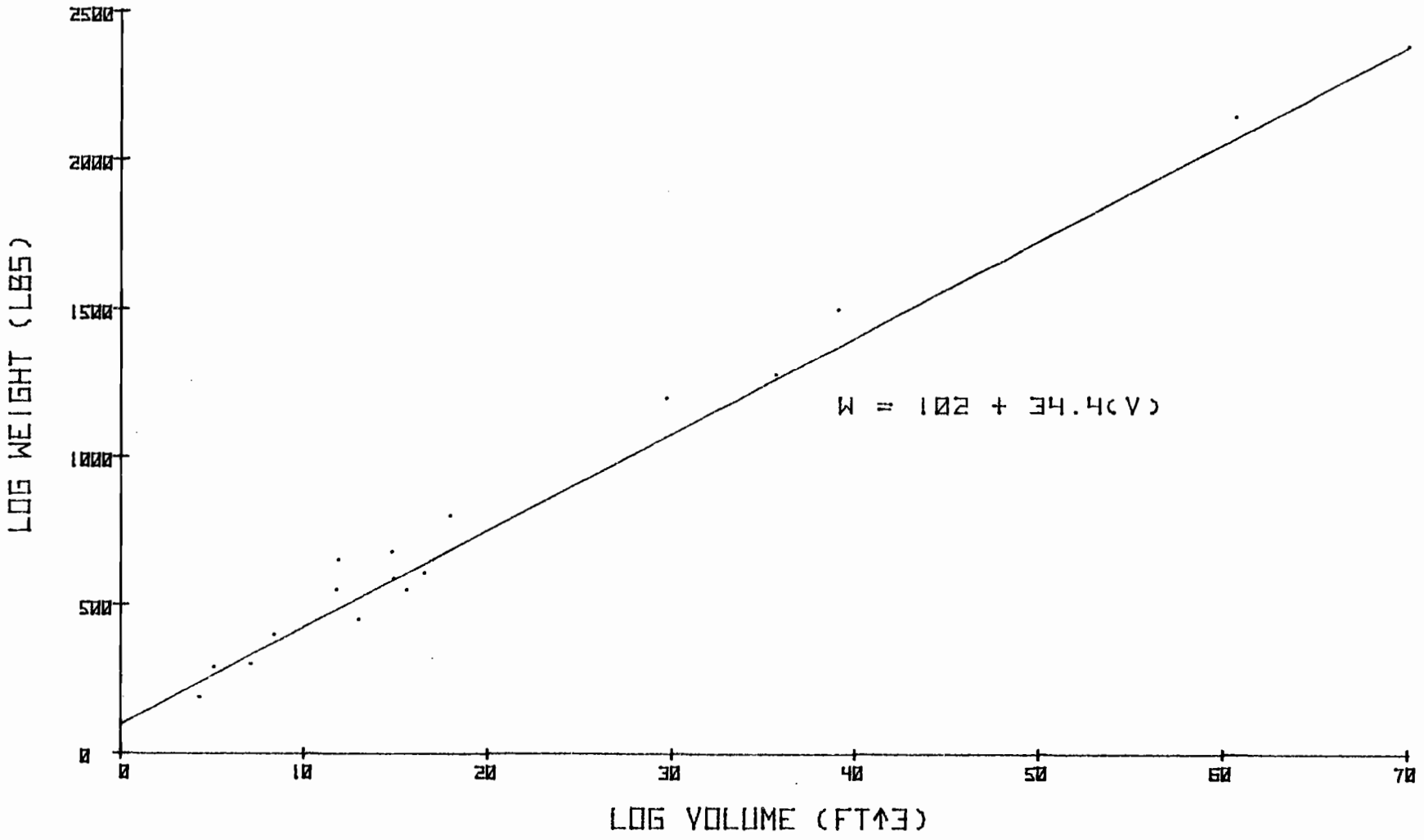

FIGURE 7. DATA PLOT OF LOG WEIGHT VERSUS LOG VOLUME

Break-out Forces

Figure 8 pictures the forces acting on the log just before movement occurs. If it is assumed that the force R acts opposite to the

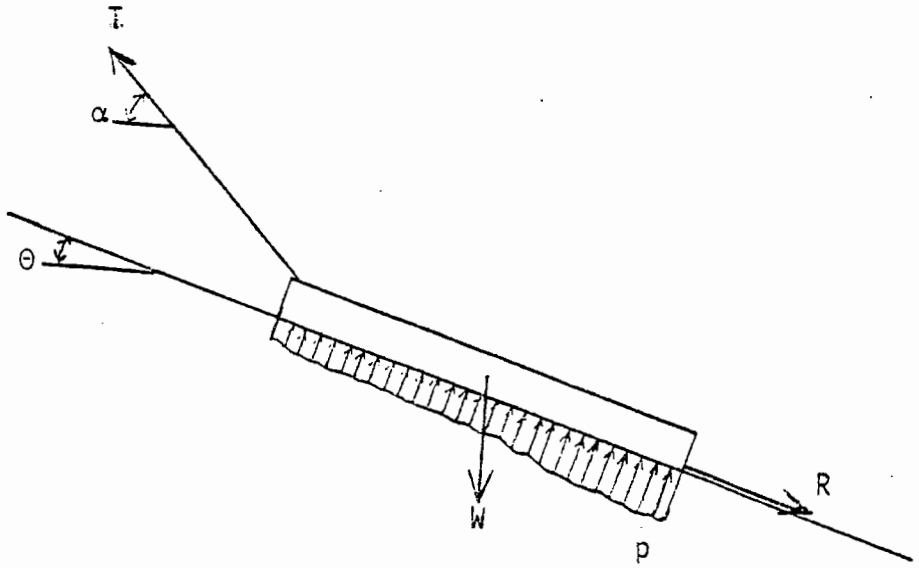

T = resultant tension at the lead end of the log

α = resultant angle of tension

Θ = ground slope

W = log weight

R = sum of the forces resisting movement of the log (Resistive Forces)

p = some unknown pressure distribution (lb/ft)

Figure 8. The forces acting on the log at impending movement.

direction of movement and that the direction of movement is along the slope, then R can be determined as long as the force T which will cause

movement is known, since the sum of the forces is zero. Resolving the forces acting on the log into components parallel and perpendicular to the ground slope (Figure 9), and summing them in these direction yields Equations 1 and 2:

1.) $R=P\cos(\alpha-\Theta)-W\sin\Theta$

2.) $N=W\cos\Theta-P\sin(\alpha-\Theta)$

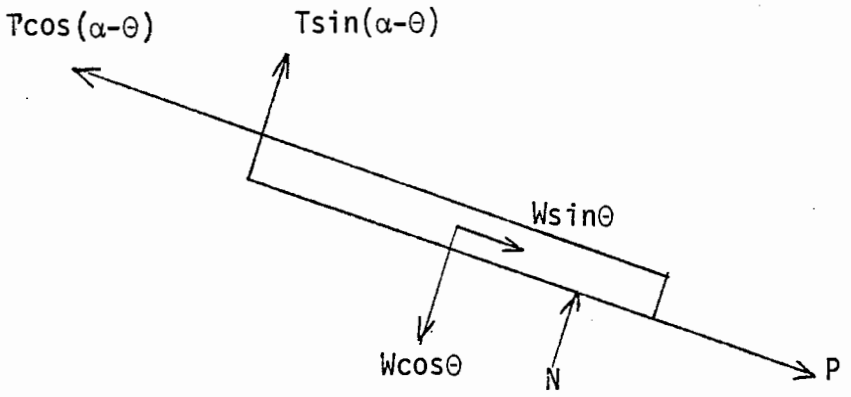

Figure 9. Resolution of forces, free body diagram.

Equation 1 is based on a highly idealized situation. The log may not always be directly on the ground (Figure 10), but as long as it is assumed that the log moves parallel to the ground slope, the variation from the idealized situation is very minor. The sum of forces parallel to the ground slope still yields Equation 1. It can also be seen that even if the front of the log rises during

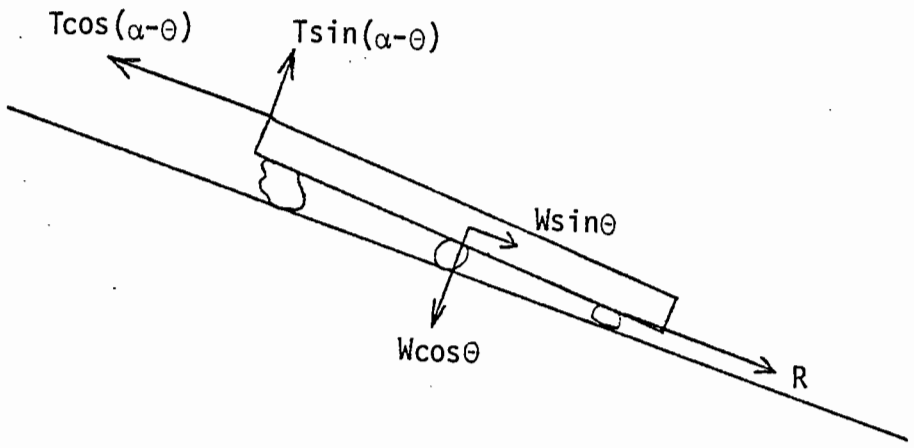

Figure 10. The resolved forces with the log not on the ground.

yarding, Equation 1 is still valid.

Equation 1, however, does not take into account that the log may not always be directly in line with the mainline (Figure 11). That is to say, β does not always equal 0. Any theoretical analysis that considers β≠0 would involve taking moments, preferably from the point about which the log would pivot upon movement. It would not only be a very cumbersome expression, but it would also be virtually impossible to measure either the magnitude or the location of these forces. Each log could, and probably would, be a completely different case depending on the number of resistive forces acting on the log and the magnitude of the individual resistive forces.

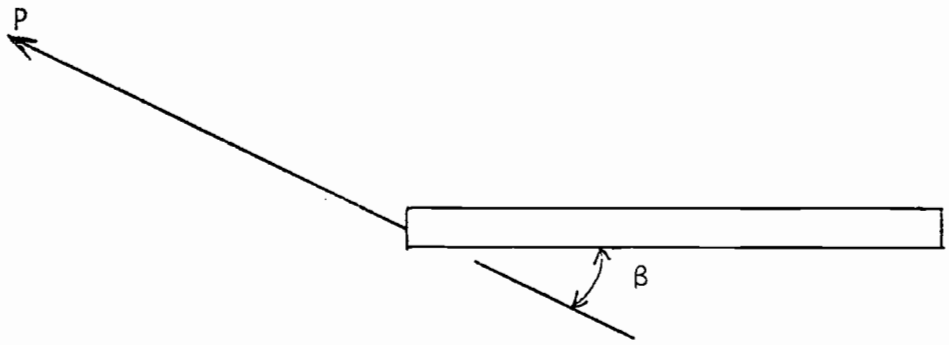

Figure 11. Plan view of log and mainline angle β.

It was observed in the field that the logs would normally pivot about a single point before actual lateral movement began only when the lead angle was large and an obstruction was encountered. These instances were rare so that lateral movement and pivoting would take place simultaneously. As long as lateral movement of the turn occurs, Equation 1 is still valid because it would take a larger force to cause lateral movement than it would to cause just pivoting under the conditions of static equilibrium. However, under those conditions when pivoting does occur, Equation 1 would introduce some error. But, since these instances were rare, Equation 1 was used for the analysis of the break-out force.

Since the tension in the mainline was measured at the yarder, the magnitude of T would be the measured tension less the product of the cable weight and the difference in elevation between the yarder and the lead end of the turn. This is based on the relationship that the difference in tension between any two points in a cable is equal to the product of the cable weight and the elevation difference between the two points (Figure 12). Since the location of the lead end of the turn and the carriage was known, each turn could be plotted (on the topographic map) and the log elevation as well as the ground slopes taken directly from these plots. The plots of the turns are shown in Appendix D.

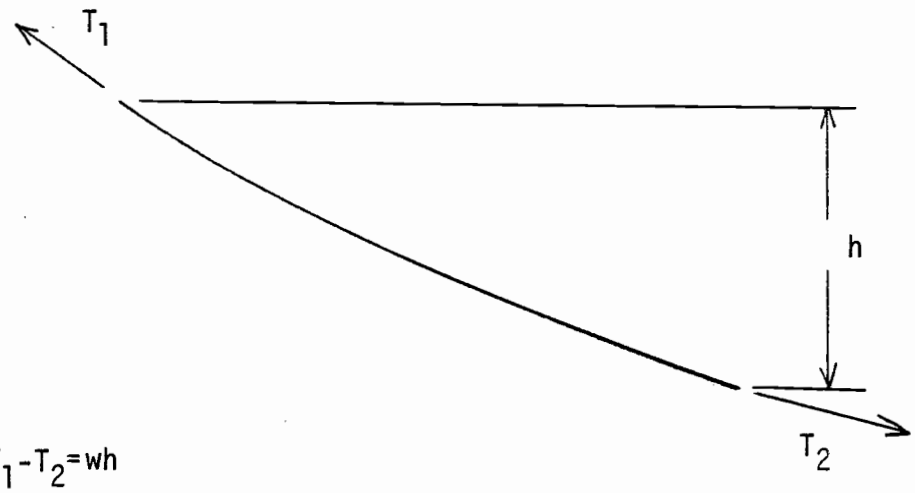

$T_1 - T_2 = wh$

where:

T_1 = Tension at upper end (lb)

T_2 = Tension at lower end (lb)

w = Cable weight (lb/ft)

h = Elevation difference

Figuire 12. Force relationships.

The resultant angle (α) is really tangent to the catenary curve at the turn and not the angle of the line of sight from the turn to the carriage. See Figure 13. The angle (α) is a function of the cable tension, the cable weight and the distance and elevation differences from the carriage, and is based on a catenary relationship. If the cable tensions are fairly high (greater than 1/3 of the cable breaking strength), the angle α is very close to the angle observed from the lead end of the turn to the carriage. For most of the turns, this angle would be quite adequate. However, since some of the tensions involved in yarding after break-out was achieved were quite small, the angle needed to be calculated using catenary relationships or large errors would have resulted. For this reason it was just as well to simply calculate all the resultant angles. The catenary iterative procedure developed by Carson (10) was used to accomplish this.

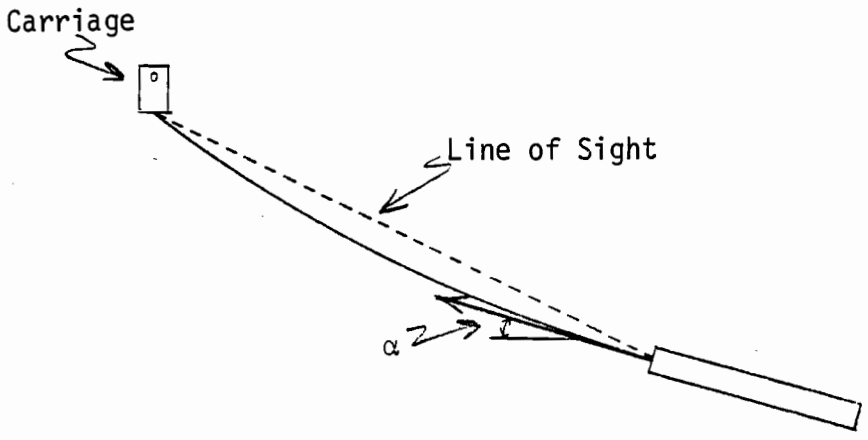

Figure 13. Resultant force angle.

The resistive force, R, determined by Equation 1 was plotted in 5 different ways as shown in Figures 14-18. These plots give no basis for suspecting that a fundamental relationship exists between the break-out force and the variables being considered, or that an empirical regression equation could be generated that could be used with any reasonable degree of confidence. For this reason, further attempts to analyze the break-out force in this way was not pursued.

An analysis of variance was performed to see if there was statistical reason to reject the hypothesis that the mean of the break-out forces for the heavily thinned units was equal to the mean of the forces for the lightly thinned units ($H_o: \mu_H = \mu_L$) in favor of the alternative hypothesis that they are significantly different ($Ha: \mu_H \neq \mu_L$). The ANOVA table (Table II) shows that H_o should be rejected at the 99% level.

Source	d.f.	SS	MS	F
Total	69	399868000		
Treatment	1	43139000	43139000	8.22
Error	68	356729000	5246000	

Table II. ANOVA of resistive force, heavy and light thinnings.

The critical F is 7.10 and the 95% confidence interval estimates are $L(\mu_H)$=1250-3190 and $L(\mu_L)$=3240-4560.

Similar analysis of variances was performed to see if the mean break-out force among the units was statistically the same. That is, the hypothesis that the mean break-out forces for each unit thinned heavily were equal (H_o:$\mu_2=\mu_3=\mu_4=\mu_8$) was tested against the alternative that the mean break-out force of one of the units was significantly different from the rest (H_a:$\mu_2\neq\mu_3\neq\mu_4\neq\mu_8$). The lightly thinned units were tested in the same way, however, unit #6 was not considered because it had only one observation. (H_o:$\mu_1=\mu_5=\mu_7$ against H_a:$\mu_1\neq\mu\neq\mu_7$). Both of these analyses resulted in accepting H_o at the 99% level. The ANOVA table are shown in Tables III and IV.

Source	d.f.	SS	MS	F
Total	47	284772000		
Treatment	3	39967000	13322000	2.39
Error	44	244805000	5564000	

Table III. ANOVA of resistive force, mean of heavily thinned units. (Critical F=4.31).

Source	d.f.	SS	MS	F
Total	20	71606000		
Treatment	2	10666000	5333000	1.57
Error	18	60940000	3390000	

Table IV. ANOVA of resistive force, mean of lightly thinned units. (Critical F=6.01)

Since these analyses showed a high probability that heavier thinnings generated higher break-out forces than lighter thinnings, it seemed wise to try to determine if it was the number of stems on the ground that might be the cause of the difference, rather than the number of stems left before progressing with the analysis. The hypothesis that the mean break-out force for units with "few" stems down ($H_o: \mu_M = \mu_F$) was tested against the alternative that they were not the same ($H_a: \mu_M \neq \mu_F$). The difference between "many" and "few" was determined to be more than the average number of trees down and less than the average number of trees down respectively, because there was a very evident break at that point. The results of this analysis are shown in Table V.

Source	d.f.	SS	MS	F
Total	69	399820000		
Treatment	1	48525000	48525000	9.39
Error	68	351295000	5166000	

Table V. ANOVA of resistive force, many stems down against few stems down.

Since the critical F for this test is also 7.10, H_o was rejected in favor of the alternative. This test strongly suggests that the difference might be due to the number of stems on the ground rather than to the number of stems left. It was anticipated that these analyses might give results such as this, in which case a more sophisticated statistical analysis would be needed which is beyond the scope of this paper.

One further analysis of variance was done to test if the number of logs per turn affected the magnitude of the break-out forces. The hypothesis that the mean break-out forces for 1, 2, and 3 or more logs per turn were equal ($H_o: \mu_1 = \mu_2 = \mu_3+$) was tested against the alternative that at least one was significantly different ($H_a: \mu_1 \neq \mu_2 \neq \mu_3+$). This resulted in rejecting H_o in favor of H_a with the 95% confidence

interval estimates indicating that the turns with 2 logs were significantly different from 1 log per turn. Table VI shows the ANOVA table and Table VII shows the sample mean and interval estimates.

Source	D.F.	SS	MS	F
Total	69	399985000		
Treatment	2	59692000	29846000	5.88
Error	67	340293000	5079000	

Table VI. ANOVA of resistive force, number of logs per turn. (Critical F=4.95)

Logs/Turn	Sample Mean	95% Confidence Interval Estimate	
		Low	High
1	2180	1300	3060
2	4140	3380	4900
3 or more	3860	2370	5350

Table VII. Sample mean and interval estimates for number of logs per turn.

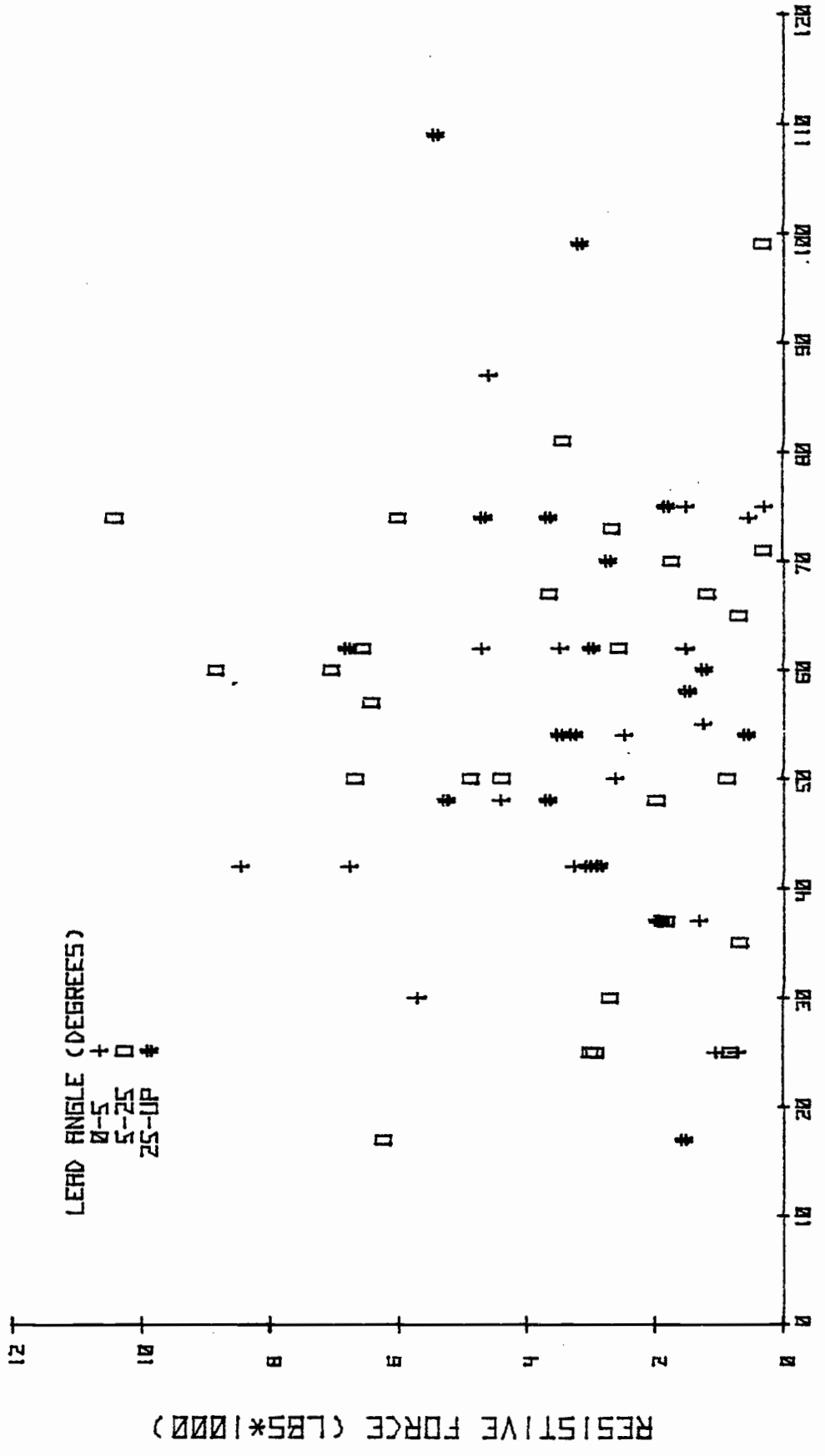

FIGURE 14. RESISTIVE FORCE VERSUS TURN LENGTH FOR VARYING LEAD ANGLES

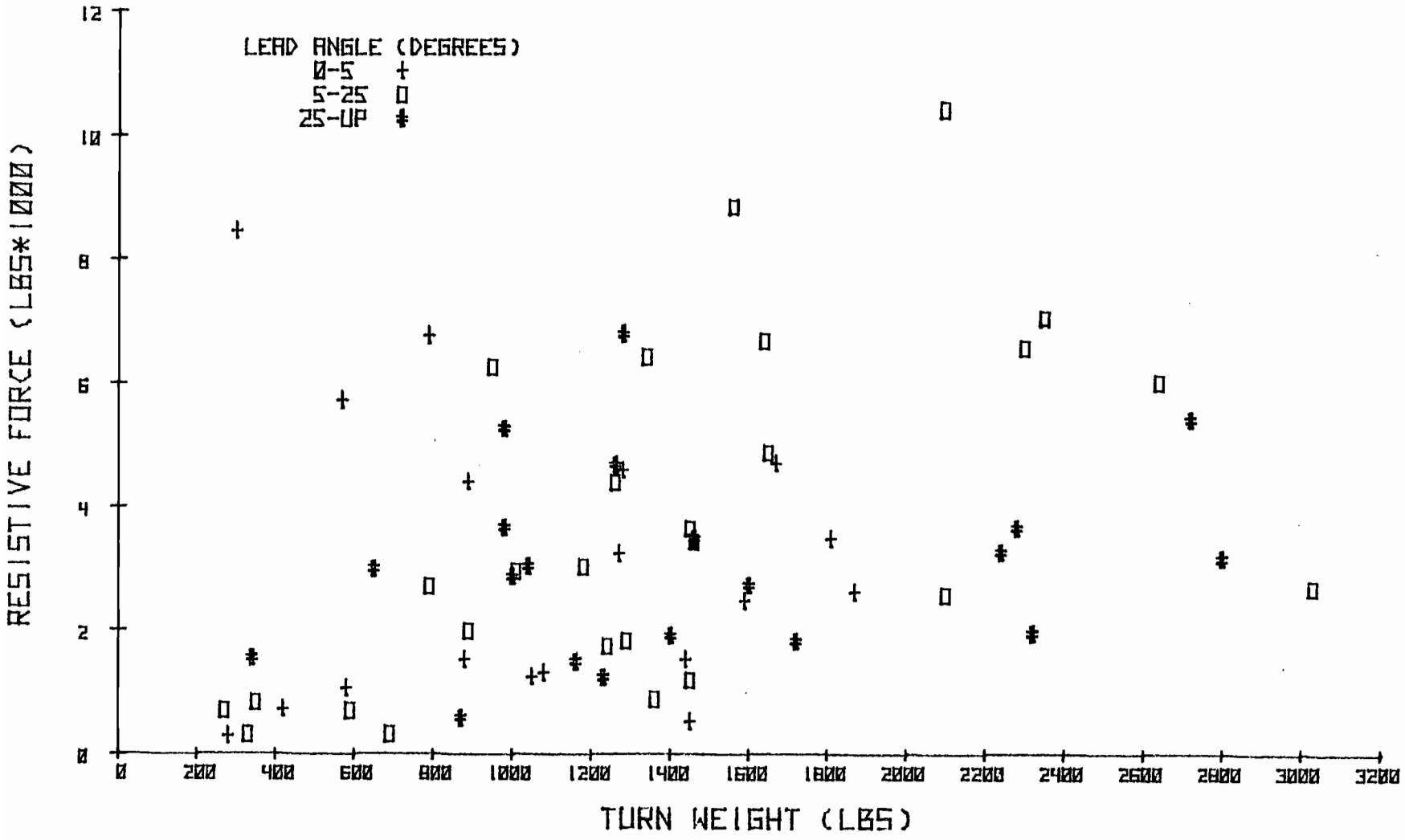

FIGURE 15. RESISTIVE FORCE VERSUS TURN WEIGHT FOR VARYING LEAD ANGLES

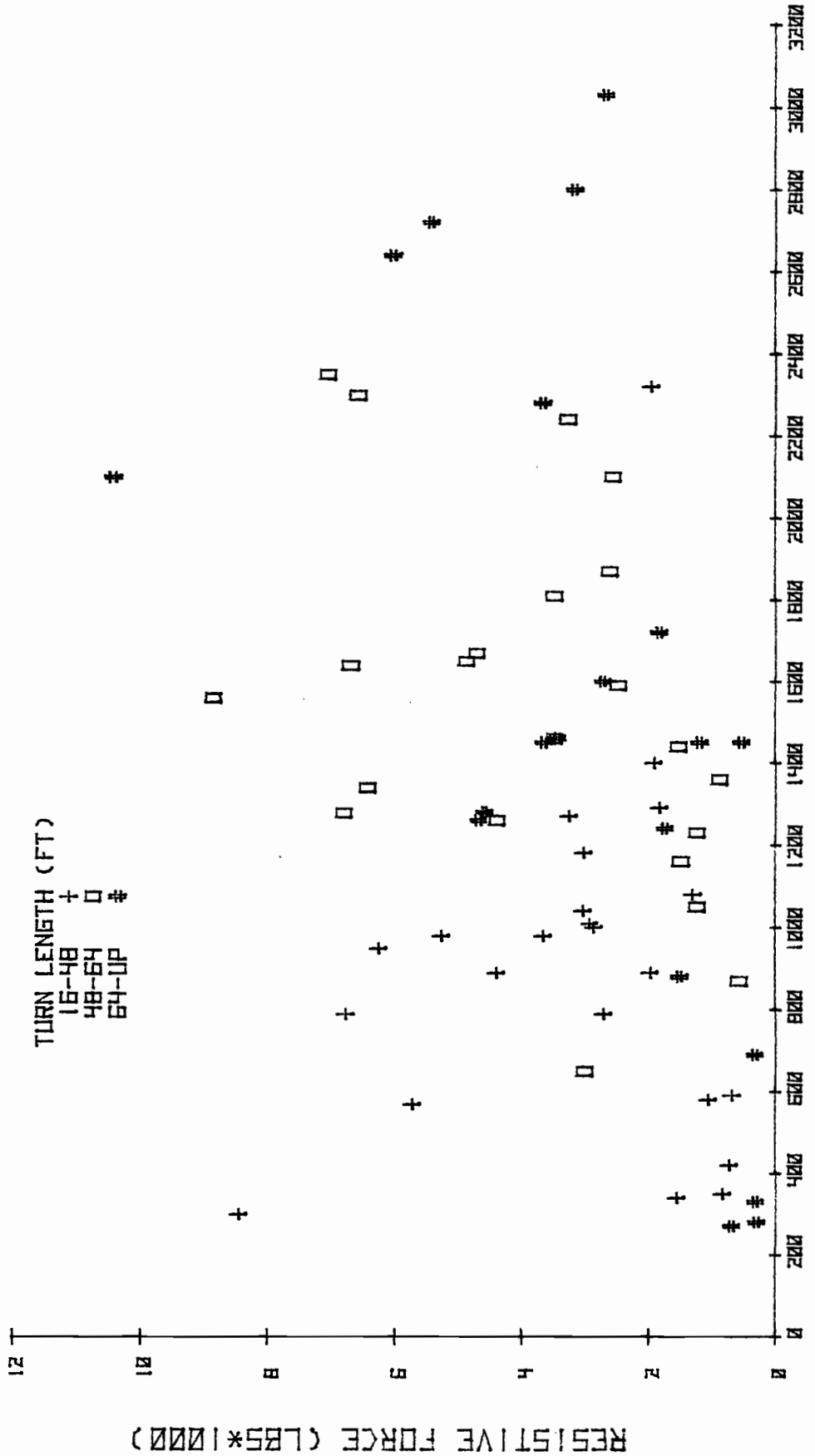

FIGURE 16. RESISTIVE FORCE VERSUS TURN WEIGHT FOR VARYING TURN LENGTH.

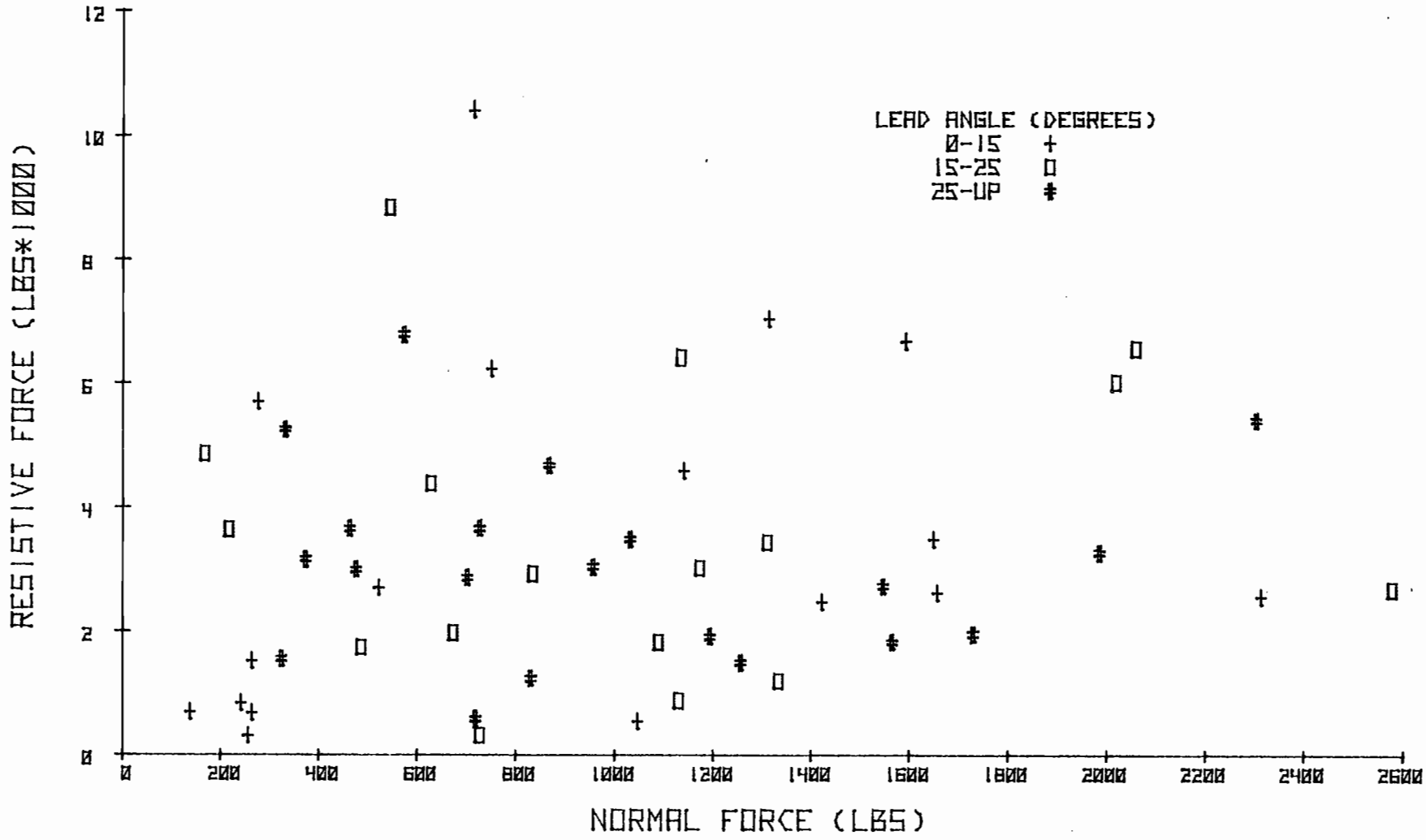

FIGURE 17. RESISTIVE FORCE VERSUS NORMAL FORCE FOR VARYING LEAD ANGLES

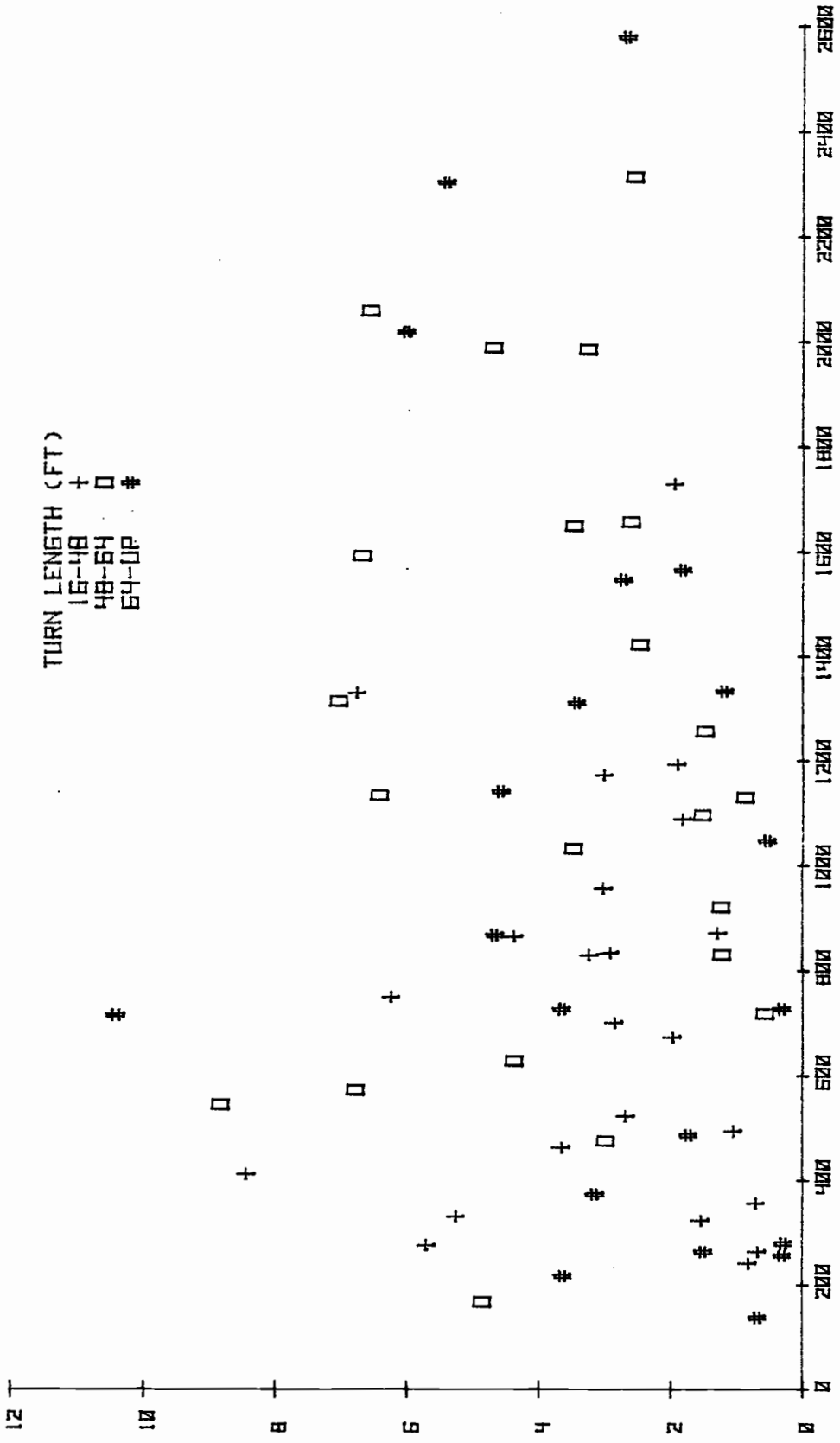

FIGURE 18. RESISTIVE FORCE VERSUS NORMAL FORCE FOR VARYING TURN LENGTH.

Discussion of Results

The results of this study are similar to those reported by Gibson (9) for a similar experiment done in hardwoods, where it was stated that "the force needed to bring in a 28 in. by 35 ft. 8189 lb. log was 6800 lb. This was handled easily. However, when two logs were winched together (6356 lb.), the maximum winching force went to 11,000 lbs.". Almost the same relationship between resistive force and number of logs was observed in this study where the average resistive force for one log turns was about half of the average for two log turns. The average resistive force for three log turns decreased from that for two log turns, but the difference was not statistically significant. There seemed to be a tendency for the choker setter to treat three log turns with more caution, choosing three logs for a turn when the circumstances would result in lower resistive forces.

Figures 19 and 20 are presented to show the effect that the mainline angle (α) and the weight component ($W\sin\Theta$) have on the total tension (T) required to break the log turn out. In Figure 19, the resultant force is the tension T and in Figure 20, the resultant tension is $T\cos(\alpha-\Theta)$. It can be seen that both α and the weight component have a significant effect, and quite clearly the variation in these plots is due to the variation in the resistive force R. This is the reason why R was examined by itself; the application of these results can be more easily extended for ground slopes and mainline angles that are outside the range of this data.

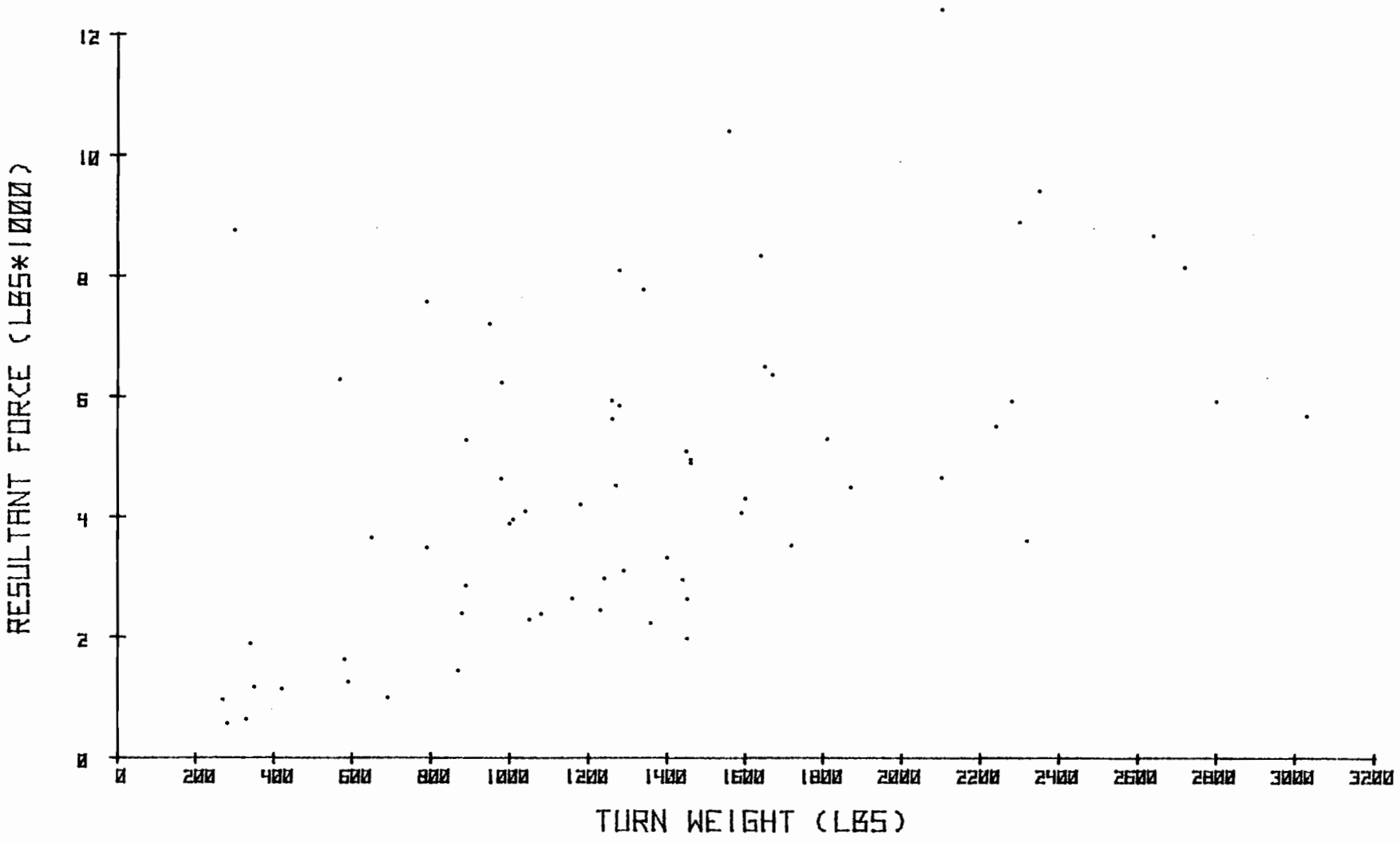

FIGURE 19. RESULTANT FORCE AT LEAD OF TURN VERSUS TURN WEIGHT.

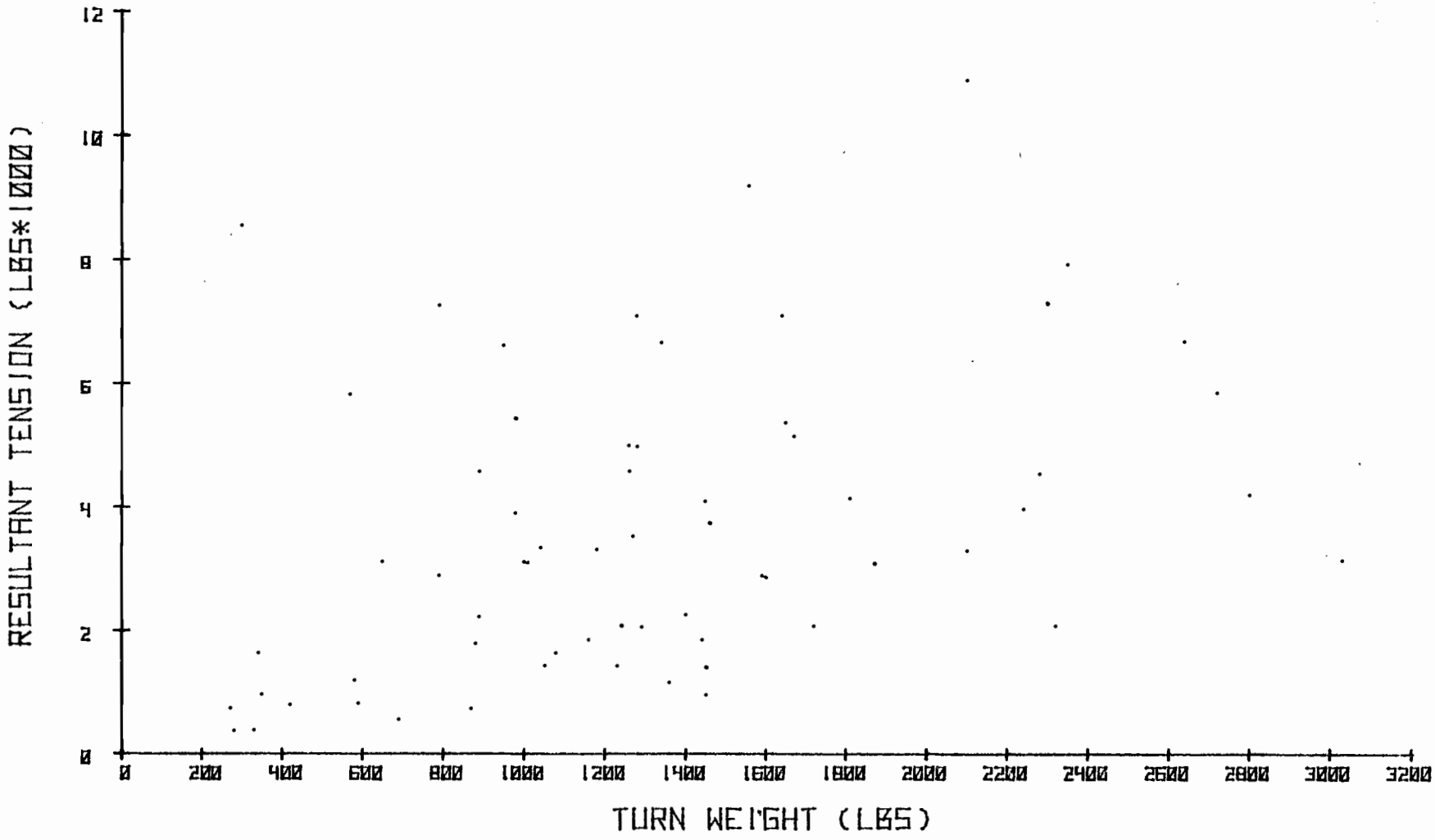

FIGURE 20. RESULTANT MAINLINE TENSION VERSUS TURN WEIGHT.

There is no doubt that the resistive force relationships have numerous interactions. For this reason even if the field measurements were taken perfectly, quite a lot of variation in the resistive forces would still be expected. The measurements introduced other sources of variations. Probably the major source was interpreting the oscillograph of mainline tensions for multiple log turns. It was difficult to know just what tensions were the break-out tensions since all the logs did not break out simultaneously. It was also difficult to get an accurate measurement of the angle from the lead end of the turn to the carriage. Since distances and the resultant force angle were calculated using this measurement, the results would reflect the error quite noticeably.

Lateral Inhaul Forces

Lateral inhaul forces were analyzed in a manner similar to the break-out forces. After movement has started the resistive force R is the frictional force. Figure 21 shows the free body diagram from which Equation 1 was derived. From it, Equation 3 is derived by replacing R with the frictional force, F.

3.) $F=P\cos(\alpha-\Theta)-W\sin\Theta$

The only difference in this analysis and the one used for the break-out force is that the magnitude of the measured tension at the yarder was less. Otherwise, the same mathematical techniques were used. Figures 22-24 show plots of the friction force, F, against the normal force, N (Equation 2).

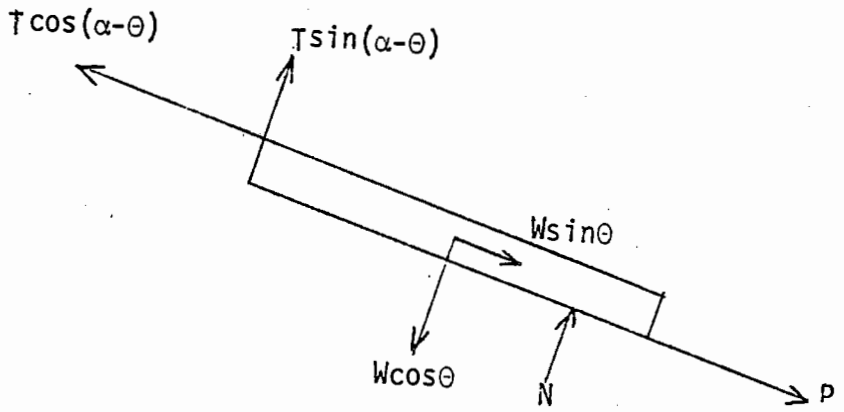

Figure 21. Free body diagram.

These plots show that although a fairly strong linear relationship between the frictional force and the normal force is indicated, there is not much reason to suspect that either the number of logs per turn, or the turn length, or thinning intensity influences the inhaul forces significantly. One other variable was calculated; d, the distance from the end of the log to the normal force (Figure 25) to see if it affected the inhaul force. Taking moments about the log end yielded Equation 4:

$$4.)\quad \frac{d}{T} = \frac{(W/2)\cos\Theta - P\sin(\alpha-\Theta)}{W\cos\Theta - P\sin(\alpha-\Theta)}$$

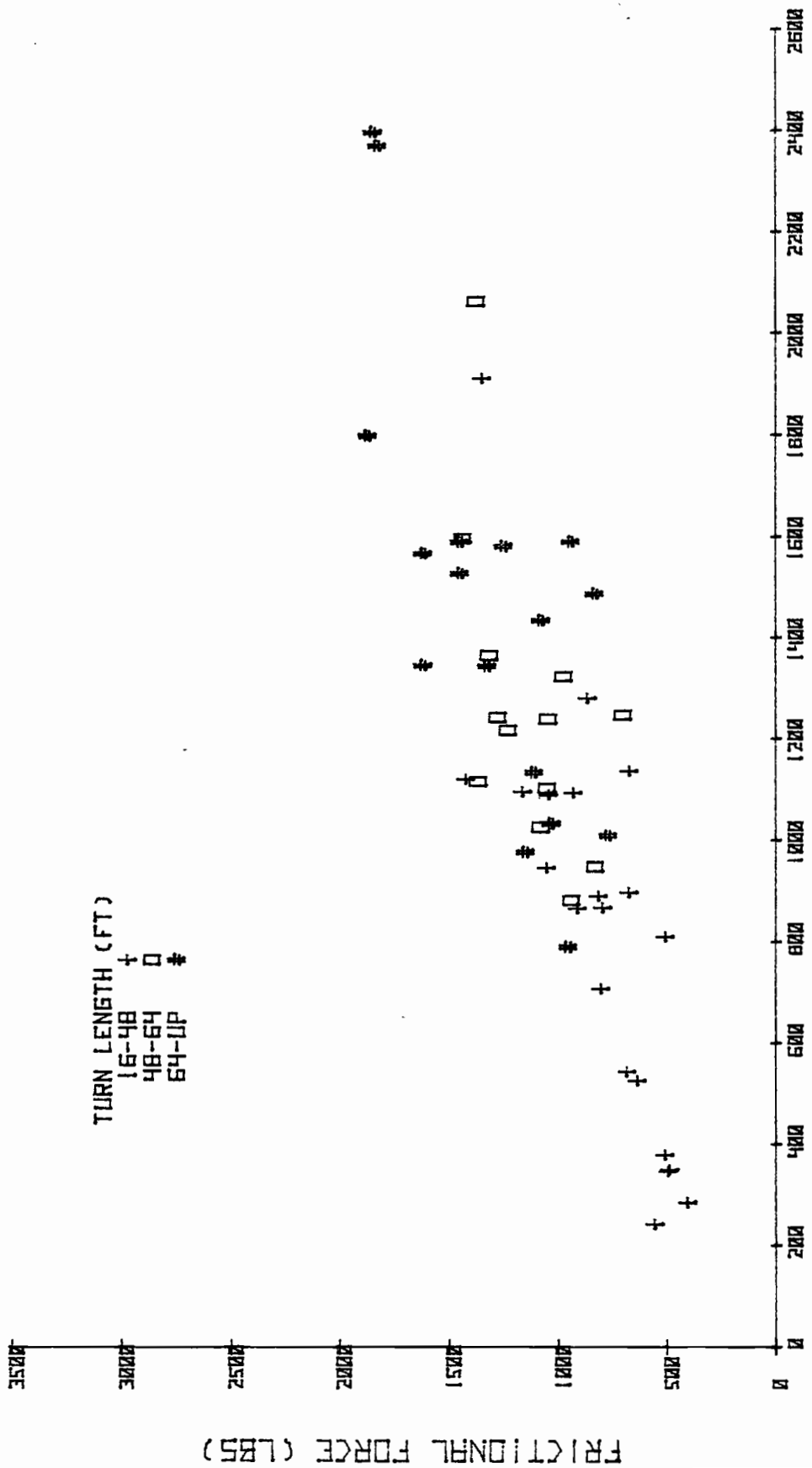

FIGURE 22. FRICTIONAL FORCE VERSUS NORMAL FORCE FOR VARYING TURN LENGTHS.

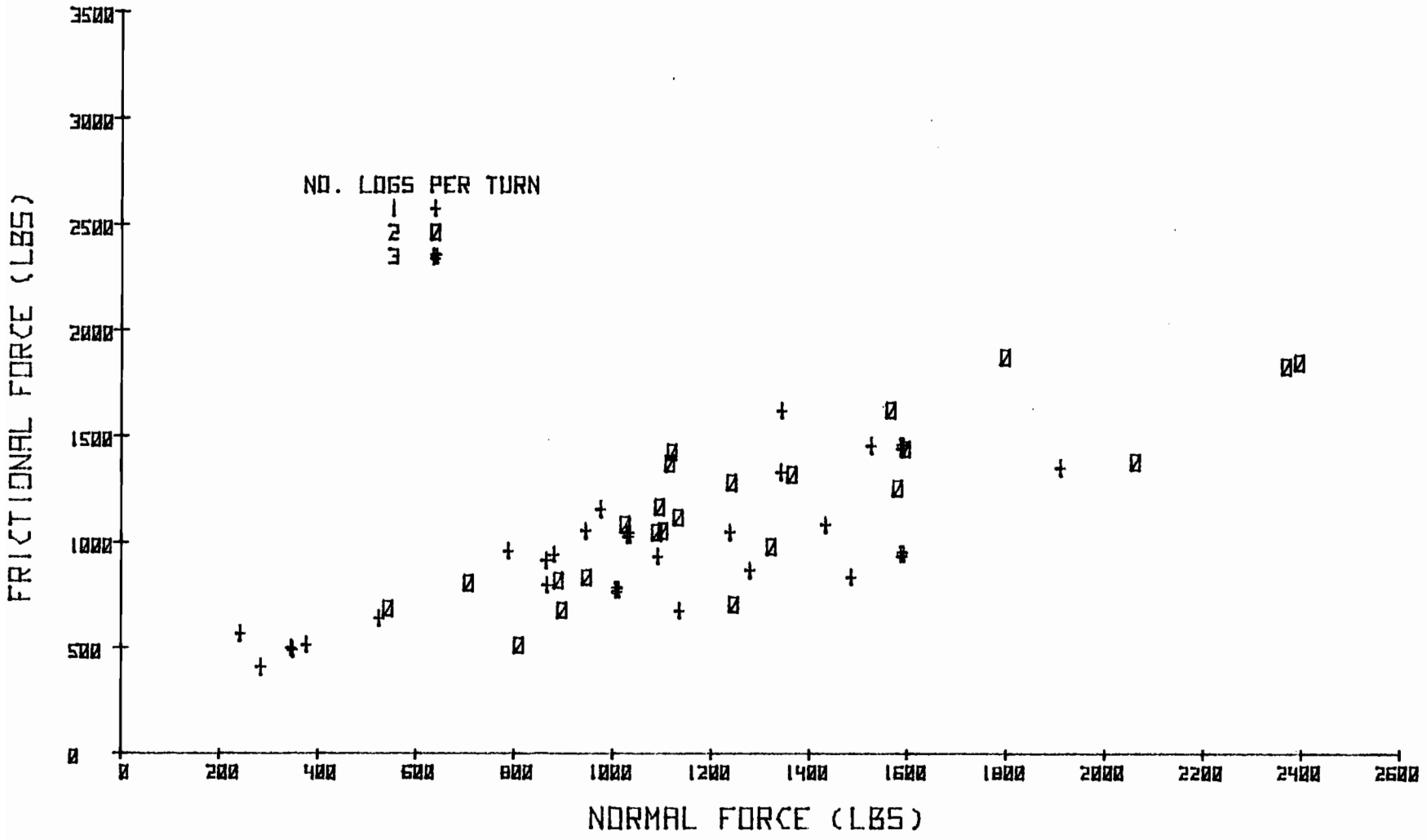

FIGURE 23. FRICTIONAL FORCE VERSUS NORMAL FORCE FOR VARYING NUMBER OF LOGS PER TURN.

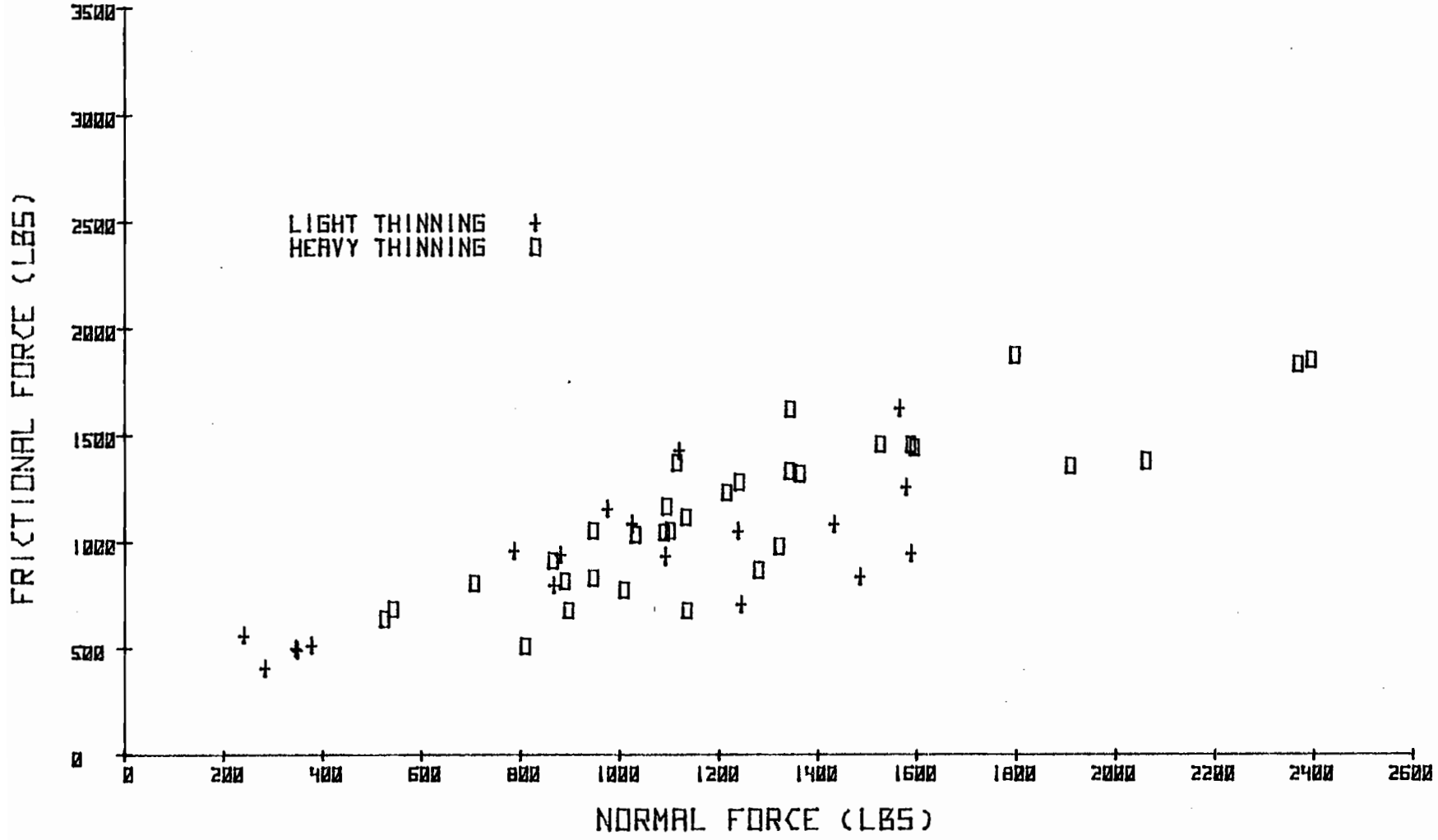

FIGURE 24. FRICTIONAL FORCE VERSUS NORMAL FORCE FOR LIGHT AND HEAVY THINNING.

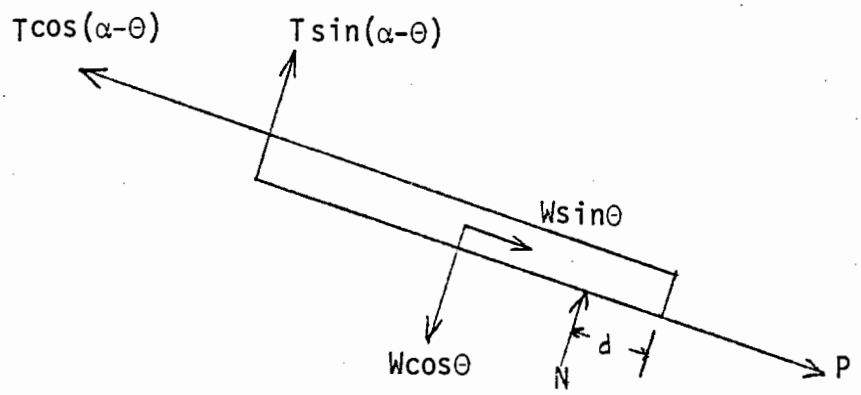

Figure 25. Moments about the log end.

A multiple linear regression was attempted using Equation 4, but the addition of the variable d/l did not significantly improve the equation obtained with just the single independent variable N.

However, Equation 3 was also used to determine if the front of the log turn remained on the ground if partial suspension occurred. Theoretically if $d/l \leq 0$, then partial suspension occurs or is about to occur, in which case the analysis would not be valid because the elevation of the lead end of the log would not be at ground elevation. This check showed that no partial suspension occurred on the turns examined.

Figure 26 shows the data points and the regression line for

frictional versus normal forces. The coefficient of determination (r^2) for this regression was 0.70. The statistics show that one can be 90% confident that the real value of a single observation will be within 300 lbs. of the value predicted by the regression line for the mean and within 320 lbs. for values at the extremes.

The regression is F=320+.64N. The intercept, because the data does not extend to N=0 does not have a physical interpretation. The slope, however, represents the frictional coefficient commonly known as "μ." This value of 0.64 is certainly not an uncommon value, in fact 0.60 is generally used as an estimate for the frictional coefficient when it is not known.

Discussion of Results

The only difference between these results and other works which deal with the coefficient of friction that can be discussed is the fact that both Caterpillar (11) and Henshaw (12) found that the frictional coefficient is dependent on ground slope, but this analysis shows no such dependency. No certain reason can be given for this difference without further investigation, but it is suspected that the differences are a result of different assumptions in dealing with the resultant force angle at the lead end of the log.

There are several things that can account for the variation observed in the data points in Figure 26. Probably the most significant would be the variation in estimating the log weight and in measuring the angle from the lead end of the log to the carriage, from which distances were calculated.

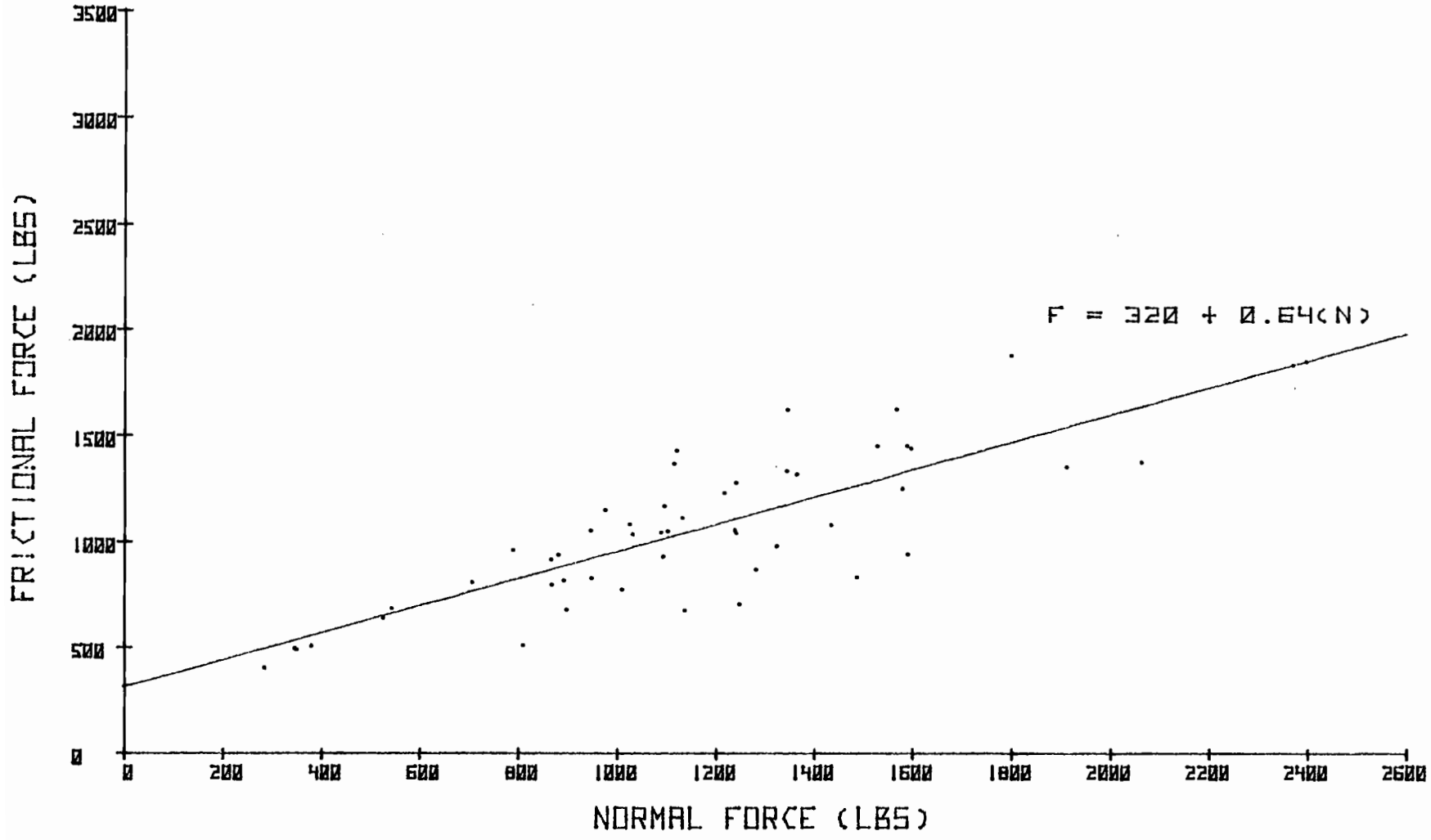

FIGURE 26. FRICTIONAL FORCE VERSUS NORMAL- REGRESSION LINE.

Another highly suspected source of variation is that very often, several turns would be taken over the same path during lateral inhaul. Each turn would have a tendency to cause the soil to become more compacted and to make a smoother path for the turn which followed, which would have a tendency to decrease the frictional resistance. Although there are variations, the data is realistically represented and it can be worthwhile in predicting the forces occurred in lateral inhaul.

SUMMARY AND APPLICATION OF RESULTS

Both the maximum and the average lateral yarding forces can be predicted with reasonable confidence for conditions similar to those under which this study was conducted. The maximum force will be encountered as initial movement of the turn is achieved. Since the analysis conducted indicates that the resistive force is independent of turn weight and length, ground slope, and the resultant force angle, Figure 27, showing the percent of resistive forces less than a particular value, was generated. This figure may be used to determine the value of the resistive force such that an arbitrary percentage of turns will fall below. For example, if one wanted the resistive force such that 95% of the turns would be less than, Figure 27 would yield a value of approximately 9800 lbs.

The value is only the resistive force. The weight component and angle of the resultant force must also be considered to determine what force is necessary to break-out the log from its bed. The equation is:

$$4.)\quad P = \frac{R+W\sin\Theta}{\cos(\alpha-\Theta)}$$

where: P = break-out force

R = resistive force

Θ = ground slope

α = mainline angle

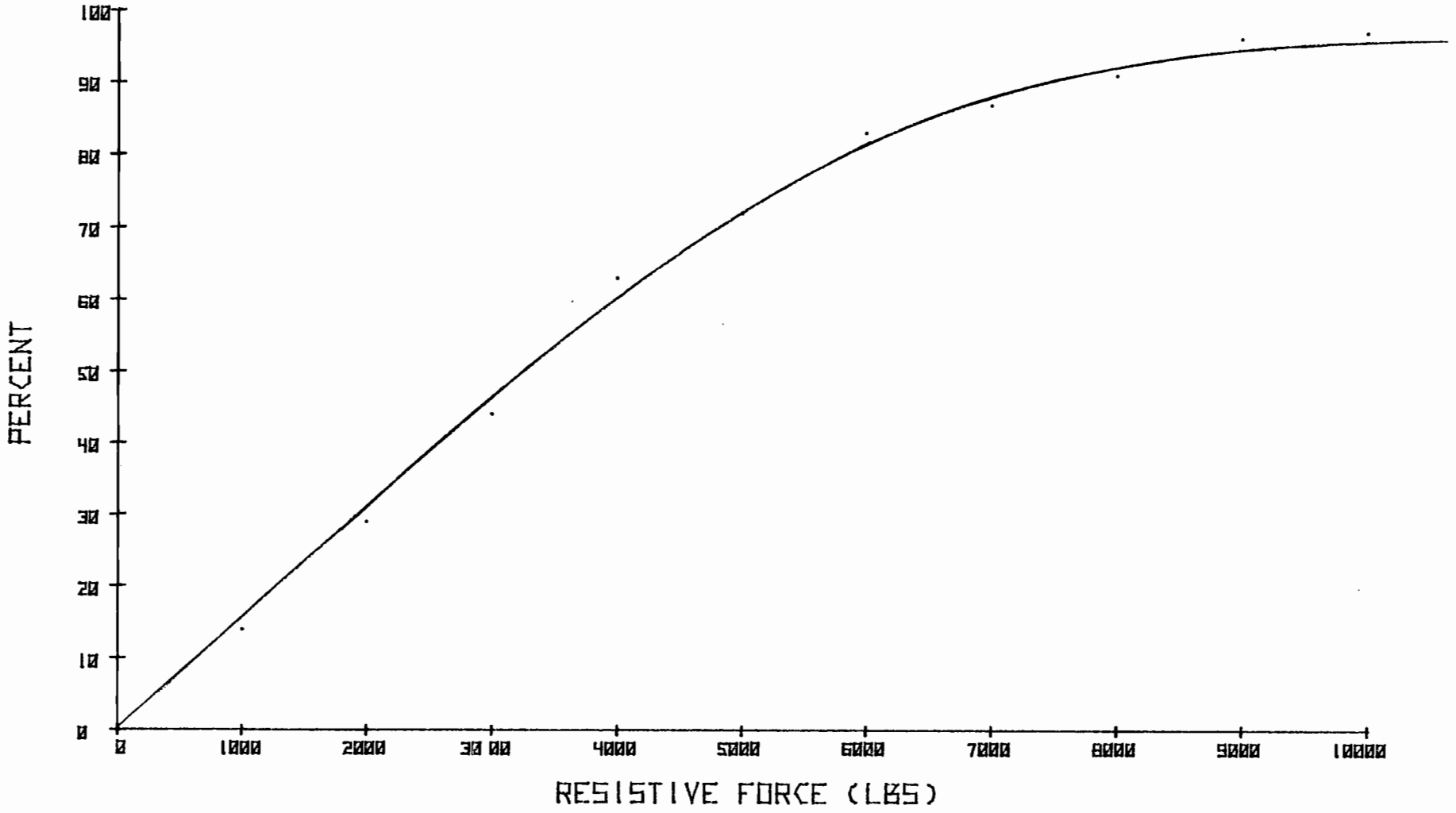

FIGURE 27. PERCENT OF RESISTIVE FORCES FALLING BELOW PARTICULAR VALUES.

With the resistive force of 9,800 lbs. and a ground slope of 30%, a mainline angle of 35%, and a turn weight of 2,000 lbs., the break-out force would be 10,400 lbs. The tension at the carriage or at the yarder would be slightly different depending on the cable weight and the difference in elevation.

Care should be used in the application of these results because Figure 27 was generated without regard to thinning intensity even though it was shown that thinning intensity does affect the break-out force. Also, intuition says that the resistive force will be dependent on turn weight under some conditions; for example in harvesting old growth timber. For these reasons extension of these results for predicting resistive forces under conditions not similar to the conditions under which this study was conducted would probably not be valid.

The "average," or lateral inhaul forces can be estimated by solving Equation 3 for T and using the regression equation for F, ignoring the intercept.

$$6.)\quad T = \frac{W(.64\cos\Theta+\sin\Theta}{\cos(\alpha-\Theta)+.64\sin(\alpha-\Theta)}$$

or more generally

$$7.)\quad \frac{T}{W} = \frac{W(\mu\cos\Theta+\sin\Theta)}{\cos(\alpha-\Theta)+\mu\sin(\alpha-\Theta)}$$

Figures 28-30 show Equation 7 solved for various values of the independent variables. To use the figure, the mainline angle (α) is not used directly, but rather the height of the carriage and the distance of the turn from the carriage is used. The carriage height is

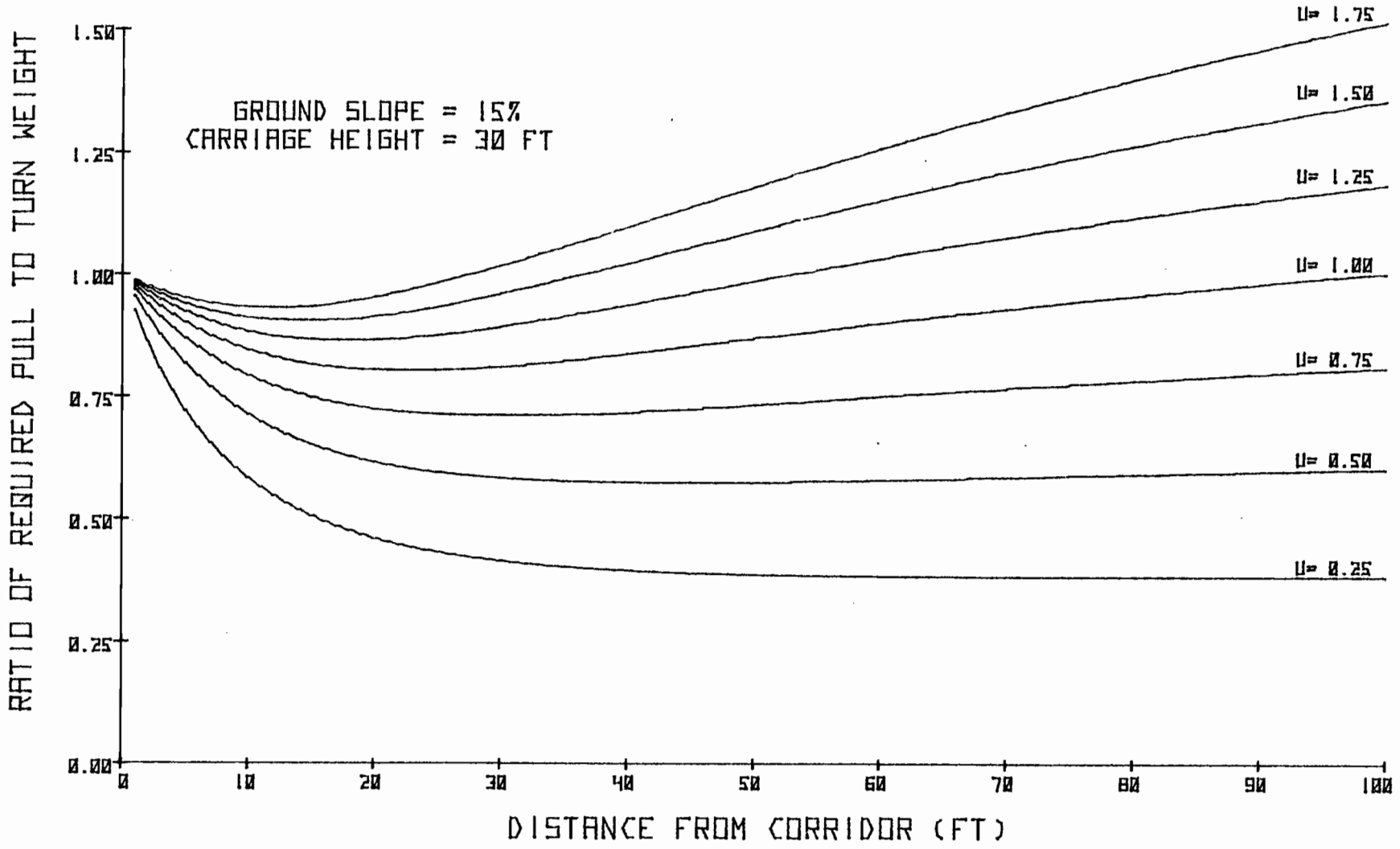

FIGURE 28. RATIO OF REQUIRED PULL TO TURN WEIGHT VERSUS DISTANCE FROM CORRIDOR

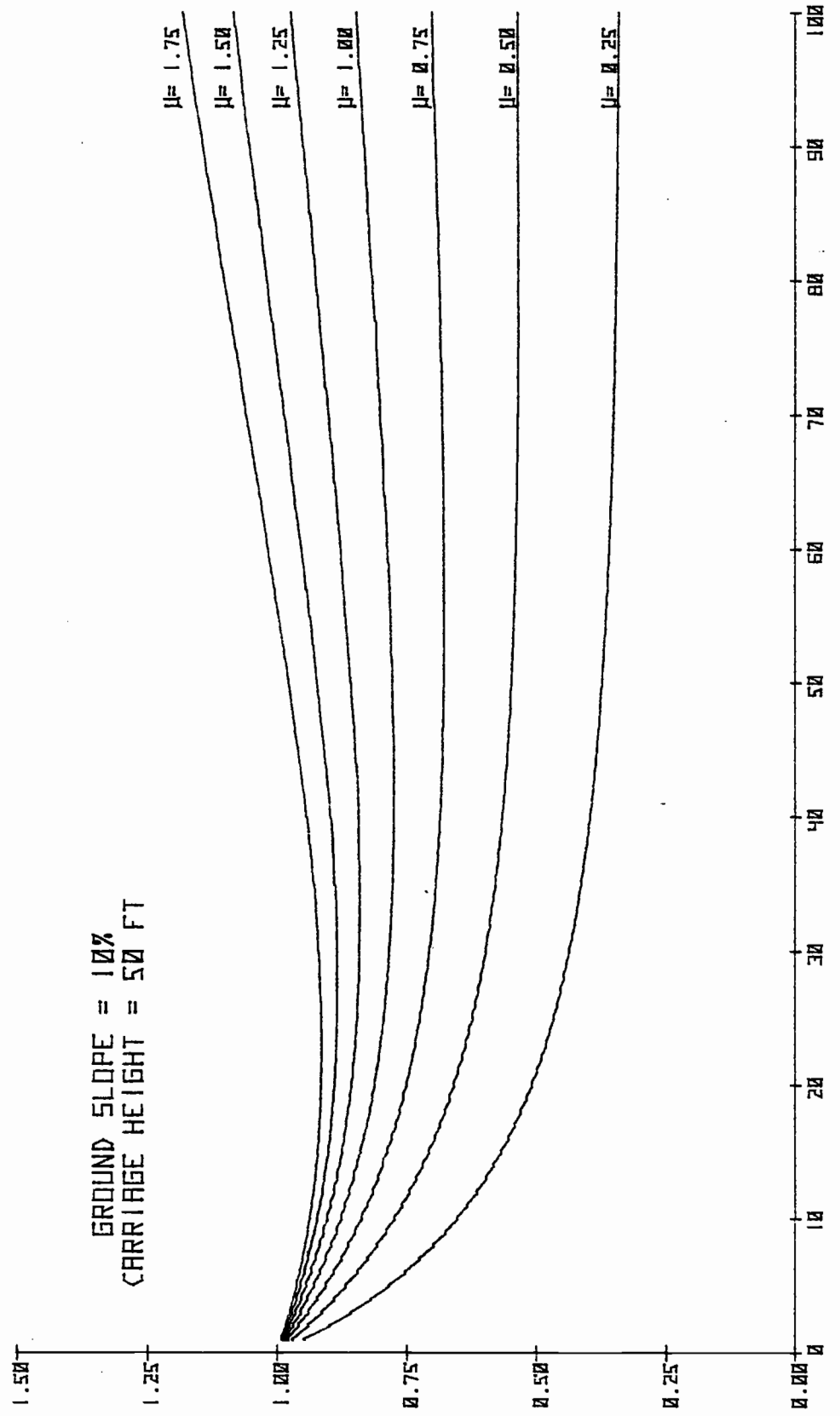

FIGURE 29. RATIO OF REQUIRED PULL TO TURN WEIGHT VERSUS DISTANCE FROM CORRIDOR

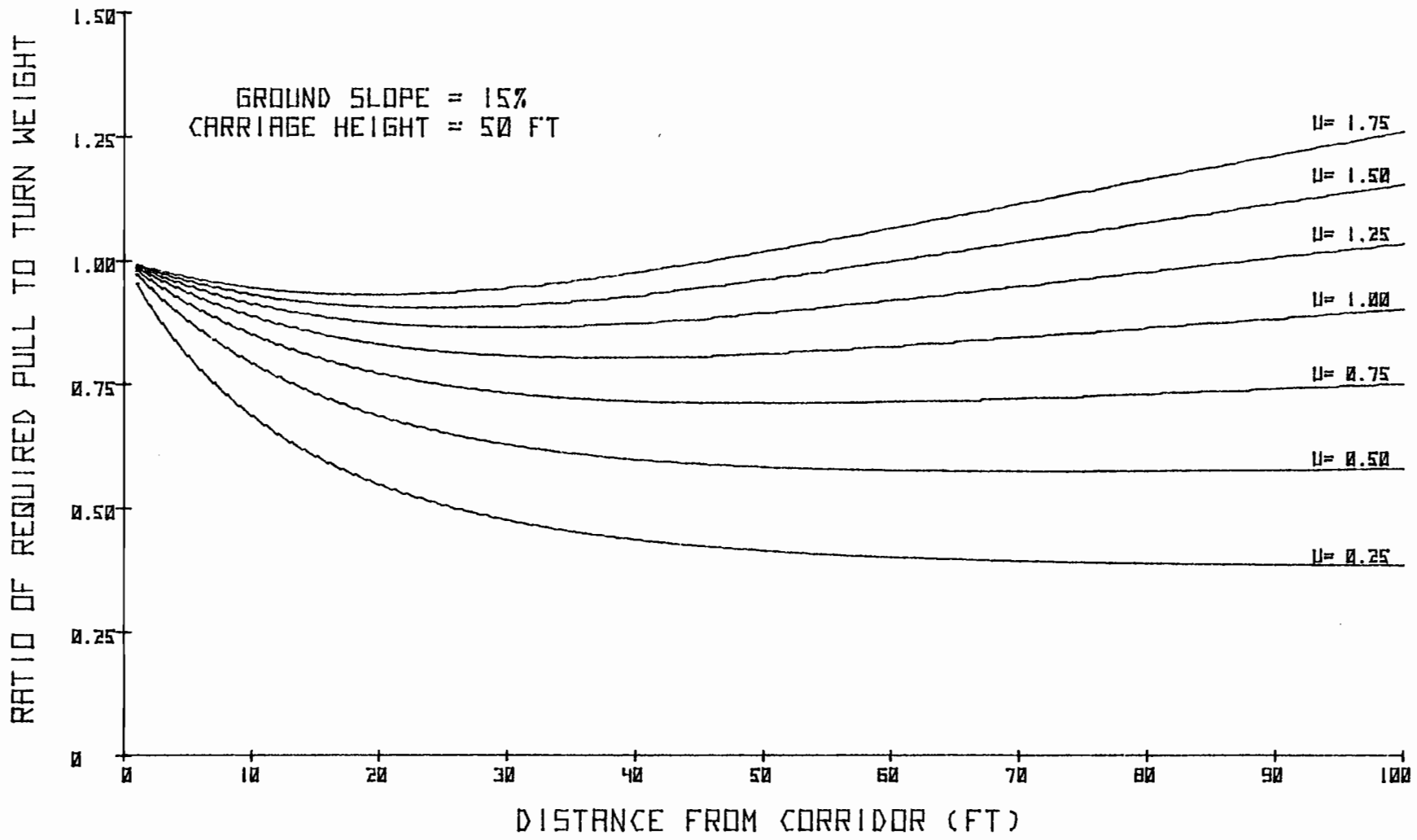

FIGURE 30. RATIO OF REQUIRED PULL TO TURN WEIGHT VERSUS DISTANCE FROM CORRIDOR

the height of the carriage in the corridor and the abcissa is the distance of the turn from the carriage. The ground slope is the slope of the ground in line with the mainline.

SUGGESTIONS FOR FURTHER RESEARCH

Being able to predict the magnitude of the maximum and average forces involved in lateral yarding operations, the resulting cable tensions can be compared to those that result when yarding the turn up the skyline corridor. In this way not only can efficient yarder design be accelerated, but also the adequacy of current methods of payload analysis be checked. It would be well to have the ability to readily analyze a system both ways, laterally and in the corridor, from the standpoint of designing systems. This would allow the possibility of operating the systems in such a way that productivity can be optimized.

It has yet to be determined just how thinning intensity affects the break-out force; whether it is stems left standing or stems cut. It may be that the number of hang-ups encountered are also influenced by thinning intensity. Both of these aspects can be investigated with the available data.

It would be good to conduct another study of this type, under similar conditions, and yet conditions that go beyond those of this study. In this way the effect of steeper slopes, heavier turns and different stand and soil conditions could be investigated. At the same time, since this is the first study of this type, the results of this study could be verified.

REFERENCES

1. Carson, W.W. 1976. Determination of skyline load capability with a programmable pocket calculator. USDA Forest Service Research Paper PNW-205, 11p.

2. Binkley, V.W. and J. Sessions. Chain and Board Handbook-Skyline Tension and Deflection. USDA Forest Service, Pacific Northwest Region. 16-65.

3. Bennett, W.D. 1962. Forces involved in skidding full trees and tree length loads of pulpwood. Tech. Tep. No. 302, Pulp and Paper Research Institute of Canada, 39p.

4. Calvert, W.W. and A.M. Garlicki. 1968. Tree-length orientation and skidding forces. Pulp and Paper Magazine of Canada, June 21, 62-64.

5. Calvert, W.W. and A.M. Garlicki. 1970. Skidding force and power requirements. Dept. of Fisheries and Forestry, Canadian Forest Service Publication No. 1279.

6. Herrick, David E. 1955. Tractive effort required to skid hardwood logs. Forest Products Journal 5(4): :250-255.

7. Kamiizada, M. and M. Shishiuchi. 1962. Tractive resistance of tractor logging. Journal of Japanese Forestry Socienty, 44-30, 4-308.

8. Wieskik, Jerzy. 1962. Resistance occurring during suspended skidding. Translation, Canadian Dept. of Forestry No. 172. 4p. Translated from Sylwan, 106(4):37-42.

9. Gibson, Harry G. 1969. Wheeled skidder performance on sloping terrain. Agricultural Engineering 50(3):152-151.

10. Carson, Ward W. and Charles N. Mann. 1970. A technique for the solution of skyline caternary equations. USDA Forest Service Research Paper PNW-110, 18p.

11. Caterpillar Tractor Co. 1968. Caterpillar performance handbook. Cat, 33-26.

12. Henshaw, John R. 1977. A study of the coefficient of drag resistance in yarding logs. Master's thesis. Oregon State University. 66-69.

APPENDIX A

SOILS DESCRIPTION

SOILS DESCRIPTION

UNIFIED SOIL CLASSIFICATION: GC

NAME: clay with rock fragments ("gravelly clay loam")

COLOR: reddish brown

ORIGIN: slope deposit

LOCATION: mid-slope

ESTIMATED THICKNESS: estimated - 60 inches+

NATURAL MOISTURE: moist (leaves moisture on hands)

PLASTICITY: APL (above plastic limit)

CONSISTENCY: medium (undisturbed) to stiff (heavy disturbance)

PERMEABILITY: slow to practically impermeable based on ring infiltrometer

DRY STRENGTH: medium (can powder with difficulty)

DILATANCY: (ability to change volume by vibration) slow reaction

TOUGHNESS: low (holds together at plastic limit)

APPENDIX B

TOPOGRAPHY

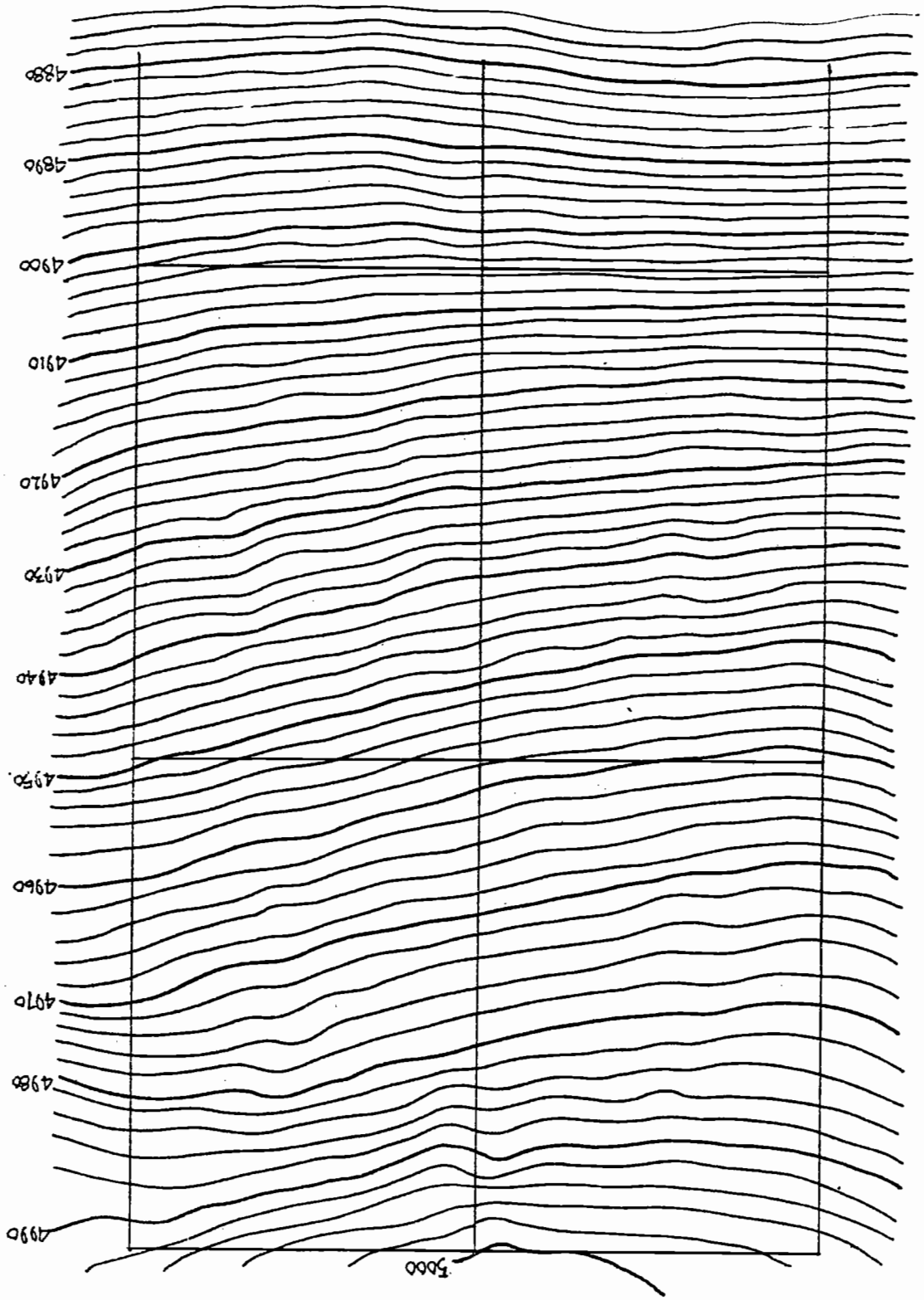

Figure 31. Topography for units 1-4. Scale 1" = 50', 2' contour interval

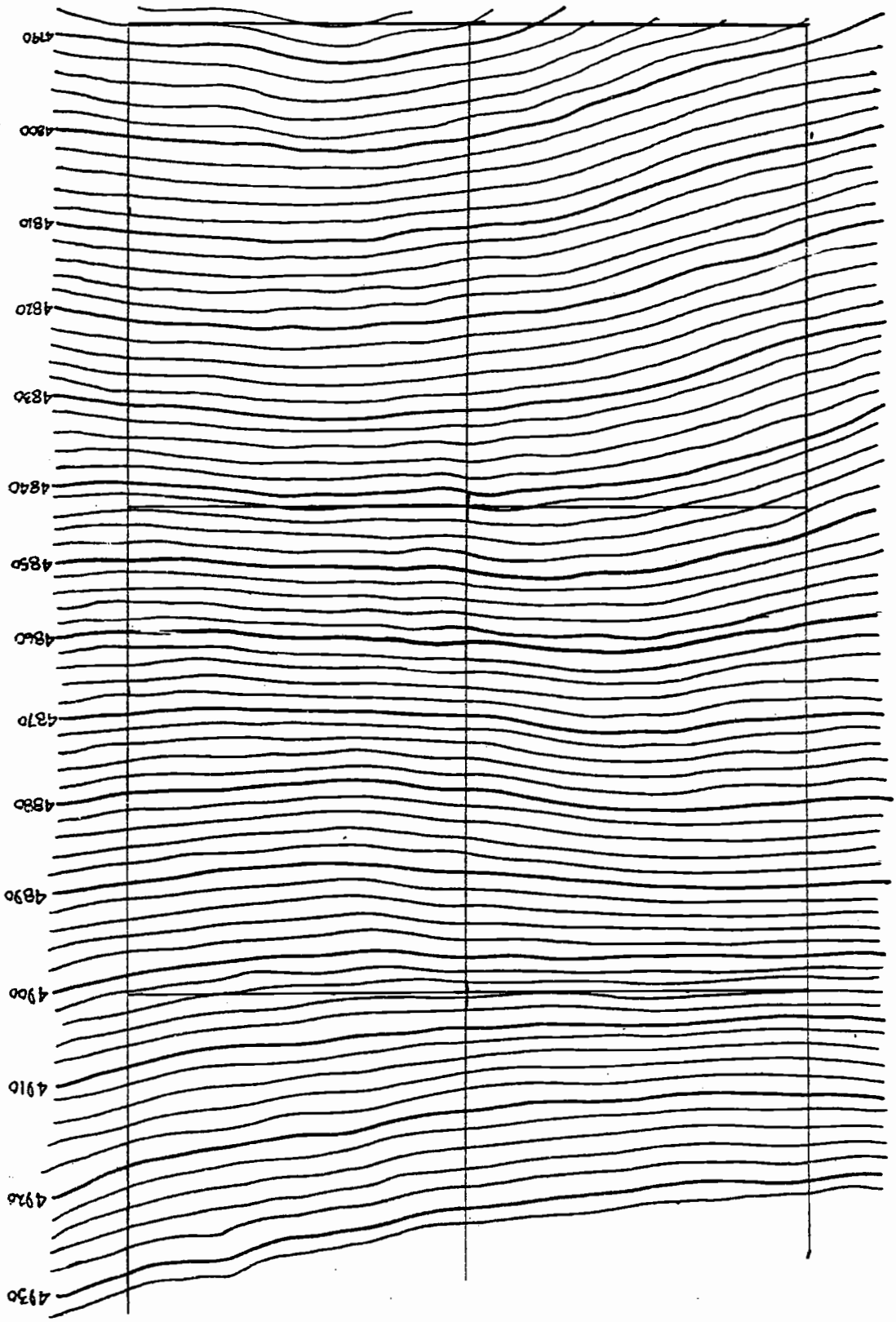

Figure 32. Topography for units 5-8. Scale 1" = 50', 2' contour interval

APPENDIX C

TREE LOCATIONS

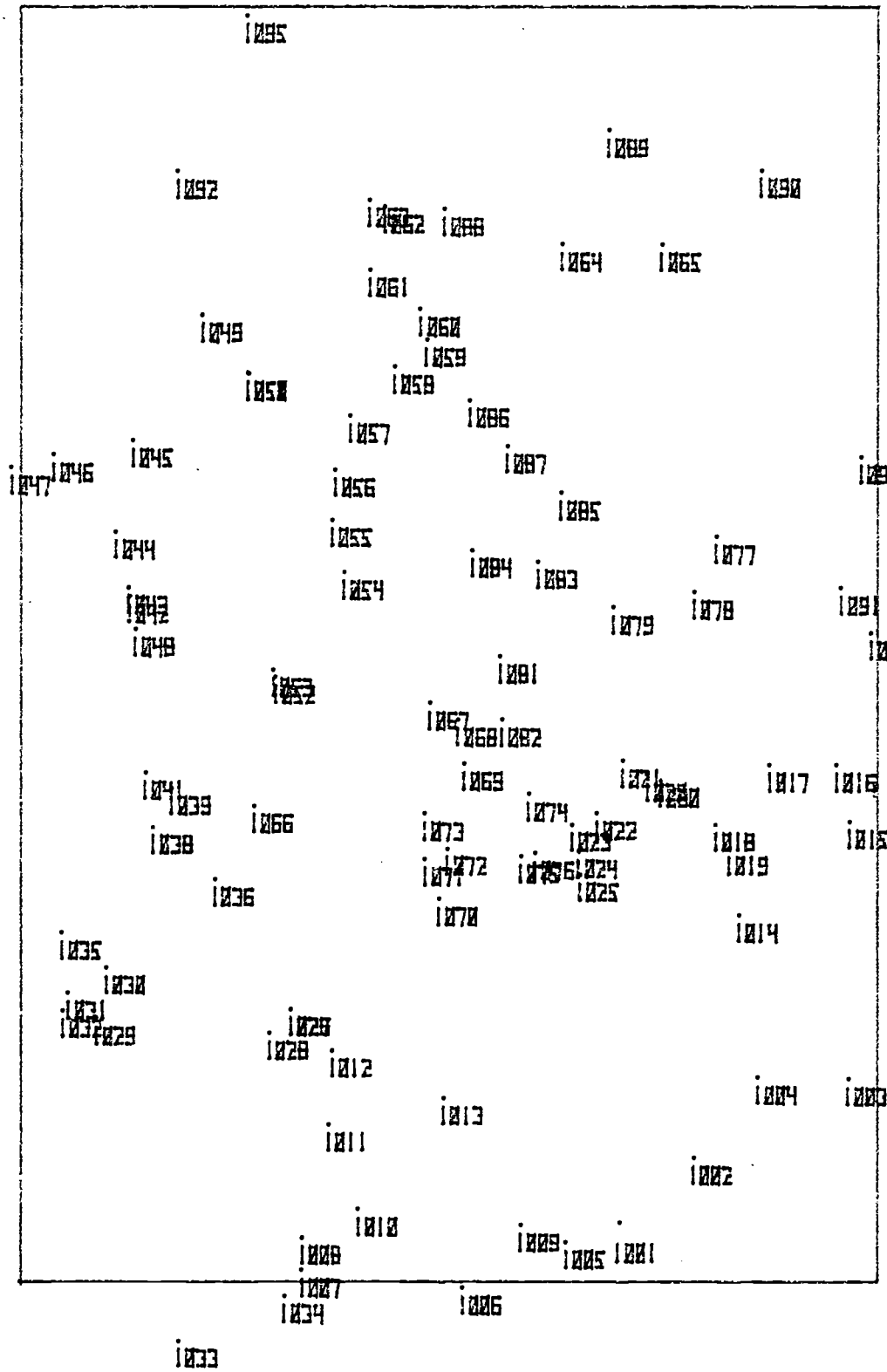

FIGURE 33. TREE LOCATION-UNIT #1.

TREE NO	X COORD	Y COORD	Z COORD
1001.0	7.1	36.1	4995.9
1002.0	14.7	27.5	4993.8
1003.0	24.0	9.8	4995.2
1004.0	24.2	20.0	4990.5
1005.0	4.7	42.4	4995.4
1006.0	-0.5	54.5	4996.2
1007.0	1.4	73.2	4993.2
1008.0	5.2	73.2	4991.9
1009.0	6.7	47.7	4994.5
1010.0	8.6	66.6	4991.5
1011.0	18.6	79.1	4988.3
1012.0	27.4	69.6	4988.2
1013.0	21.6	56.7	4988.9
1014.0	43.3	22.2	4983.8
1015.0	54.3	9.3	4982.0
1016.0	61.0	10.8	4979.5
1017.0	61.0	18.6	4979.2
1018.0	74.0	25.0	4980.0
1019.0	51.2	23.4	4981.4
1020.0	59.3	32.3	4978.6
1021.0	61.5	35.9	4977.9
1022.0	55.4	38.6	4979.3
1023.0	54.0	41.8	4979.1
1024.0	50.9	41.0	4980.4
1025.0	48.1	40.8	4980.7
1026.0	32.3	74.5	4985.6
1027.0	32.5	74.0	4985.6
1028.0	29.5	77.0	4985.7
1029.0	31.2	97.2	4985.6
1030.0	37.2	96.0	4984.3
1031.0	34.2	100.5	4985.5
1032.0	32.1	101.1	4985.9
1033.0	-5.9	87.6	4993.4
1034.0	-1.6	75.2	4993.0
1035.0	41.3	101.2	4983.1

Table VIII. Tree coordinates for unit 1.

1036.0	47.6	83.4	4969.2
1038.0	53.7	90.8	4977.7
1039.0	58.3	88.4	4975.9
1041.0	69.1	94.6	4975.4
1042.0	80.9	93.3	4968.7
1043.0	81.9	93.4	4968.2
1044.0	88.5	94.9	4968.9
1045.0	99.2	92.8	4963.7
1046.0	97.5	102.2	4963.4
1047.0	96.0	107.1	4963.5
1048.0	77.8	92.6	4969.2
1049.0	113.9	84.7	4959.6
1050.0	107.1	79.5	4962.7
1051.0	107.1	79.5	4962.7
1052.0	71.4	76.2	4972.2
1053.0	72.2	76.6	4971.9
1054.0	83.7	68.3	4970.1
1055.0	89.9	69.6	4968.1
1056.0	95.7	69.3	4966.9
1057.0	102.1	67.5	4965.3
1058.0	107.8	62.4	4963.9
1059.0	111.0	58.7	4963.5
1060.0	114.6	59.3	4962.0
1061.0	119.3	58.3	4961.1
1062.0	125.7	63.5	4958.4
1063.0	127.5	63.3	4958.5
1064.0	122.3	42.9	4959.6
1065.0	122.2	31.9	4962.3
1066.0	56.2	78.3	4977.0
1067.0	68.3	58.3	4974.6
1068.0	56.4	55.0	4974.9
1069.0	61.2	54.7	4976.3
1070.0	45.3	57.2	4966.3

Table VIII. (cont)

1071.0	56.0	56.2	4973.4
1072.0	51.2	56.2	4979.1
1073.0	55.1	58.9	4977.6
1074.0	57.6	46.8	4976.6
1075.0	50.3	47.7	4979.8
1076.0	50.7	46.0	4979.8
1077.0	67.9	24.1	4972.2
1078.0	81.4	27.5	4973.1
1079.0	79.6	36.8	4973.4
1080.0	69.2	31.4	4979.1
1081.0	73.9	50.0	4973.0
1082.0	66.4	43.9	4975.4
1083.0	65.0	45.6	4971.7
1084.0	86.4	53.3	4970.0
1085.0	93.1	42.0	4969.2
1086.0	104.0	53.5	4966.0
1087.0	98.6	49.3	4967.3
1088.0	126.1	36.6	4959.5
1089.0	125.6	37.4	4958.6
1090.0	130.9	19.6	4961.0
1091.0	81.9	10.2	4974.6
1092.0	130.7	37.7	4958.0
1093.0	97.3	8.0	4970.8
1094.0	76.6	6.7	4976.0
1095.0	142.0	73.6	4951.2
2.0	11.9	0.8	4996.5
4.0	57.5	2.0	4980.9
7.0	110.7	1.4	4965.2
9.0	96.6	3.7	4971.4
10.0	83.8	1.6	4972.1

Table VIII. (cont)

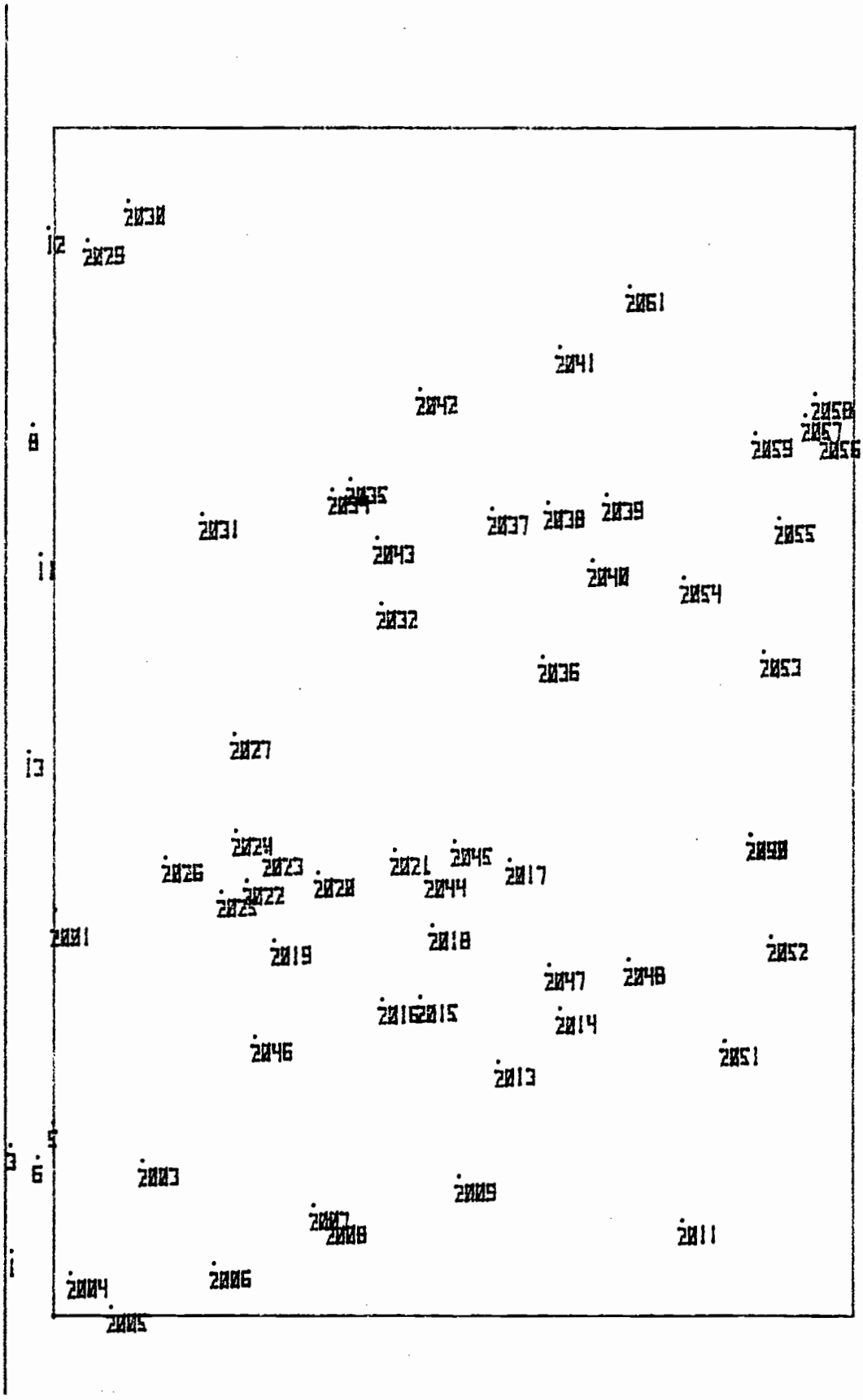

FIGURE 34. TREE LOCATION-UNIT #2.

TREE NO	XCOORD	YCOORD	Z COORD
2001.0	5.0	-6.4	4967.1
2003.0	19.6	-17.1	4994.2
2004.0	5.5	-8.2	4999.0
2005.0	1.4	-12.8	5000.0
2006.0	6.6	-26.1	4998.0
2007.0	14.0	-38.3	4995.2
2008.0	12.1	-40.4	4996.4
2009.0	17.7	-56.7	4994.3
2011.0	12.2	-64.6	4994.9
2013.0	22.7	-61.5	4990.0
2014.0	39.0	-58.2	4987.4
2015.0	40.4	-52.0	4988.0
2016.0	40.2	-47.1	4988.0
2017.0	57.0	-63.0	4983.5
2018.0	45.5	-53.5	4984.7
2019.0	47.4	-53.5	4985.0
2020.0	56.2	-39.1	4982.9
2021.0	54.0	-48.7	4982.7
2022.0	60.2	-50.2	4982.5
2023.0	58.9	-32.6	4982.4
2024.0	61.5	-29.7	4981.7
2025.0	72.7	-26.9	4985.1
2026.0	58.1	-28.0	4982.0
2027.0	73.1	-28.5	4978.7
2028.0	136.3	-19.1	4962.0
2030.0	140.8	-19.3	4960.3
2031.0	131.5	-24.6	4971.1
2032.0	98.2	-48.8	4975.6
2034.0	104.6	-40.8	4971.3
2035.0	105.8	-43.1	4970.4

Table IX. Tree coordinates for unit 2.

2036.0	83.7	-67.1	4977.2
2037.0	102.1	-60.7	4971.5
2038.0	102.8	-57.7	4973.0
2039.0	103.9	-59.1	4972.7
2040.0	95.6	-73.2	4974.3
2041.0	122.4	-66.2	4967.9
2042.0	117.2	-61.6	4969.0
2043.0	98.4	-46.5	4972.9
2044.0	56.2	-53.9	4983.4
2045.0	50.2	-56.1	4982.5
2046.0	35.4	-31.2	4988.2
2047.0	44.5	-67.9	4985.4
2048.0	45.1	-77.8	4986.1
2049.0	61.0	-93.1	4982.5
2050.0	61.0	-93.1	4982.8
2051.0	24.9	-85.5	4986.1
2052.0	48.1	-95.8	4984.4
2053.0	54.1	-54.8	4977.6
2054.0	93.4	-84.8	4975.6
2055.0	131.0	-56.6	4973.4
2056.0	111.5	-102.2	4970.7
2057.0	113.9	-99.3	4969.5
2056.0	116.8	-101.2	4965.1
2059.0	111.7	-93.7	4970.5
2061.0	130.1	-77.9	4966.1
1.0	8.2	-0.8	4998.1
3.0	21.6	-8.7	4992.1
5.0	24.7	-5.6	4991.5
6.0	20.1	-3.9	4992.5
8.0	112.7	-3.4	4957.1
11.0	96.3	-4.3	4971.0
12.0	137.4	-5.4	4960.9
13.0	71.5	-2.7	4977.8

Table IX. (cont)

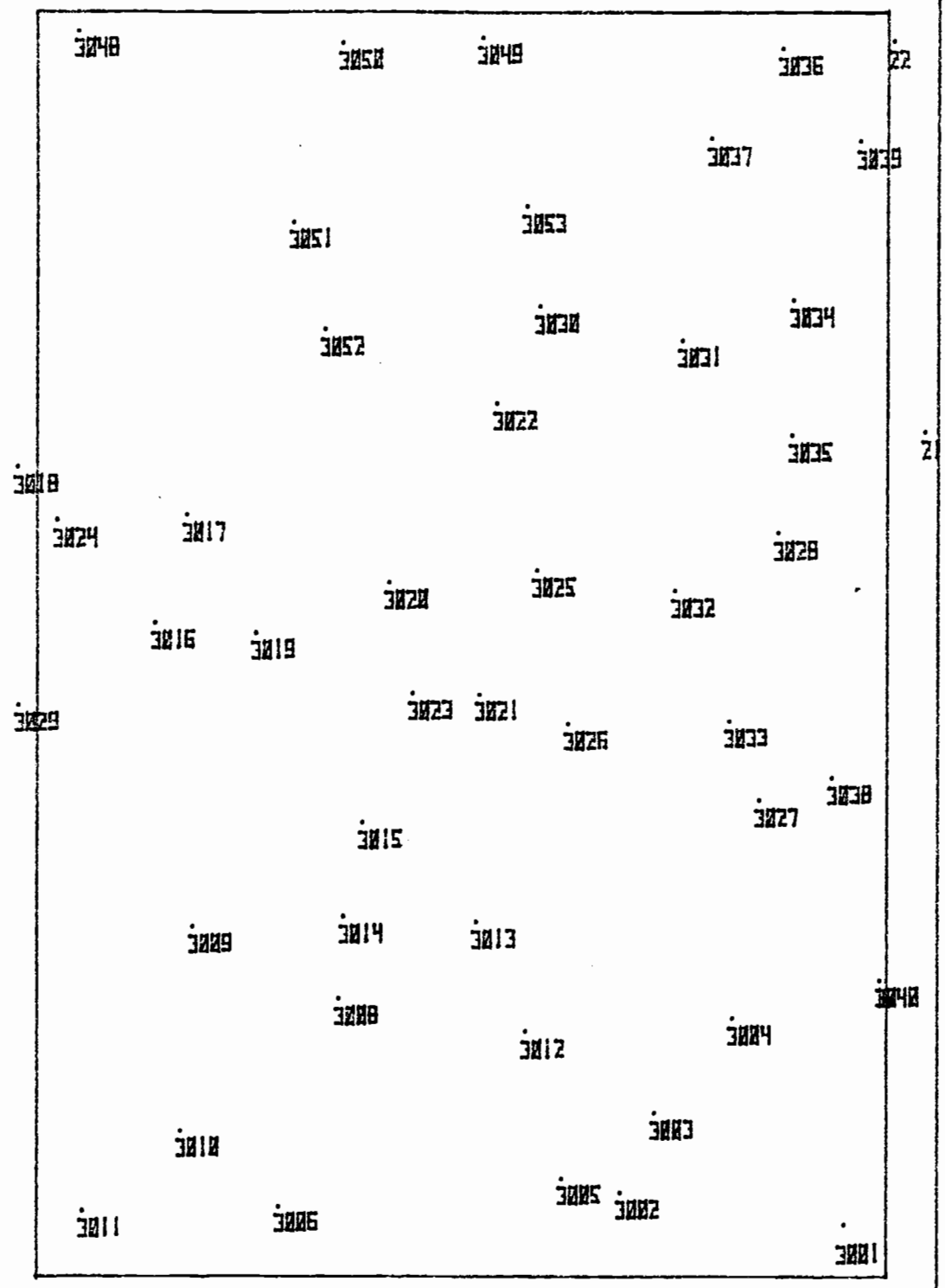

FIGURE 35. TREE LOCATION-UNIT #3.

TREE NO	XCOORD	YCOORD	Z COORD
3001. 0	172. 2	11. 0	4954. 9
3002. 0	160. 0	37. 3	4951. 3
3003. 0	169. 3	33. 2	4948. 5
3004. 0	180. 0	24. 2	4945. 4
3005. 0	161. 7	44. 2	4950. 1
3006. 0	158. 5	77. 5	4948. 0
3008. 0	182. 1	72. 4	4944. 4
3009. 0	191. 7	87. 7	4937. 8
3010. 0	167. 4	98. 2	4944. 1
3011. 0	157. 6	106. 6	4946. 2
3012. 0	179. 1	46. 5	4944. 7
3013. 0	192. 3	54. 3	4938. 5
3014. 0	182. 0	69. 0	4939. 1
3015. 0	204. 0	67. 7	4933. 3
3016. 0	227. 7	62. 1	4926. 2
3017. 0	210. 6	86. 4	4932. 7
3018. 0	246. 2	196. 2	4918. 7
3019. 0	226. 5	88. 3	4927. 7
3020. 0	232. 8	64. 1	4929. 5
3021. 0	219. 3	53. 9	4931. 6
3022. 0	253. 7	51. 4	4920. 3
3023. 0	240. 0	41. 8	4928. 7
3024. 0	239. 0	103. 6	4920. 1
3025. 0	234. 0	47. 3	4927. 1
3026. 0	214. 7	43. 6	4933. 2
3027. 0	205. 7	21. 0	4938. 2
3028. 0	233. 4	18. 3	4927. 7
3029. 0	218. 0	100. 2	4927. 5
3030. 0	265. 2	47. 0	4917. 3
3031. 0	261. 2	30. 1	4918. 6
3032. 0	234. 0	30. 0	4929. 1
3033. 0	215. 1	24. 5	4934. 8
3034. 0	266. 1	16. 9	4918. 2
3035. 0	250. 0	17. 1	4924. 5
3036. 0	286. 7	18. 4	4905. 9
3037. 0	283. 1	25. 7	4910. 5
3038. 0	248. 4	12. 9	4922. 7
3039. 0	284. 8	5. 1	4911. 6
3040. 0	195. 3	5. 8	4945. 7
3046. 0	227. 4	181. 2	4902. 1
3049. 0	257. 0	52. 7	4905. 2
3050. 0	296. 3	70. 0	4904. 8
3051. 0	275. 2	75. 9	4912. 5
3052. 0	262. 5	72. 1	4916. 4
3053. 0	277. 1	43. 5	4912. 4
15. 0	196. 4	6. 9	4943. 7
21. 0	250. 4	1. 5	4924. 5
22. 0	296. 6	5. 4	4906. 4

Table X. Tree coordinates for unit 3.

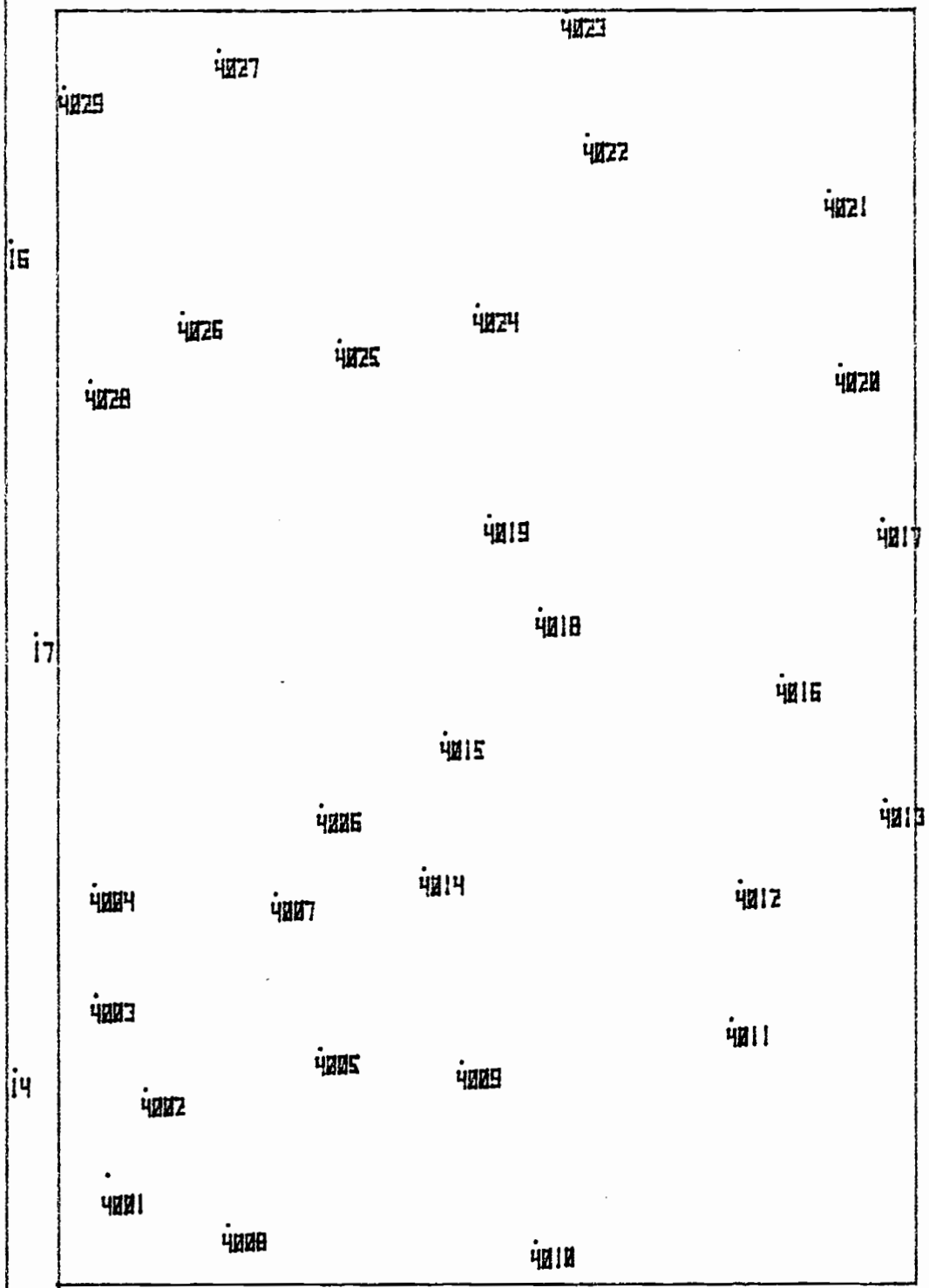

FIGURE 36. TREE LOCATIONS-UNIT #4.

TREE NO	XCOORD	YCOORD	Z COORD
4001.0	163.9	-11.9	4954.1
4002.0	173.0	-15.2	4950.9
4003.0	184.2	-12.3	4947.6
4004.0	197.2	-10.3	4943.7
4005.0	178.0	-36.6	4951.1
4006.0	206.5	-36.9	4941.4
4007.0	196.1	-31.4	4944.7
4008.0	157.0	-25.7	4956.4
4009.0	174.2	-52.1	4951.0
4010.0	153.0	-61.5	4958.5
4011.0	161.3	-84.5	4951.5
4012.0	197.5	-83.6	4945.4
4013.0	207.1	-102.4	4943.3
4014.0	199.1	-48.8	4944.5
4015.0	245.1	-51.2	4939.3
4016.0	221.9	-30.4	4937.9
4017.0	240.1	-102.2	4931.7
4018.0	223.7	-52.3	4934.0
4019.0	240.7	-56.3	4930.5
4020.0	258.4	-97.3	4923.9
4021.0	279.9	-96.8	4916.9
4022.0	295.4	-57.9	4912.8
4023.0	299.9	-65.4	4905.2
4024.0	268.8	-33.1	4921.2
4025.0	261.4	-39.0	4922.1
4026.0	264.6	-20.7	4920.5
4027.0	245.3	-25.0	4907.3
4028.0	256.5	-9.8	4902.9
4029.0	291.0	-5.7	4906.3
14.0	175.4	-0.8	4949.7
16.0	273.1	-3.7	4917.2
17.0	226.8	-3.5	4933.0

Figure XI. Tree coordinates for unit 4.

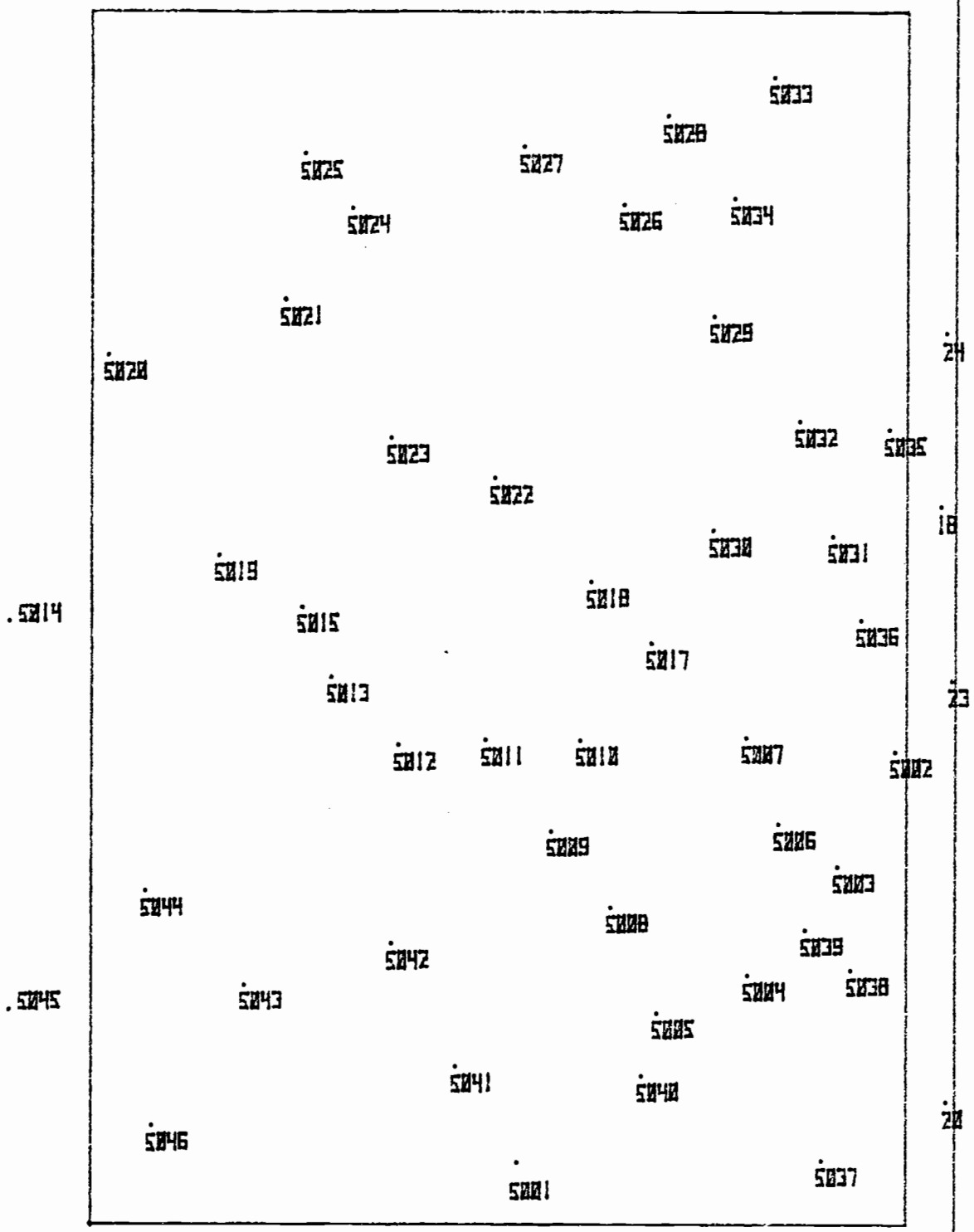

FIGURE 37. TREE LOCATION-UNIT #5.

TREE NO	X COORD	Y COORD	Z COORD
5001.0	307.7	53.6	4901.5
5002.0	356.7	7.4	4861.5
5003.0	344.4	14.5	4887.7
5004.0	331.0	28.3	4893.3
5005.0	325.3	36.5	4893.2
5006.0	343.7	81.0	4856.2
5007.0	360.4	25.7	4862.0
5008.0	339.4	42.3	4890.2
5009.0	348.9	49.6	4886.1
5010.0	360.1	46.0	4881.2
5011.0	360.1	57.5	4881.2
5012.0	359.1	68.9	4881.2
5013.0	367.9	76.5	4877.5
5014.0	374.7	116.7	4873.2
5015.0	370.6	88.2	4875.5
5017.0	372.1	37.4	4875.2
5018.0	379.7	44.8	4873.1
5019.0	382.9	90.9	4871.4
5020.0	407.7	103.9	4861.1
5021.0	414.5	82.3	4858.4
5022.0	392.4	56.5	4867.0
5023.0	397.5	58.2	4866.1
5024.0	425.8	74.1	4853.2
5025.0	420.0	79.0	4856.6
5026.0	426.3	40.9	4852.5
5027.0	433.4	53.8	4849.3
5028.0	437.1	96.5	4847.4
5029.0	412.5	28.7	4858.4
5030.0	386.1	29.7	4870.2
5031.0	385.4	15.1	4870.1
5032.0	399.5	19.2	4864.2
5033.0	442.0	22.8	4845.1
5034.0	427.1	27.2	4852.2
5035.0	398.5	8.2	4864.1
5036.0	375.0	11.4	4874.6
5037.0	366.9	16.6	4902.1
5038.0	331.6	12.9	4892.0
5039.0	336.6	18.4	4892.0
5040.0	340.0	58.6	4887.7
5041.0	319.6	61.2	4896.7
5042.0	334.9	69.2	4891.0
5043.0	329.0	87.1	4891.6
5044.0	341.4	96.3	4887.0
5045.0	325.6	113.4	4891.1
5046.0	319.0	98.5	4897.6
18.0	389.0	1.9	4856.5
20.0	315.2	1.0	4898.3
23.0	357.6	0.4	4877.8
24.0	410.4	1.1	4852.8

Figure XII. Tree Coordinates for unit 5.

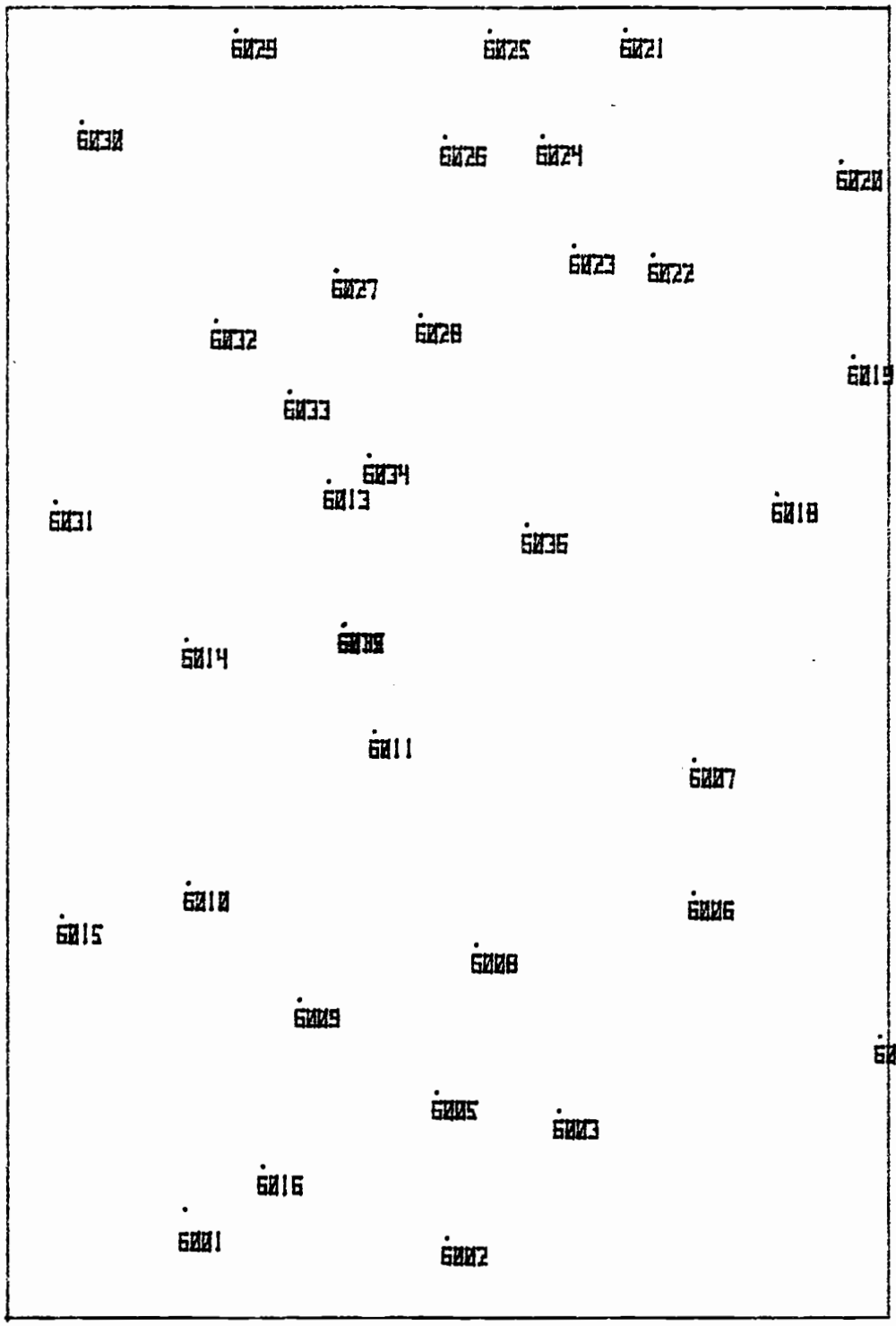

FIGURE 38. TREE LOCATION-UNIT #6.

TREE NO	XCOORD	YCOORD	Z COORD
6001.0	312.8	-26.3	4859.2
6002.0	309.2	-56.0	4900.9
6003.0	323.8	-68.6	4894.1
6004.0	312.4	-105.0	4890.8
6005.0	326.0	-54.9	4893.0
6006.0	348.9	-83.9	4883.5
6007.0	364.1	-84.1	4877.0
6008.0	342.9	-59.3	4885.5
6009.0	336.3	-79.2	4888.8
6010.0	350.0	-26.6	4861.4
6011.0	367.4	-47.7	4875.4
6012.0	379.5	-44.1	4870.5
6013.0	356.8	-42.8	4863.9
6014.0	377.9	-26.4	4871.3
6015.0	346.2	-12.2	4885.8
6016.0	317.4	-35.0	4897.1
6017.0	370.5	-109.3	4876.1
6018.0	394.5	-95.3	4866.7
6019.0	418.2	-101.9	4862.4
6020.0	432.5	-100.7	4854.6
6021.0	447.4	-76.1	4846.5
6022.0	421.9	-79.5	4858.9
6023.0	422.9	-70.3	4855.3
6024.0	435.4	-66.6	4850.1
6025.0	447.4	-60.7	4845.0
6026.0	435.2	-55.8	4849.0
6027.0	420.1	-43.5	4854.0
6028.0	415.0	-55.8	4857.1
6029.0	447.4	-32.1	4843.1
6030.0	437.0	-14.5	4846.2
6031.0	393.5	-11.3	4865.9
6032.0	414.4	-29.7	4856.2
6033.0	406.3	-38.1	4859.7
6034.0	398.9	-47.0	4863.0
6035.0	379.7	-44.2	4870.5
6036.0	391.0	-65.0	4867.1
19.0	363.3	-2.0	4889.0

Figure XIII. Tree coordinates for unit 6.

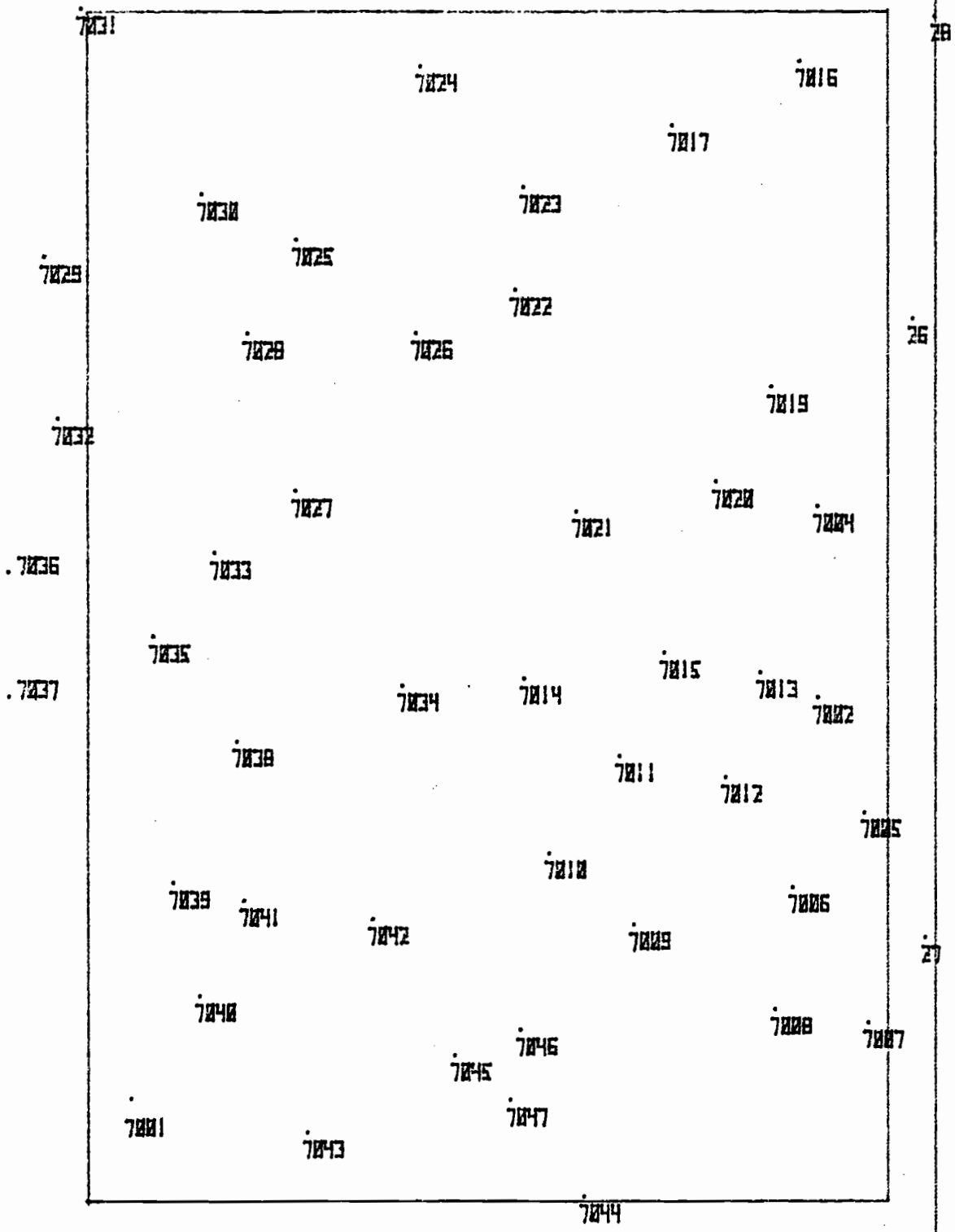

FIGURE 39. TREE LOCATION-UNIT#7.

TREE NO	XCOORD	YCOORD	Z COORD
7001.0	463.0	100.6	4837.7
7002.0	512.7	14.9	4817.2
7004.0	537.8	14.6	4809.2
7005.0	439.2	8.9	4822.6
7006.0	489.8	17.3	4825.7
7007.0	472.6	6.5	4812.6
7008.0	474.3	20.2	4831.6
7009.0	469.0	37.0	4826.6
7010.0	494.1	43.4	4823.4
7011.0	506.3	39.6	4819.3
7012.0	503.6	64.4	4829.0
7013.0	516.8	21.3	4816.2
7014.0	516.1	51.5	4816.3
7015.0	519.3	34.0	4814.9
7016.0	593.7	18.9	4788.9
7017.0	585.7	32.9	4799.6
7018.0	582.9	20.6	4802.6
7020.0	540.9	27.4	4806.8
7021.0	537.2	44.9	4808.0
7022.0	565.1	51.7	4797.0
7023.0	578.0	51.3	4793.6
7024.0	593.1	64.4	4789.8
7025.0	571.1	73.9	4796.6
7026.0	589.6	73.0	4800.3
7027.0	529.8	52.0	4807.6
7028.0	559.5	82.1	4800.9
7029.0	569.3	111.4	4793.1
7030.0	577.1	91.8	4795.1
7031.0	599.4	106.0	4790.4
7032.0	548.9	109.9	4805.6
7033.0	531.9	90.2	4810.9
7034.0	513.2	86.7	4815.0
7035.0	521.4	97.9	4815.0
7036.0	529.6	122.9	4813.6
7037.0	513.9	124.0	4819.0
7038.0	506.2	87.4	4819.1
7039.0	490.1	55.4	4826.2
7040.0	475.0	52.1	4832.2
7041.0	488.1	86.0	4826.0
7042.0	485.7	70.5	4827.8
7043.1	459.7	79.6	4838.9
7044.0	450.6	44.1	4841.3
7045.0	468.5	69.1	4833.9
7046.0	471.7	82.0	4832.6
7047.0	462.0	53.1	4835.9
26.0	561.5	2.9	4800.7
27.0	493.4	1.2	4823.0
28.0	599.4	0.0	4787.8

Table XIV. Tree coordinates for unit 7.

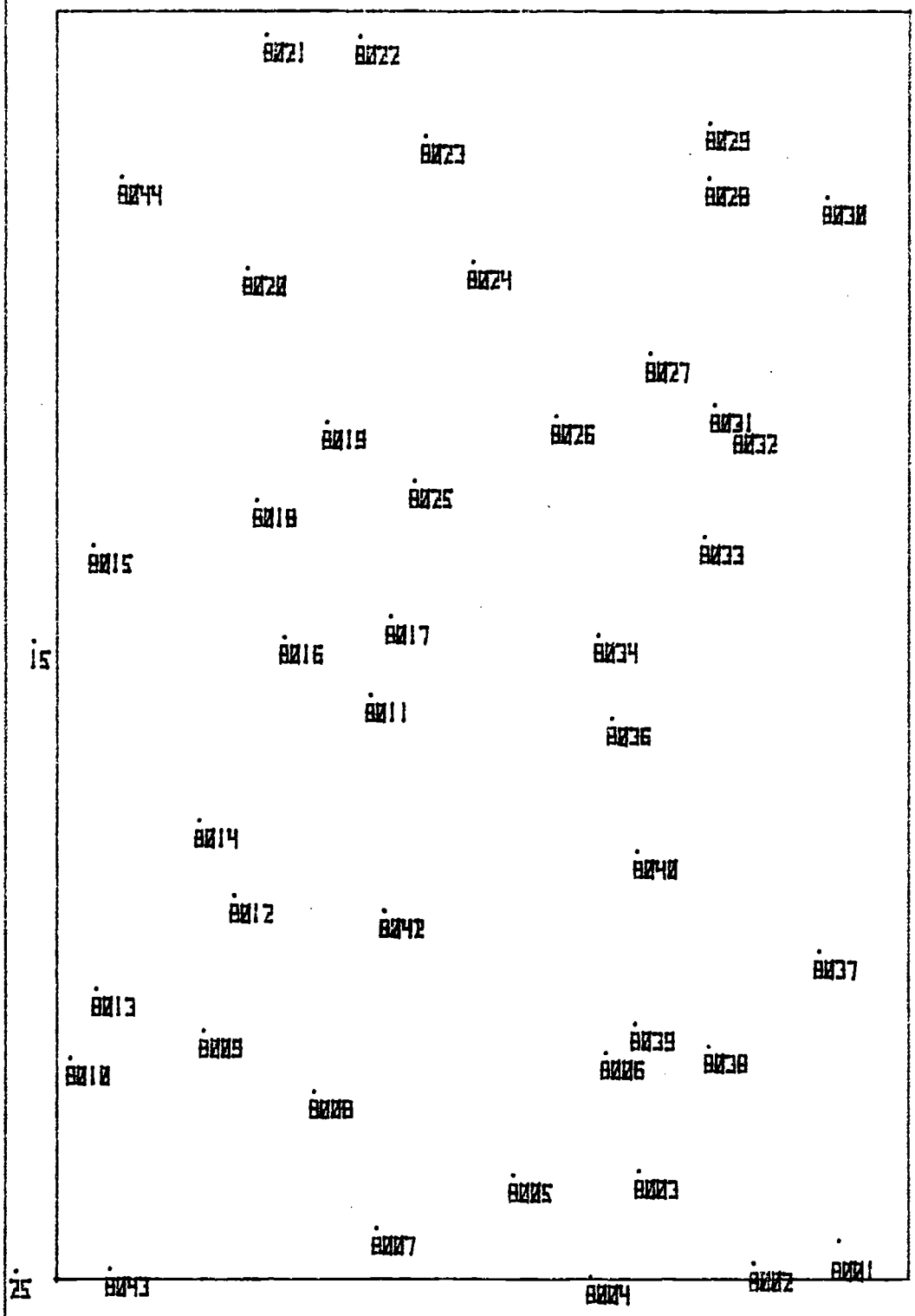

FIGURE 40. TREE LOCATION-UNIT #8.

TREE NO	XCOORD	YCOORD	Z COORD
8001.0	454.7	-97.9	4847.5
8002.0	451.8	-68.0	4846.6
8003.0	462.8	-74.4	4841.3
8004.0	456.3	-68.7	4844.8
8005.0	462.4	-59.6	4839.4
8006.0	476.9	-79.4	4835.9
8007.0	455.1	-47.8	4840.7
8008.0	472.3	-36.3	4834.1
8009.0	479.5	-23.2	4830.9
8010.0	476.0	-7.9	4821.8
8011.0	519.3	-42.3	4819.1
8012.0	495.6	-26.9	4825.4
8013.0	484.5	-10.6	4826.0
8014.0	504.4	-22.7	4822.3
8015.0	537.0	-18.3	4810.2
8016.0	525.2	-32.7	4815.6
8017.0	528.6	-45.2	4816.4
8018.0	542.4	-26.5	4809.7
8019.0	551.5	-27.8	4807.6
8020.0	569.8	-28.4	4801.0
8021.0	597.2	-30.8	4792.1
8022.0	596.9	-41.5	4794.0
8023.0	585.1	-49.3	4798.6
8024.0	570.3	-54.8	4803.9
8025.0	544.6	-47.9	4811.4
8026.0	552.3	-54.5	4810.9
8027.0	559.7	-75.7	4806.7
8028.0	548.4	-68.5	4803.1
8029.0	526.9	-82.7	4801.3
8030.0	578.2	-96.4	4805.1
8031.0	551.6	-93.0	4811.6
8032.0	551.2	-85.5	4812.9
8033.0	538.0	-82.0	4817.2
8034.0	526.5	-69.6	4819.4
8036.0	516.5	-71.2	4823.0
8037.0	489.0	-95.4	4834.8
8038.0	477.2	-82.5	4837.5
8039.0	490.4	-73.2	4835.2
8040.0	500.8	-74.3	4828.9
8041.0	493.8	-44.0	4827.5
8042.0	493.8	-44.6	4827.5
8043.0	481.3	-12.3	4841.2
8044.0	500.6	-13.7	4795.2
15.0	525.6	-3.3	4814.5
25.0	451.0	-1.1	4846.5

Table XV. Tree coordinates for unit 8.

APPENDIX D

TURN LOCATIONS AND LOG TO MAINLINE LEAD ANGLES

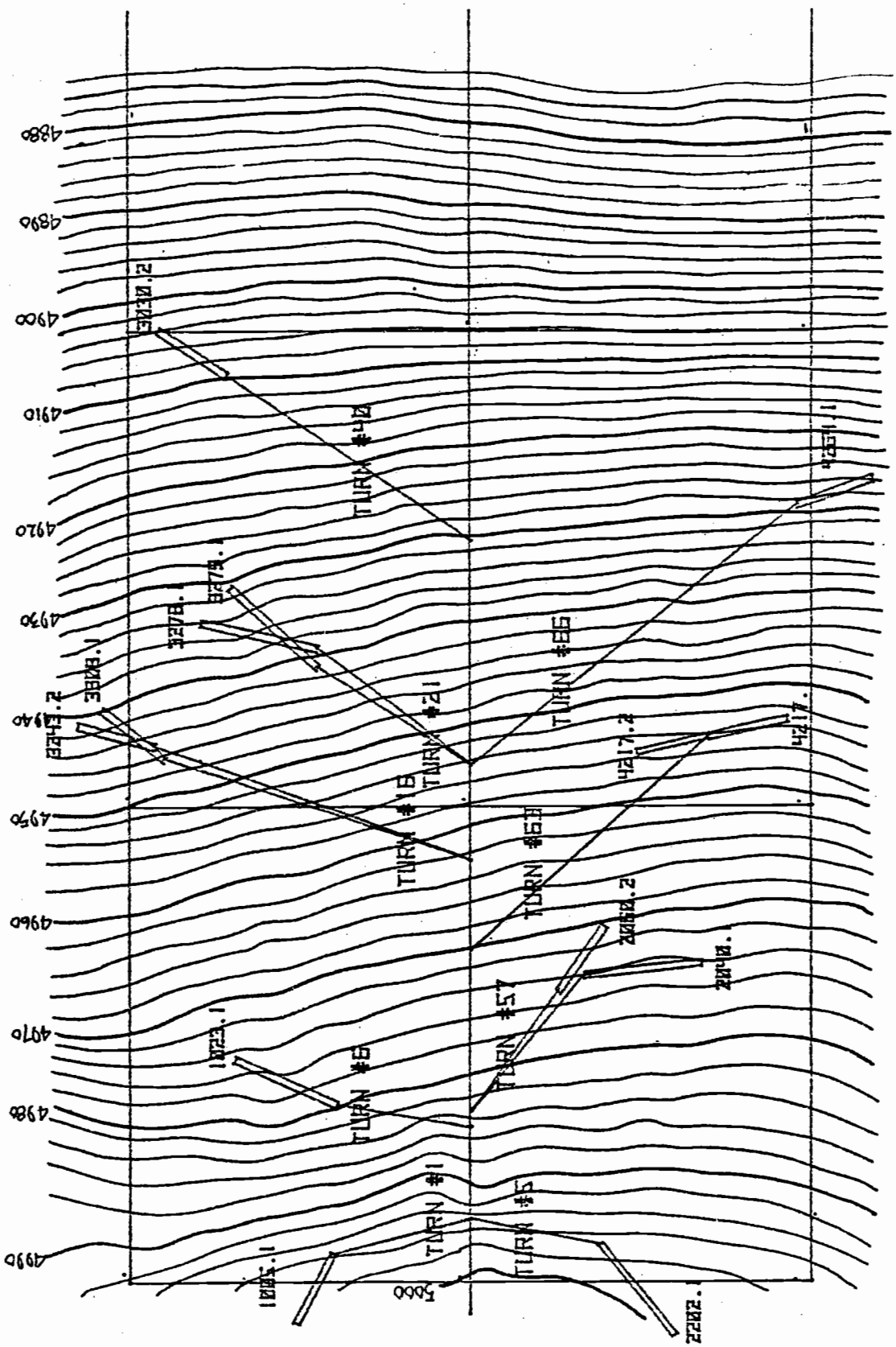

FIGURE 41. TURN LOCATION AND LOG TO MAINLINE LEAD ANGLE.

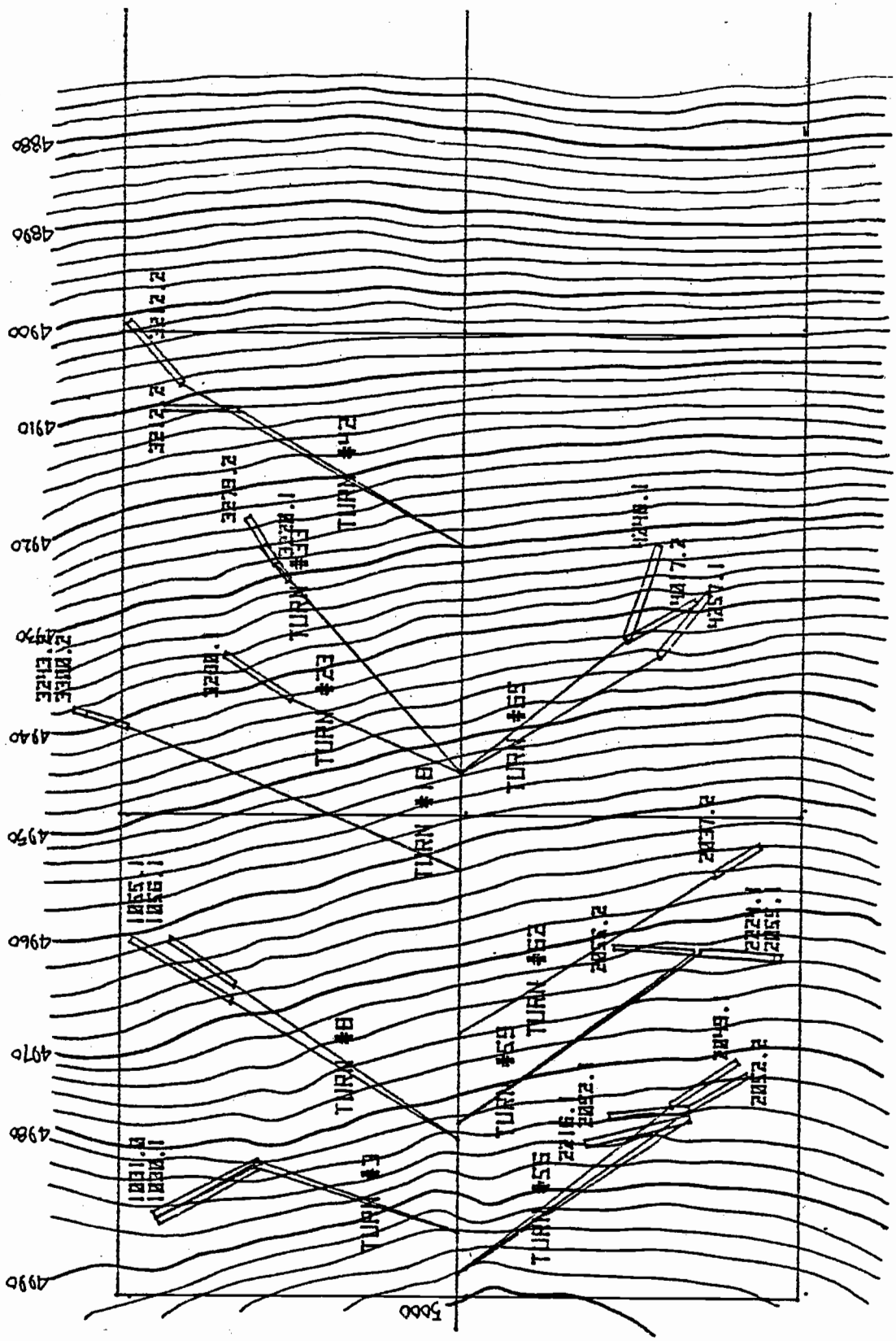

FIGURE 42. TURN LOCATION AND LOG TO MAINLINE LEAD ANGLE.

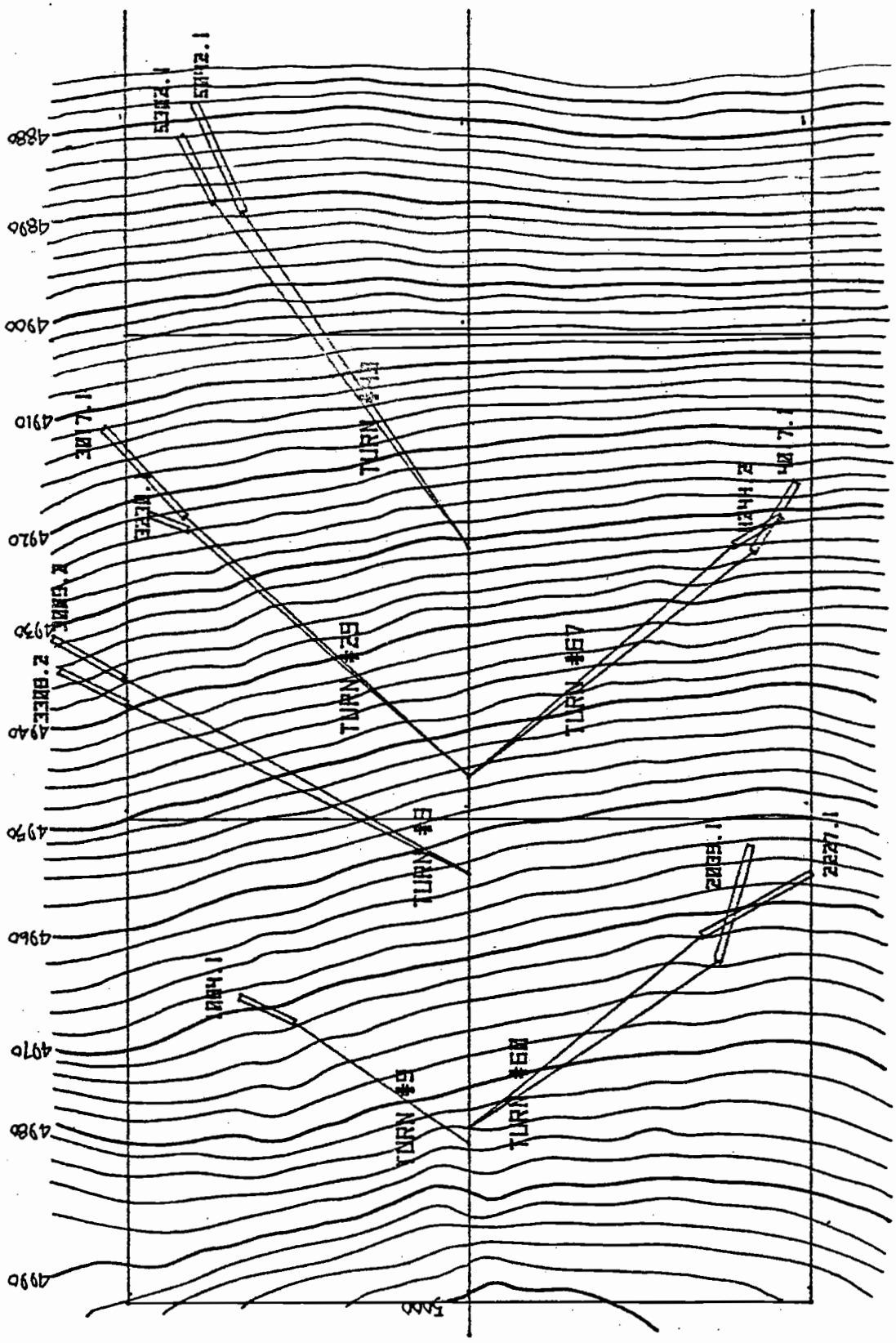

FIGURE 43. TURN LOCATION AND LOG TO MAINLINE LEAD ANGLE.

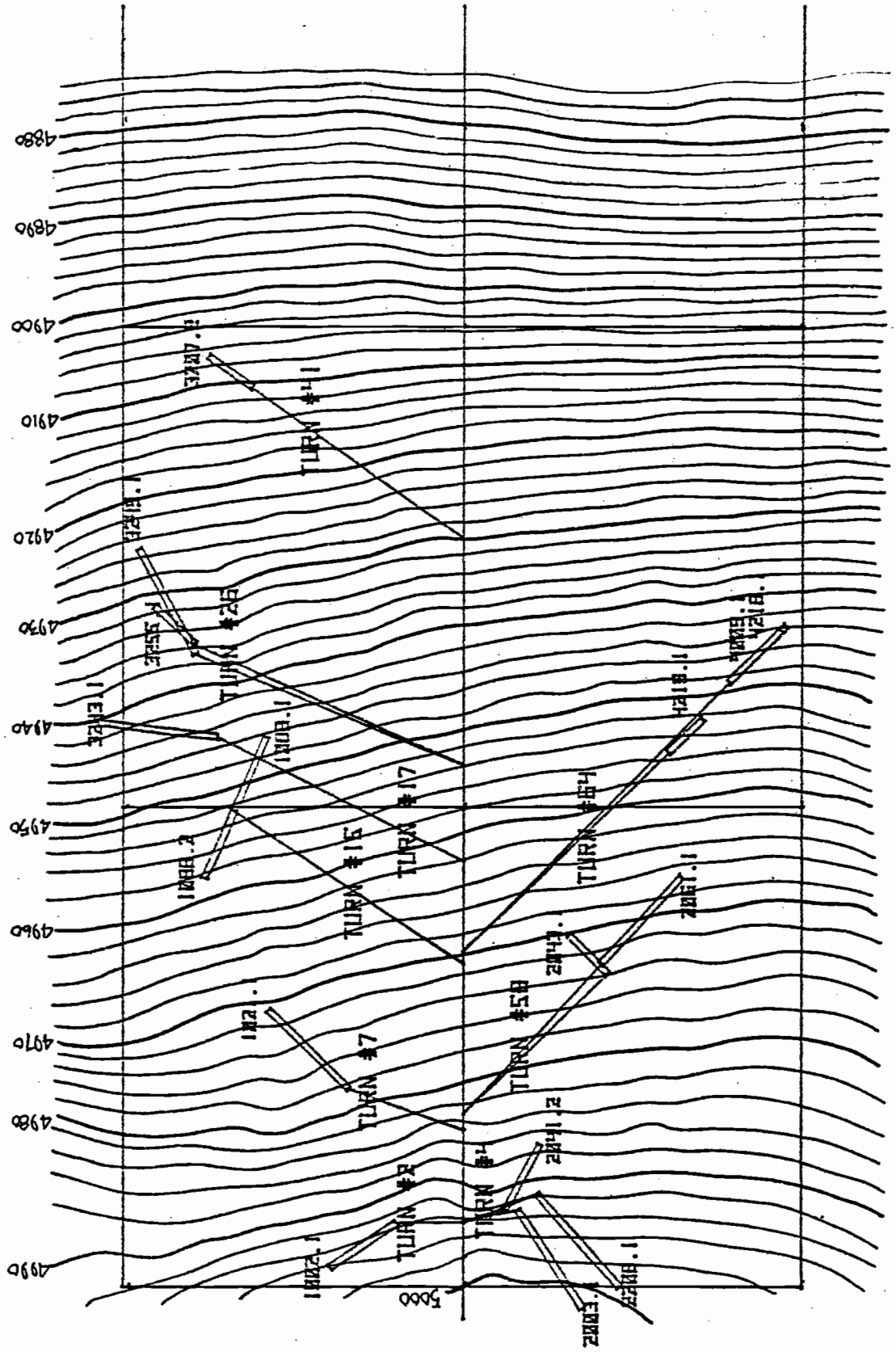

FIGURE 44. TURN LOCATION AND LOG TO MAINLINE LEAD ANGLE.

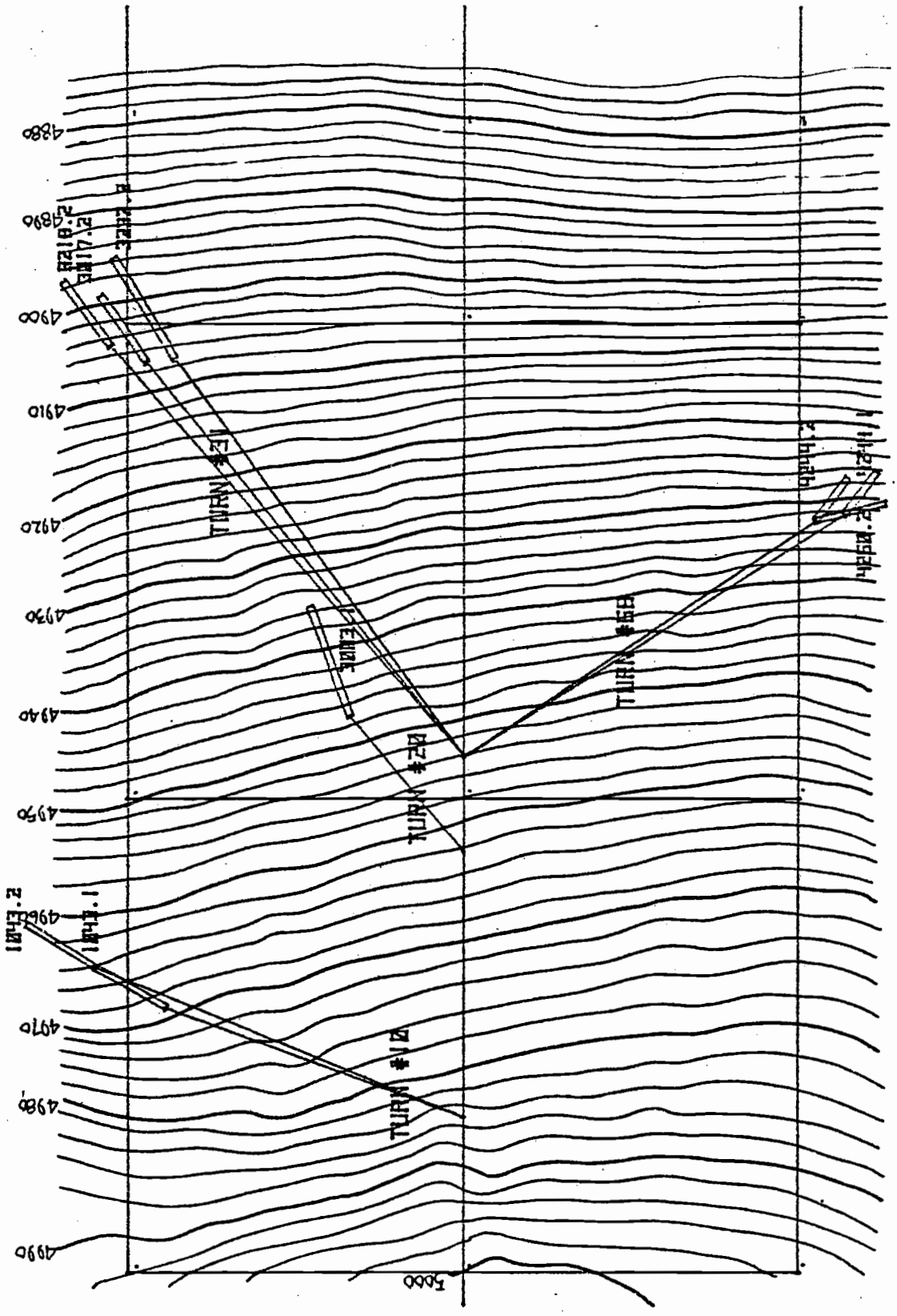

FIGURE 45. TURN LOCATION AND LOG TO MAINLINE LEAD ANGLE.

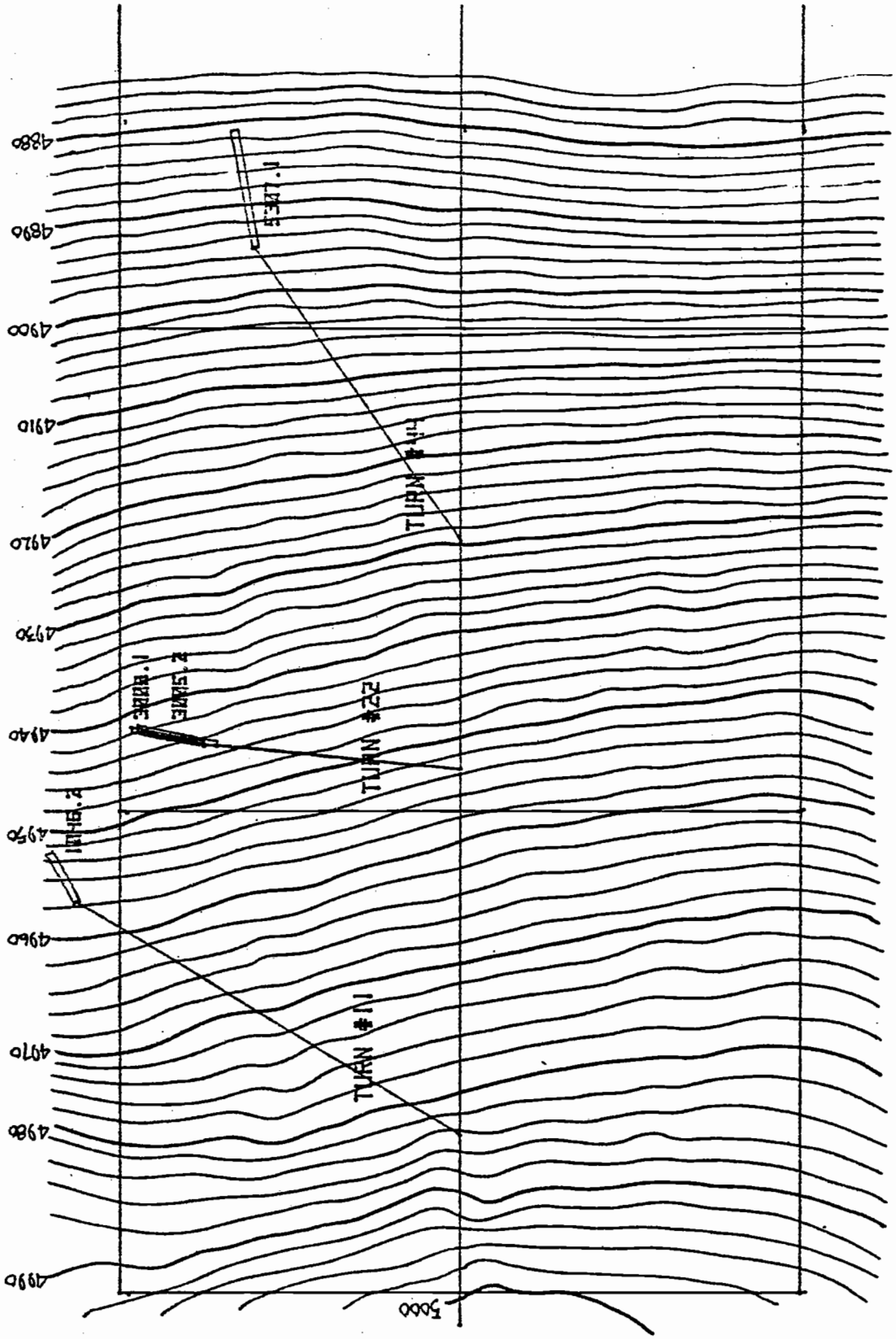

FIGURE 46. TURN LOCATION AND LOG TO MAINLINE LEAD ANGLE.

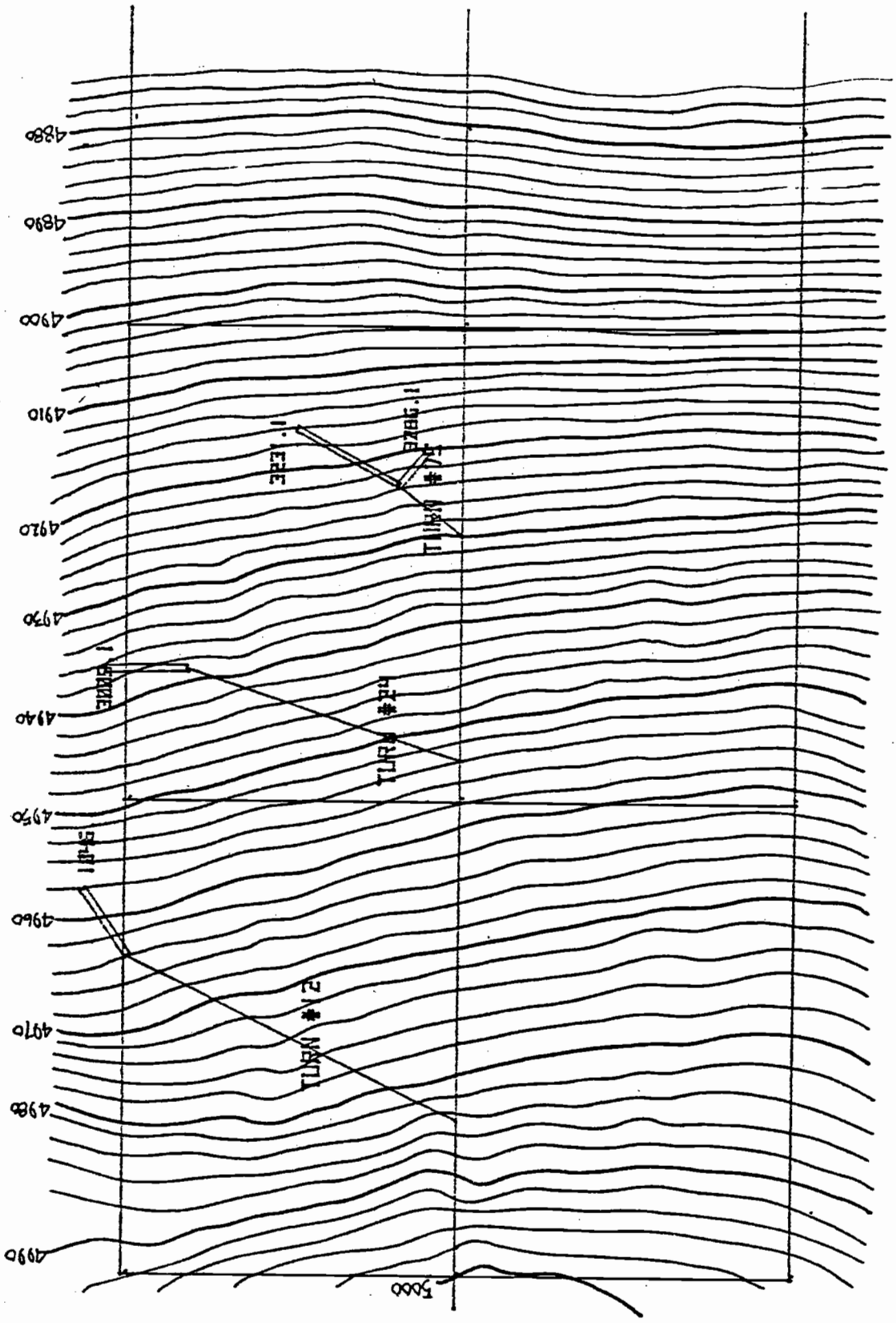

FIGURE 47. TURN LOCATION AND LOG TO MAINLINE LEAD ANGLE.

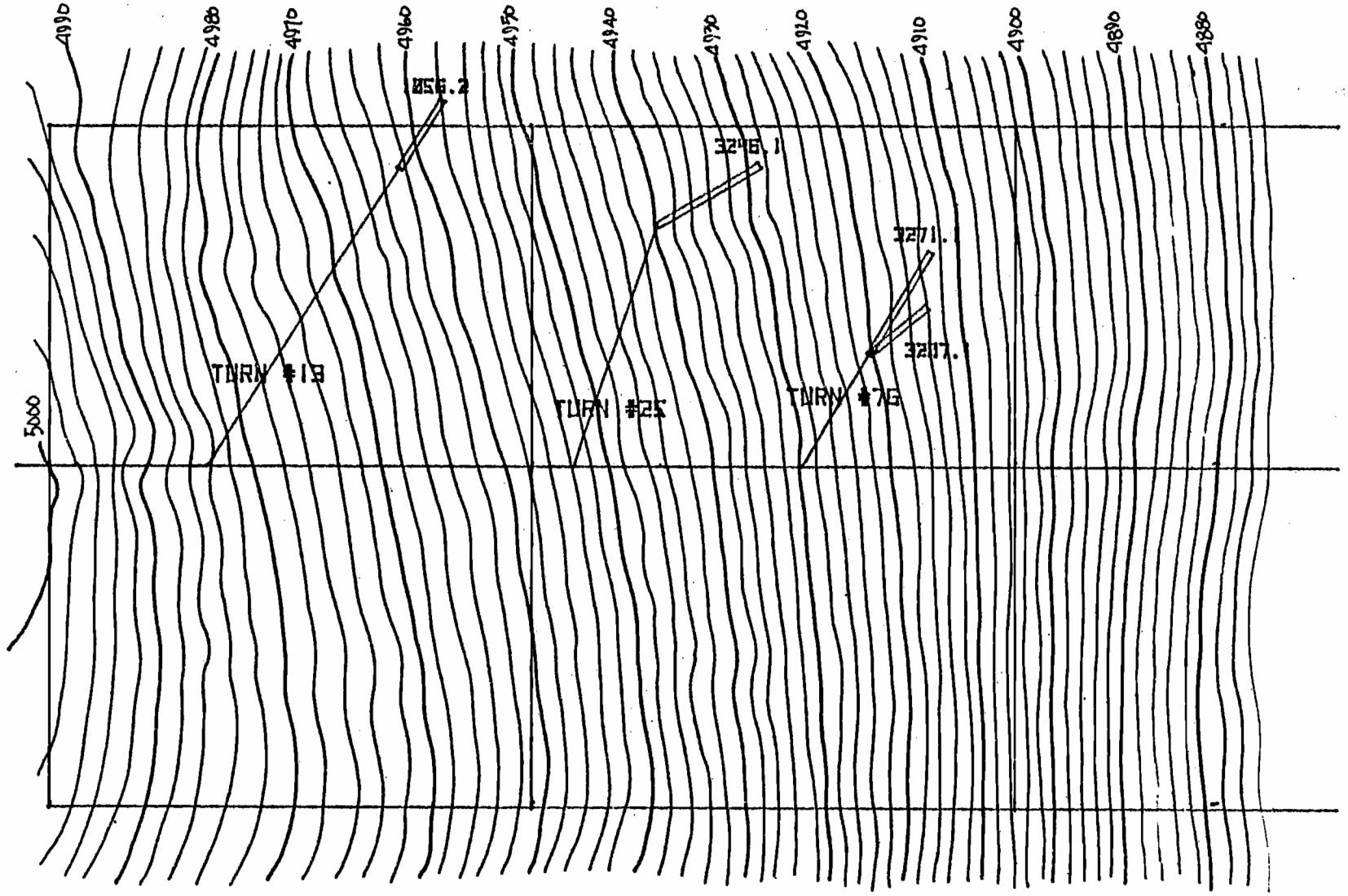

FIGURE 48. TURN LOCATION AND LOG TO MAINLINE LEAD ANGLE.

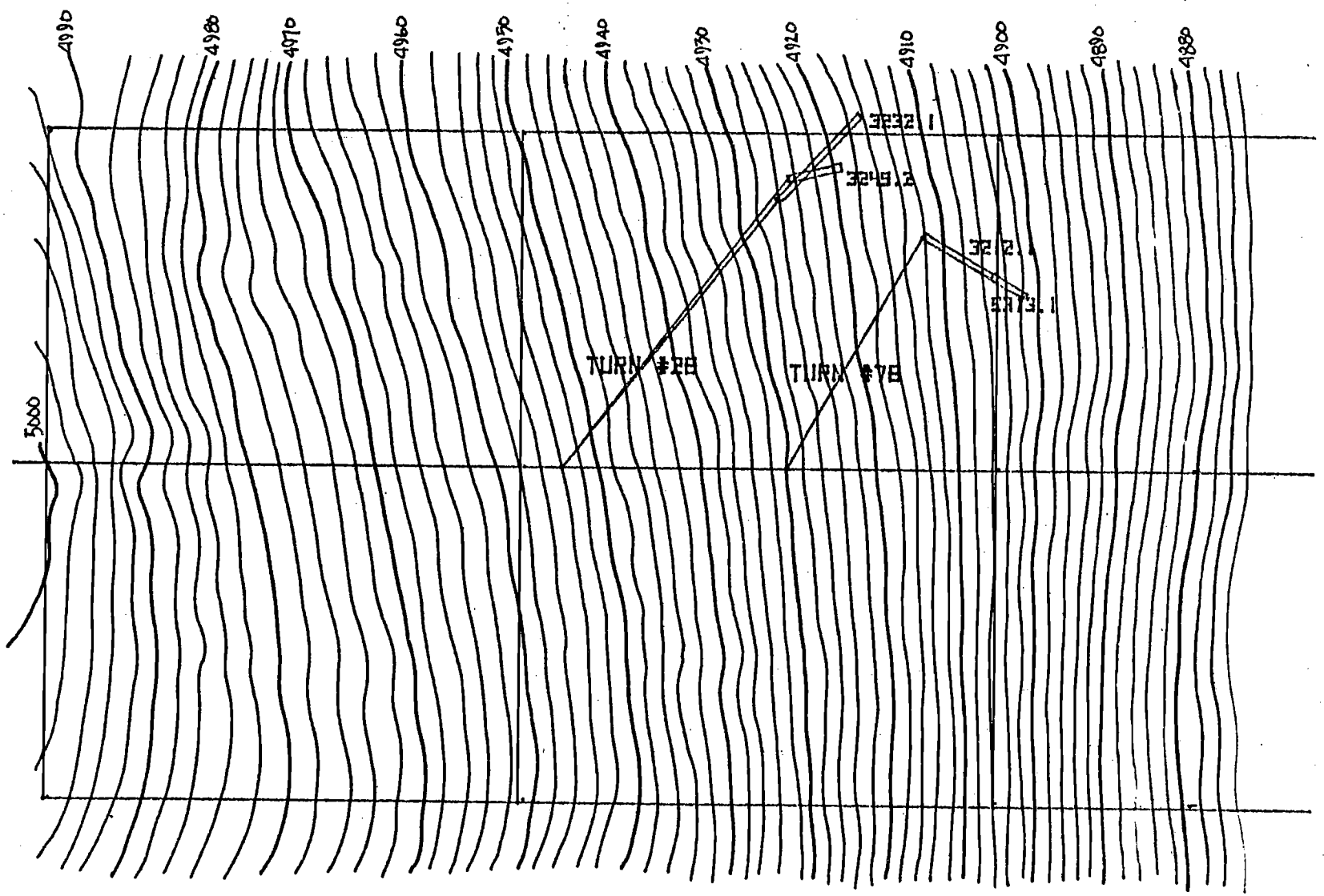

FIGURE 49. TURN LOCATION AND LOG TO MAINLINE LEAD ANGLE.

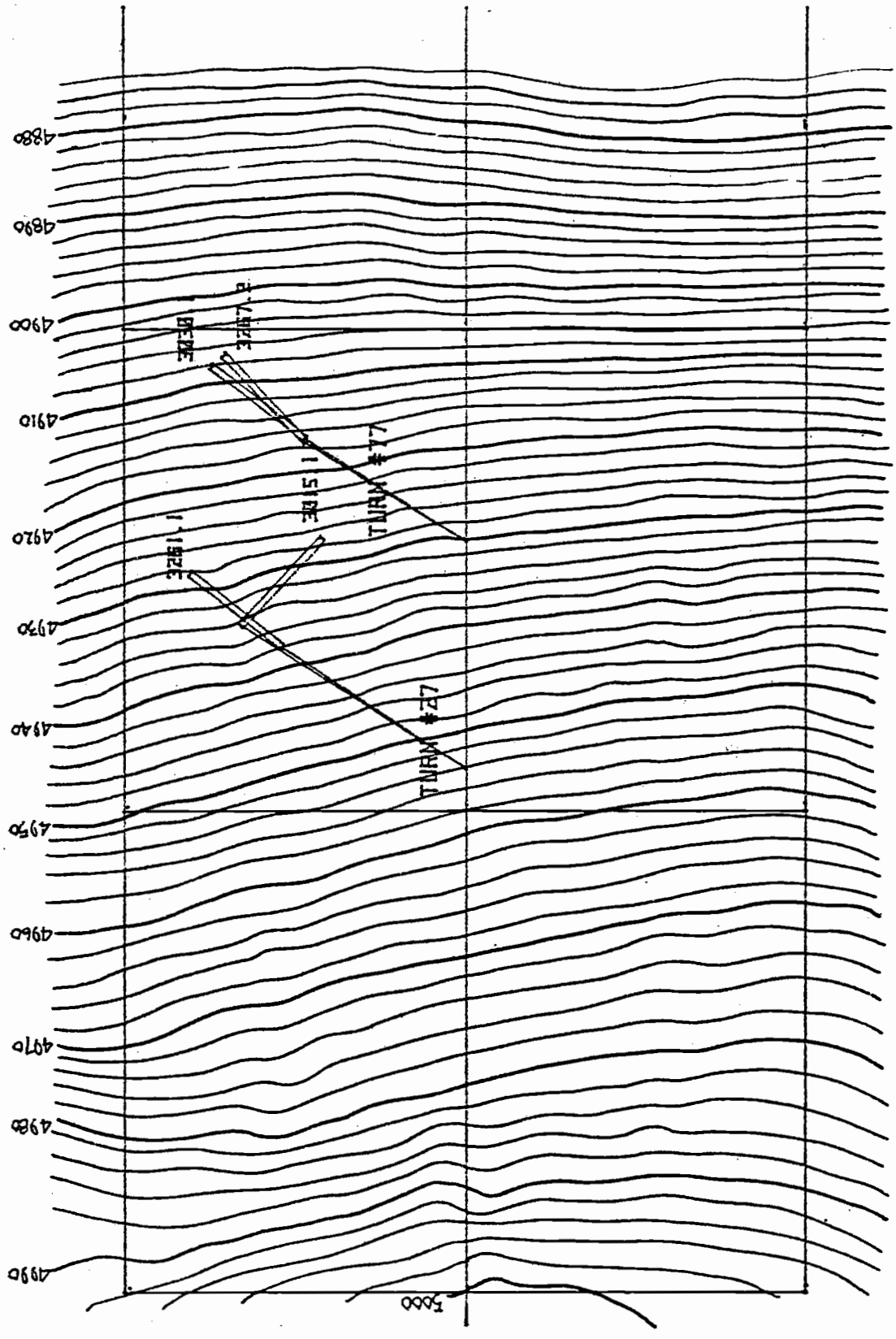

FIGURE 50. TURN LOCATION AND LOG TO MAINLINE LEAD ANGLE.

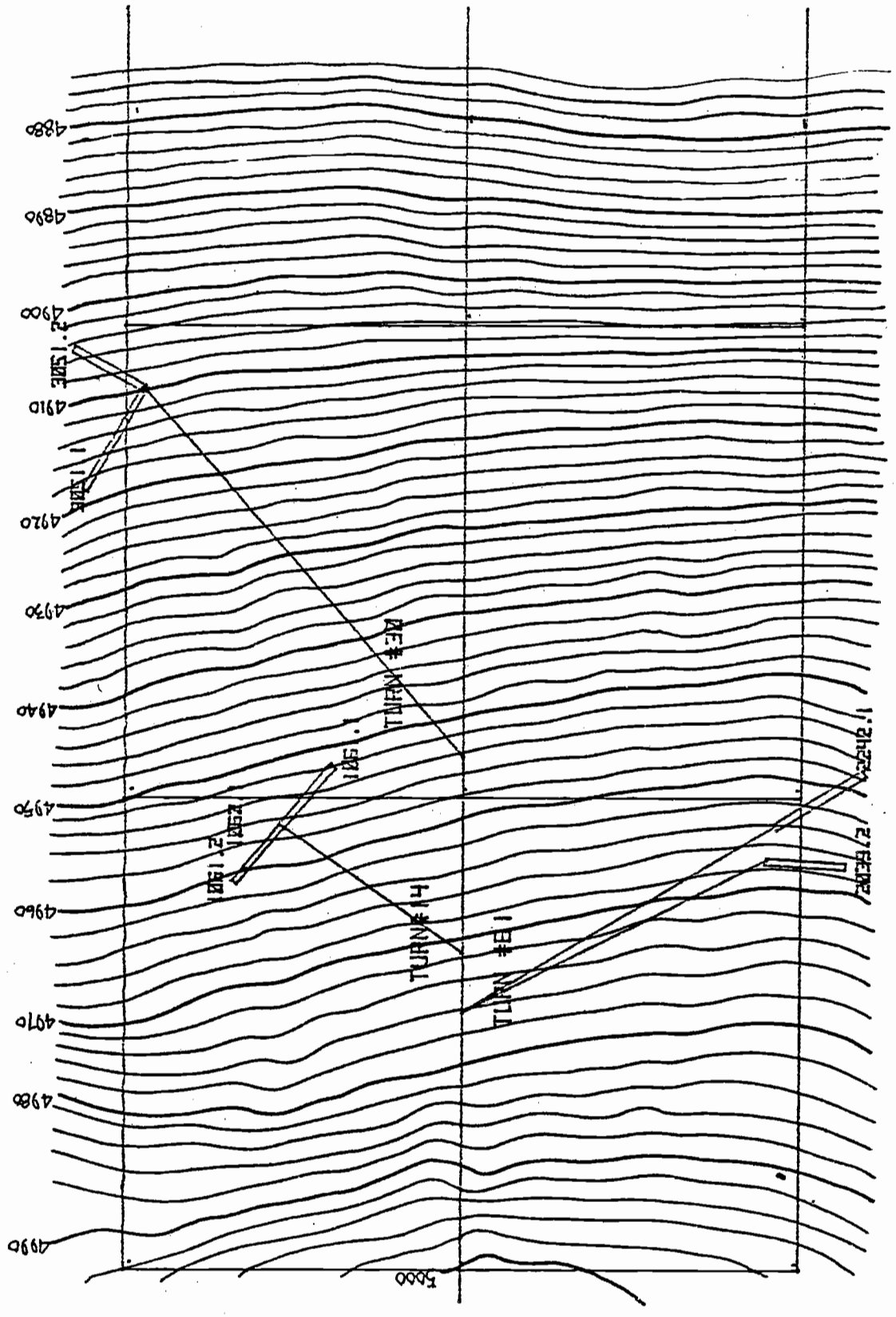

FIGURE 50 TURN LOCATION AND LOG TO MAINLINE LEAD ANGLE.

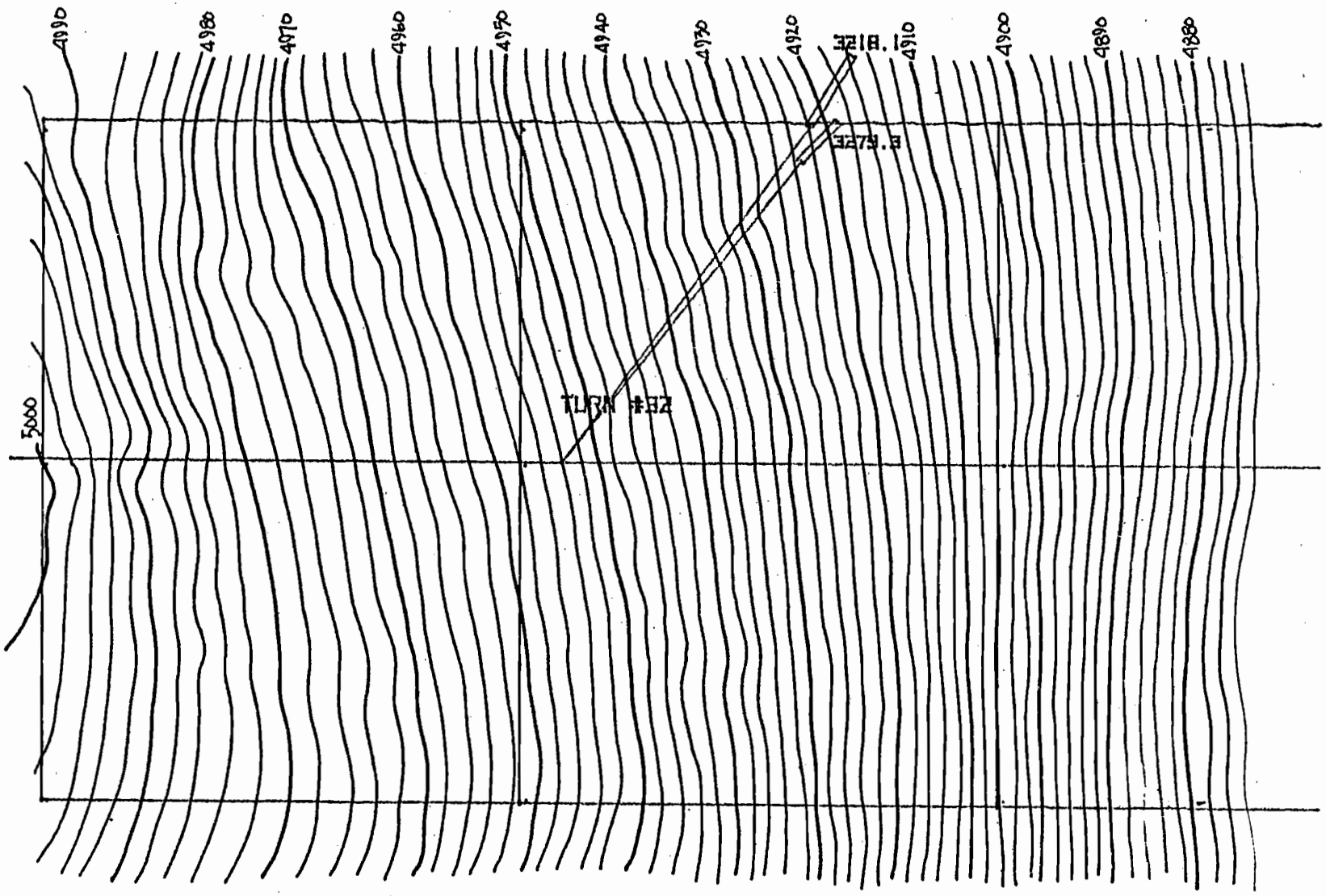

FIGURE 52. TURN LOCATION AND LOG TO MAINLINE LEAD ANGLE.

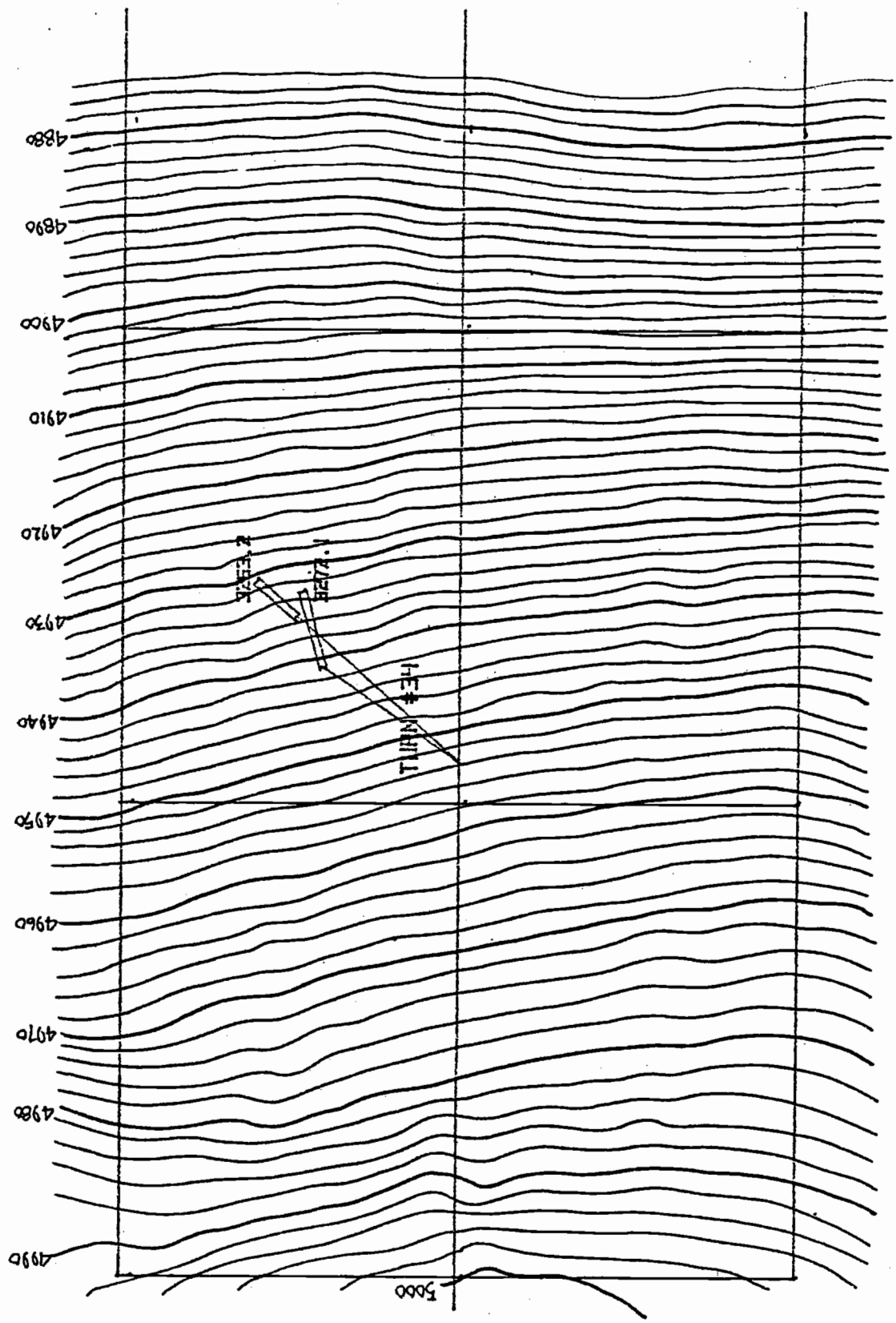

FIGURE 53. TURN LOCATION AND LOG TO MAINLINE LEAD ANGLE.

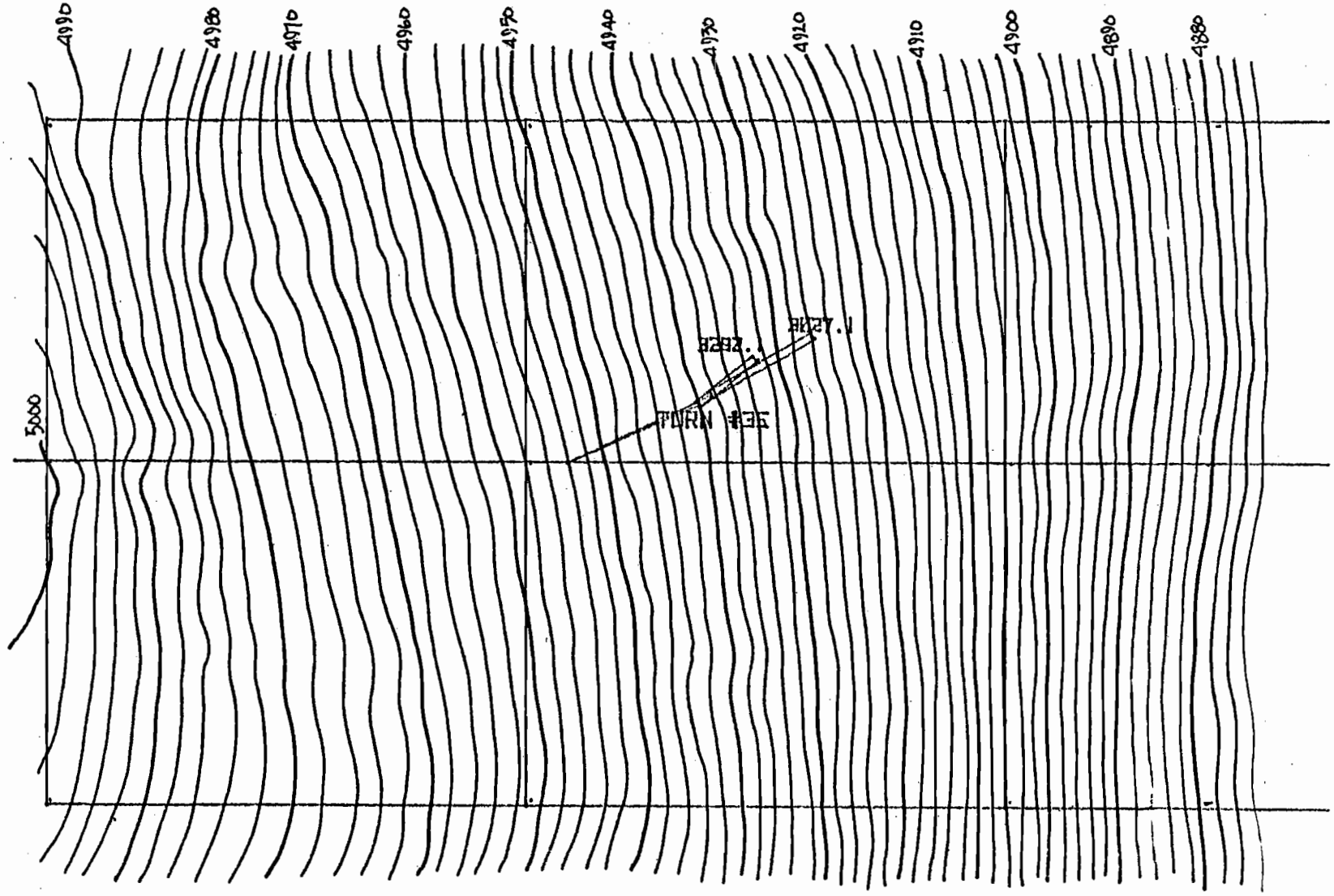

FIGURE 54. TURN LOCATION AND LOG TO MAINLINE LEAD ANGLE.

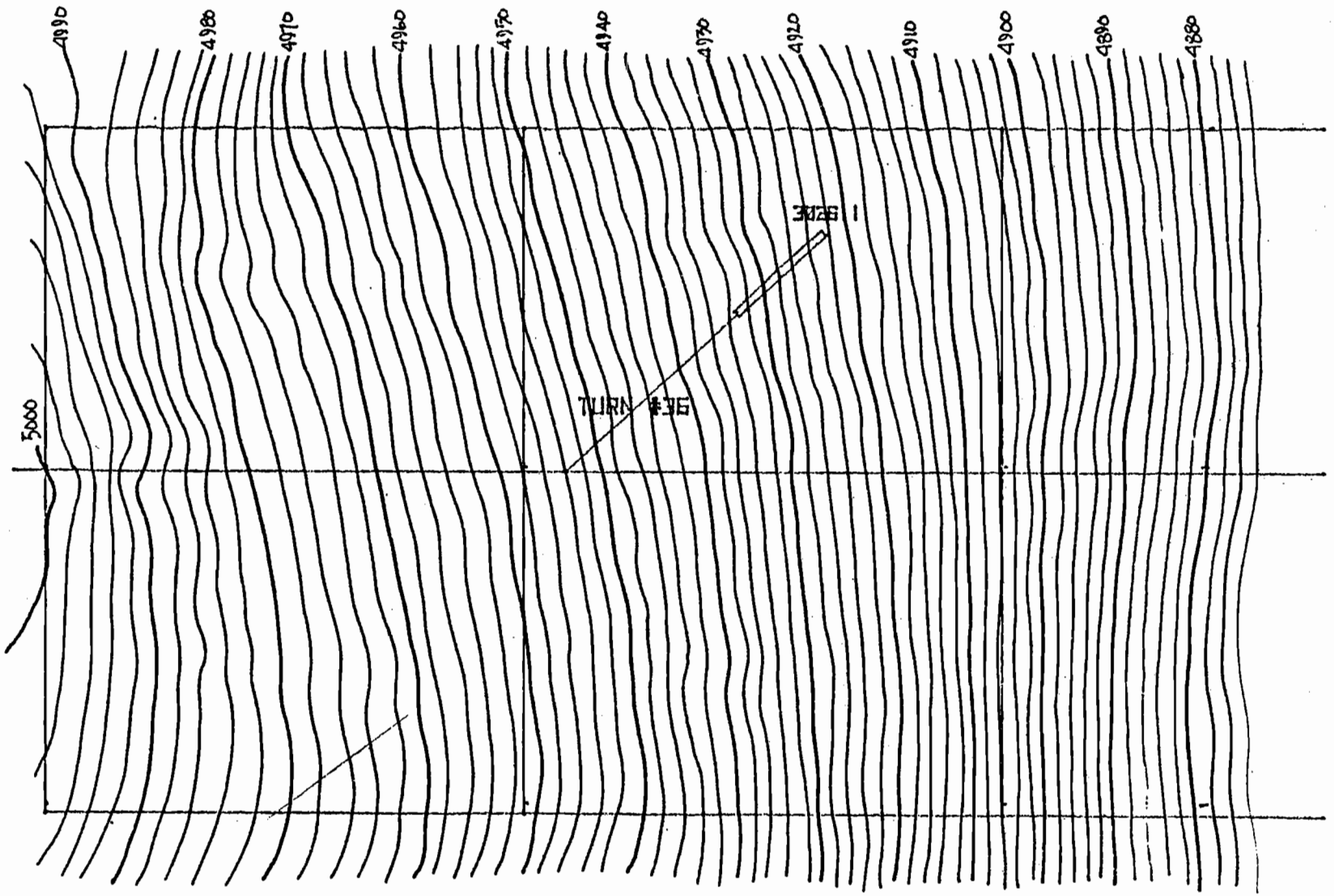

FIGURE 55. TURN LOCATION AND LOG TO MAINLINE LEAD ANGLE.

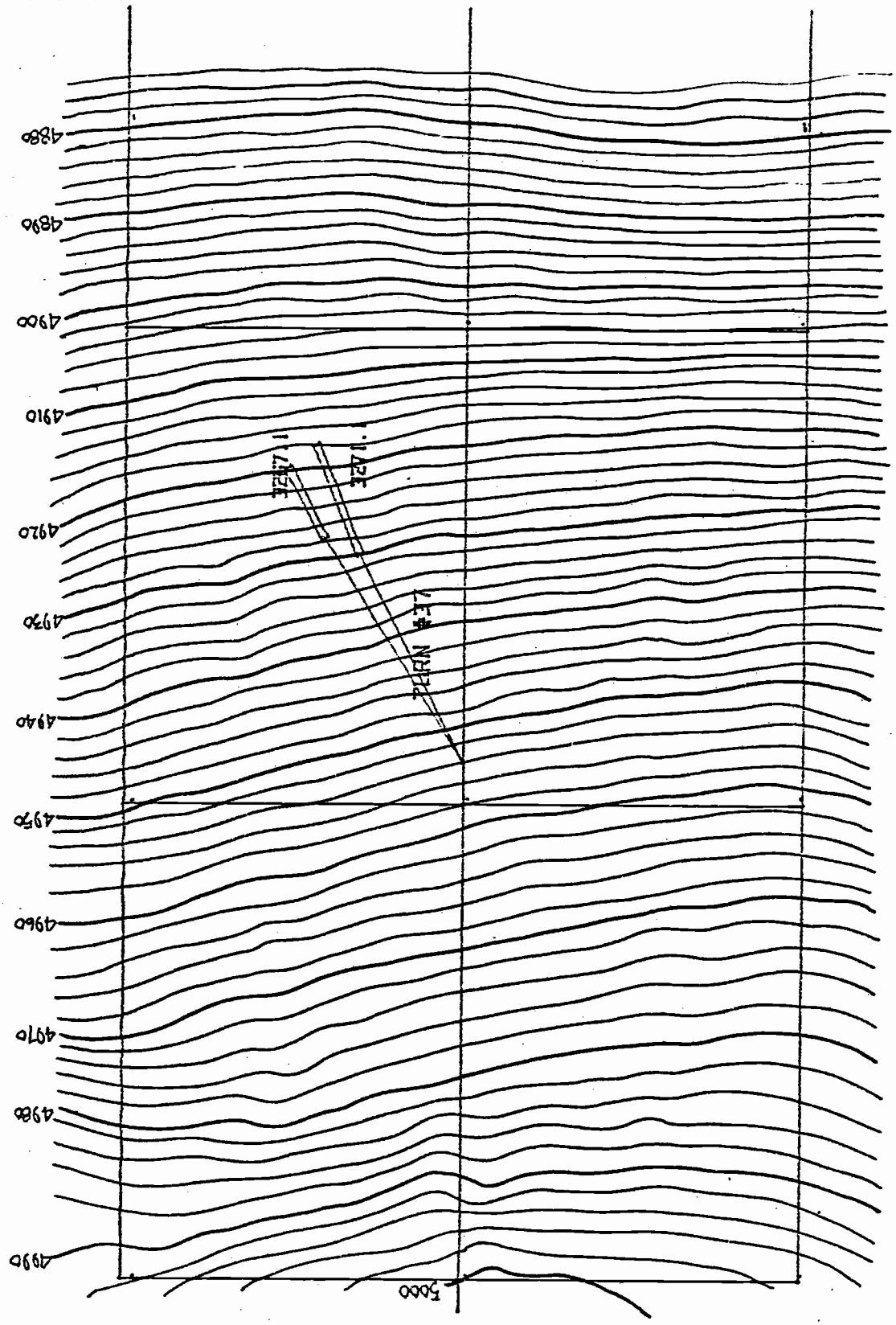

FIGURE 56. TURN LOCATION AND LOG TO MAINLINE LEAD ANGLE.

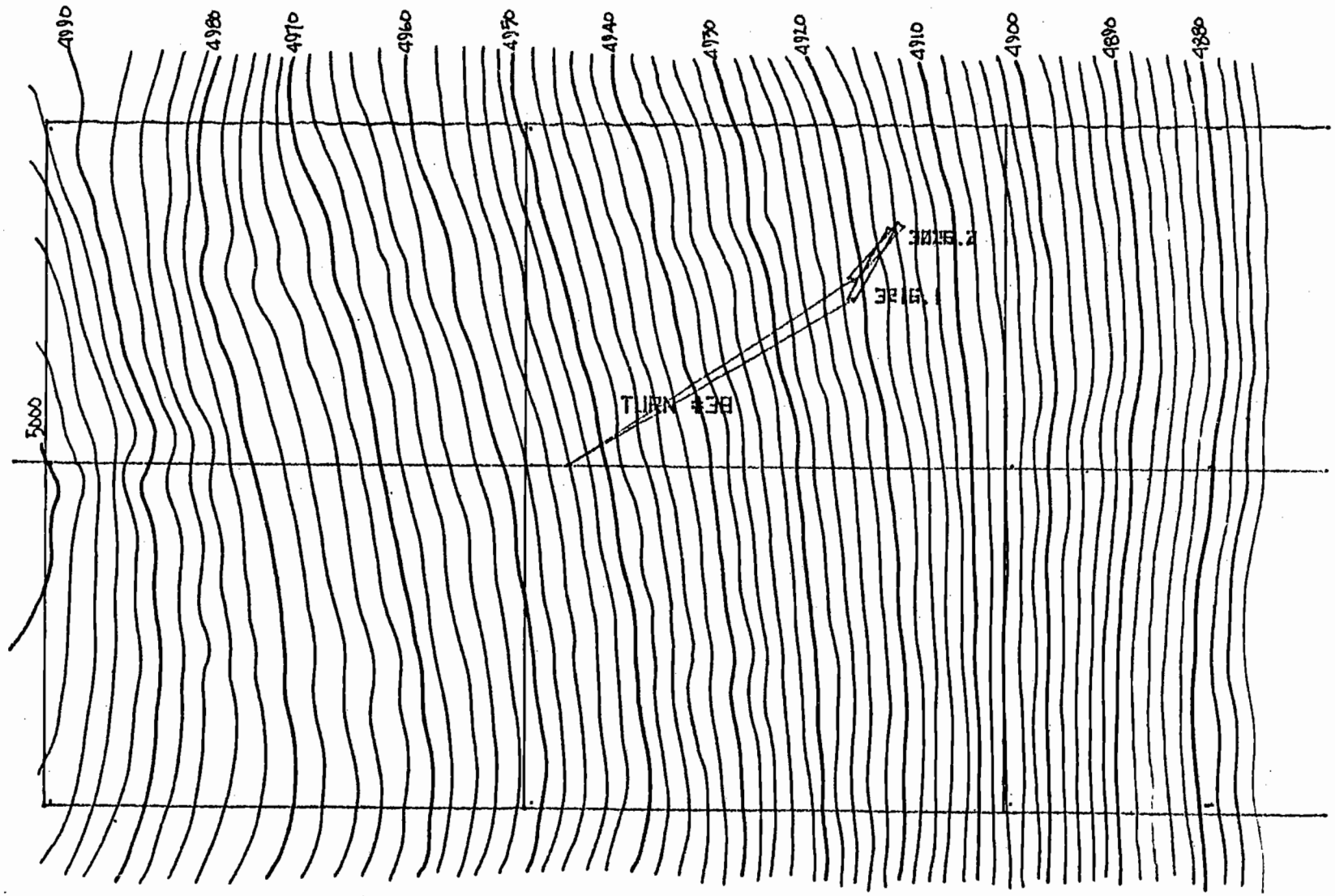

FIGURE 57. TURN LOCATION AND LOG TO MAINLINE LEAD ANGLE.

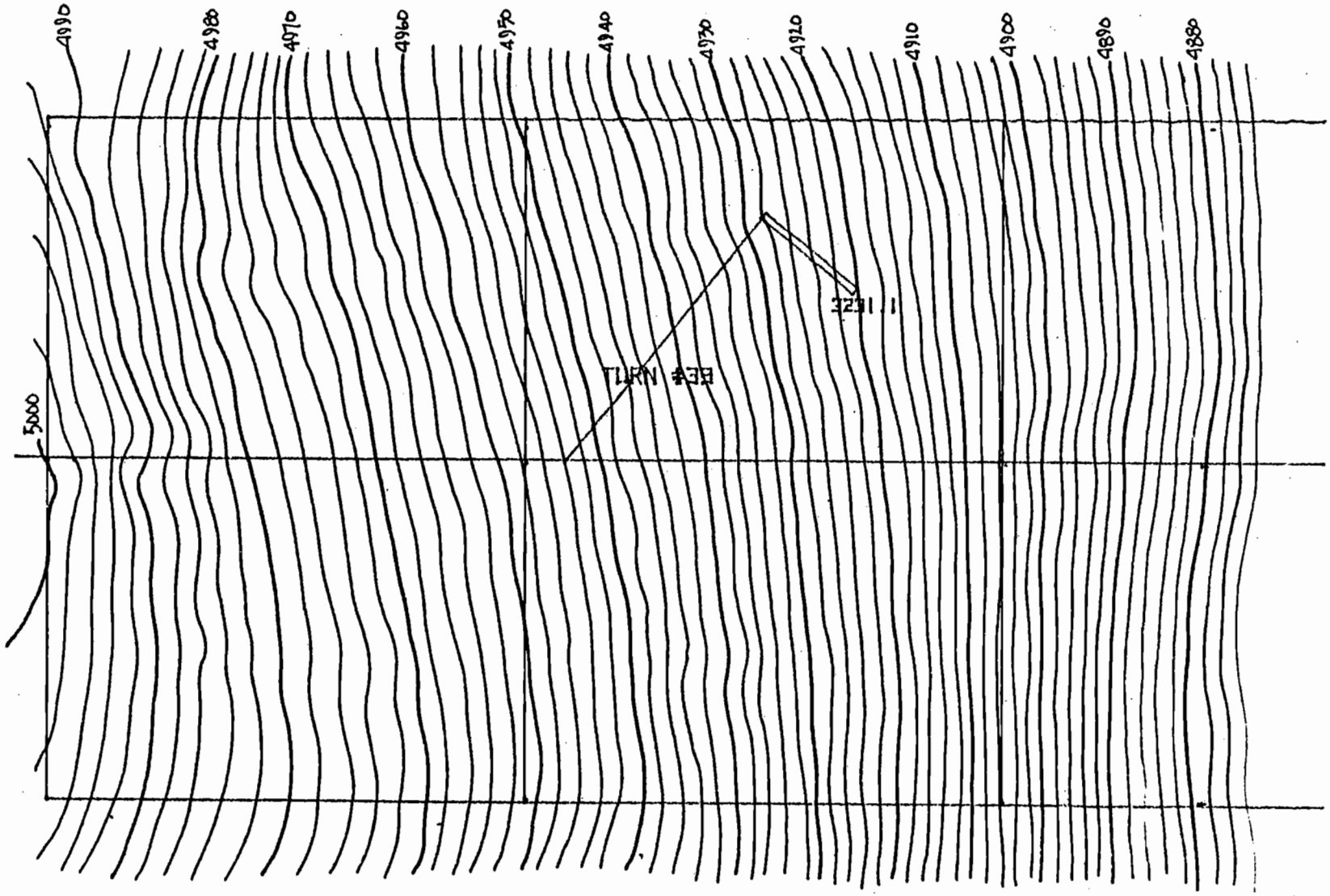

FIGURE 58. TURN LOCATION AND LOG TO MAINLINE LEAD ANGLE.

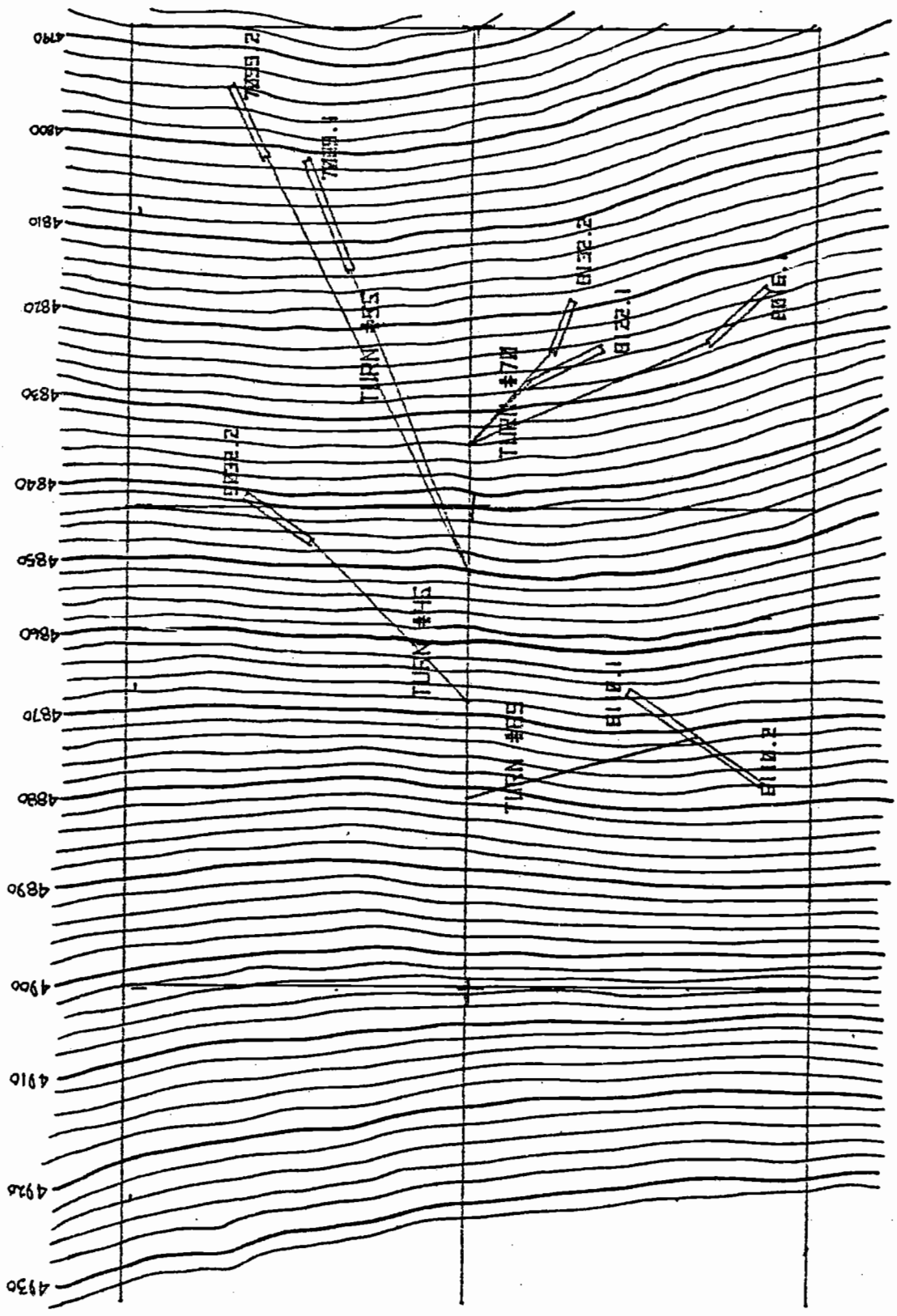

FIGURE 59. TURN LOCATION AND LOG TO MAINLINE LEAD ANGLE.

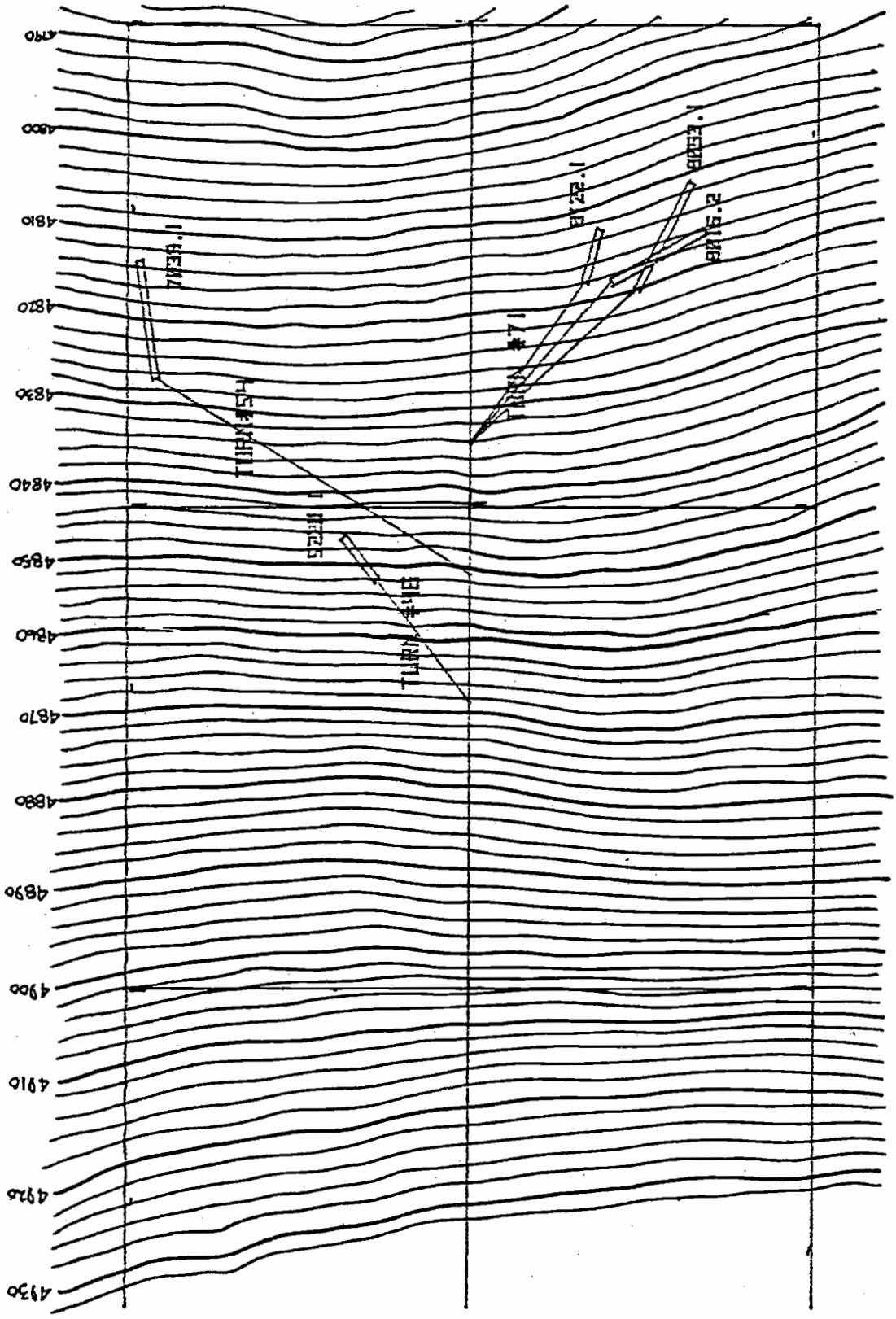

FIGURE 60. TURN LOCATION AND LOG TO MAINLINE LEAD ANGLE.

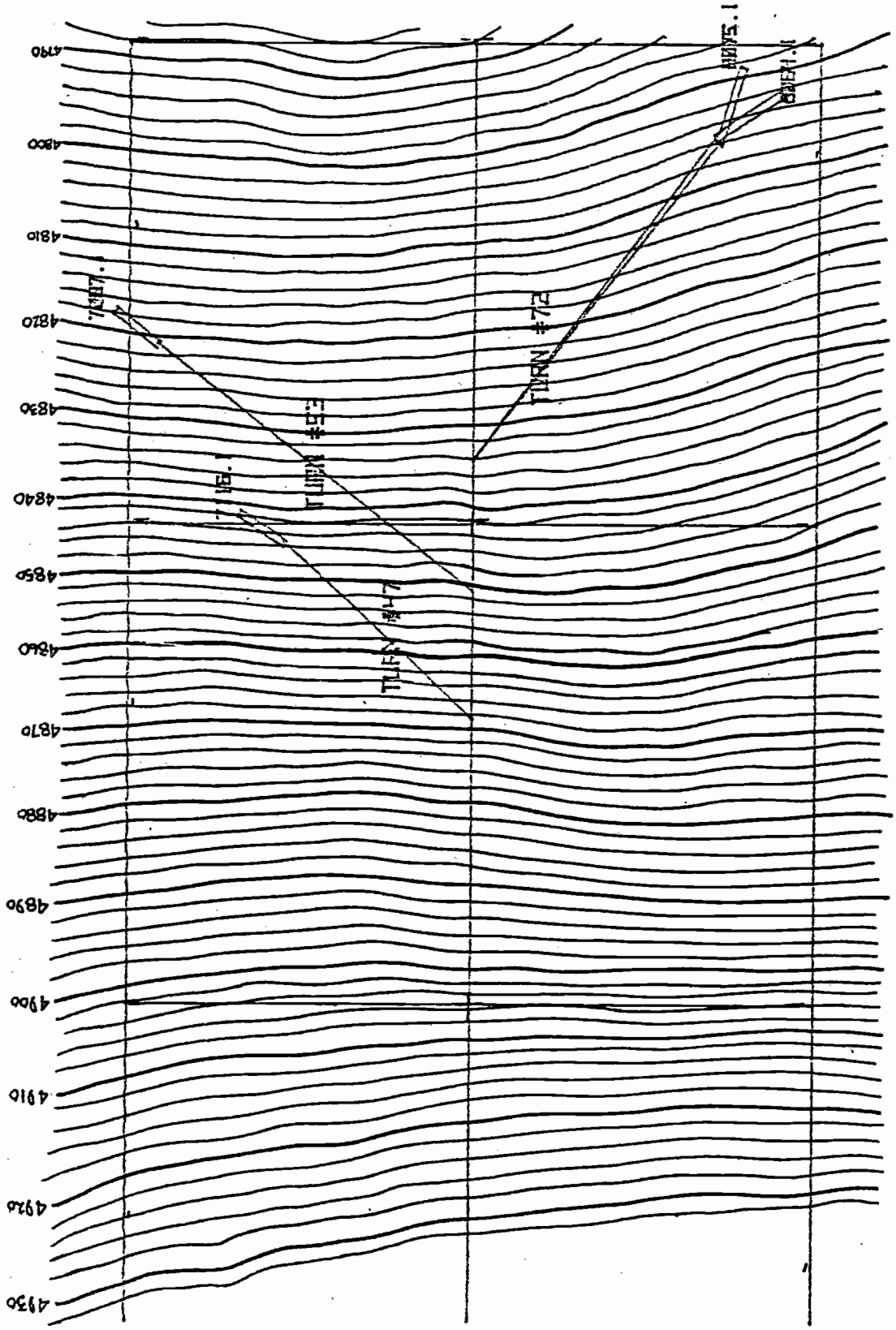

FIGURE 61. TURN LOCATION AND LOG TO MAINLINE LEAD ANGLE.

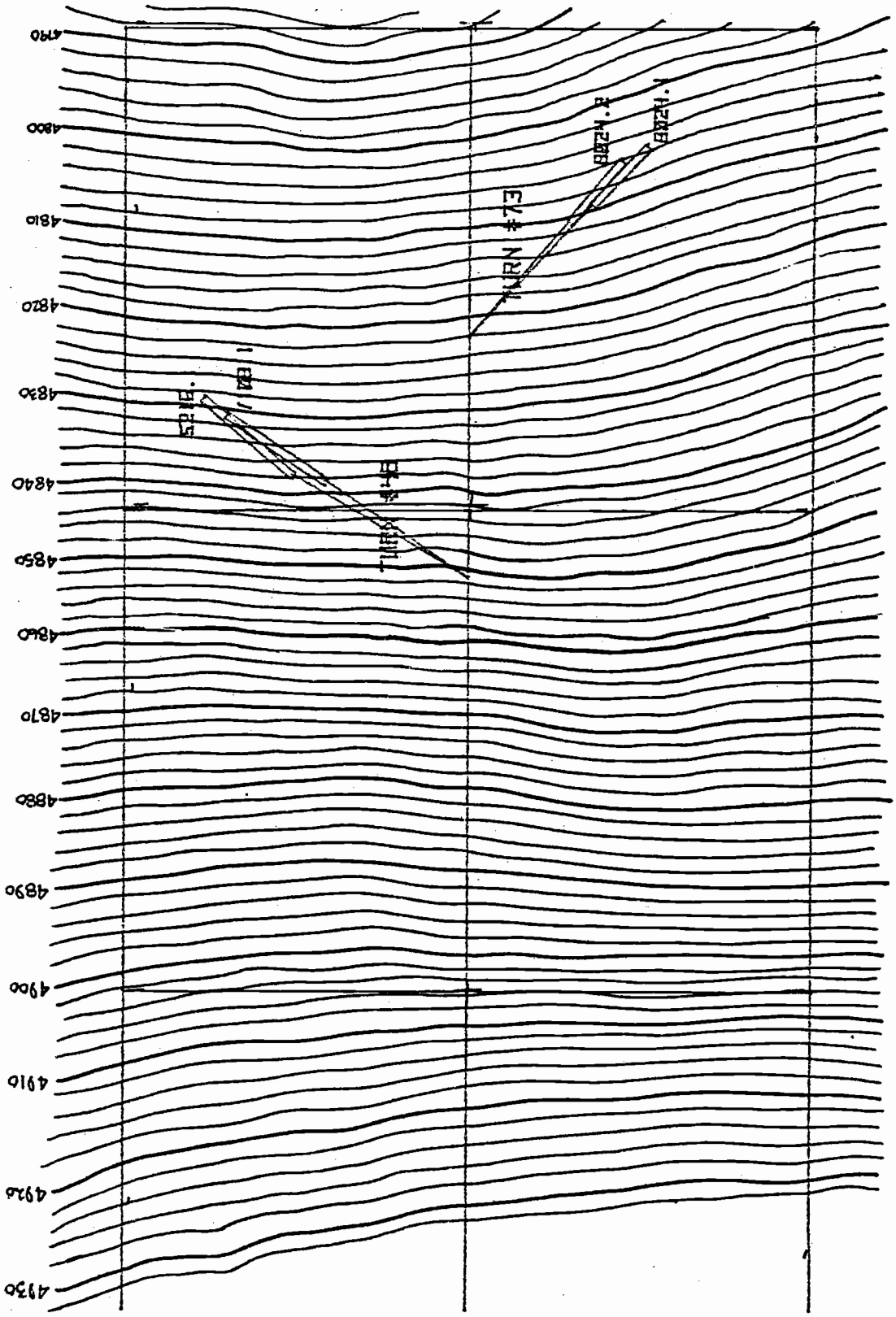

FIGURE 62. TURN LOCATION AND LOG TO MAINLINE LEAD ANGLE.

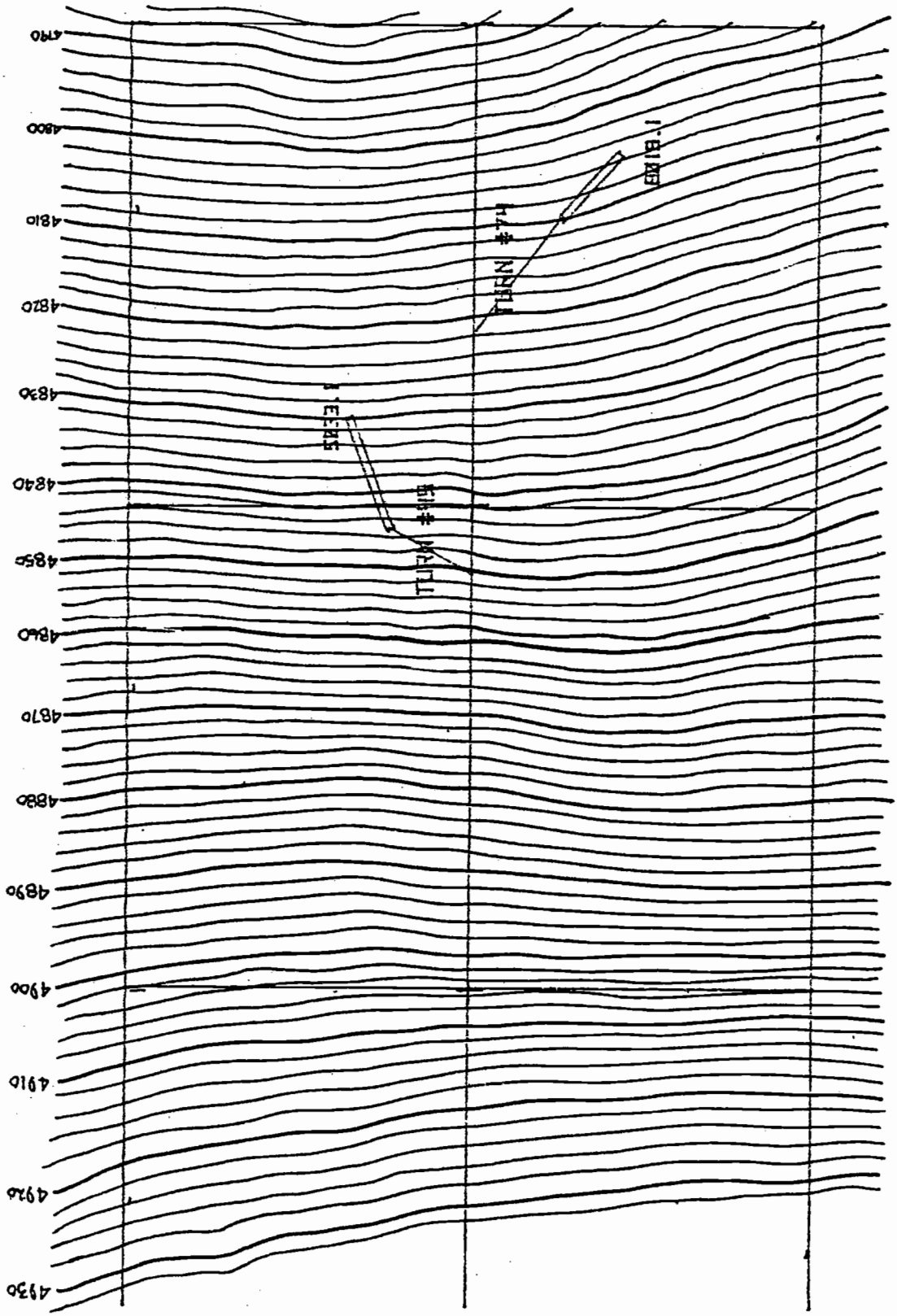

FIGURE 63. TURN LOCATION AND LOG TO MAINLINE LEAD ANGLE.

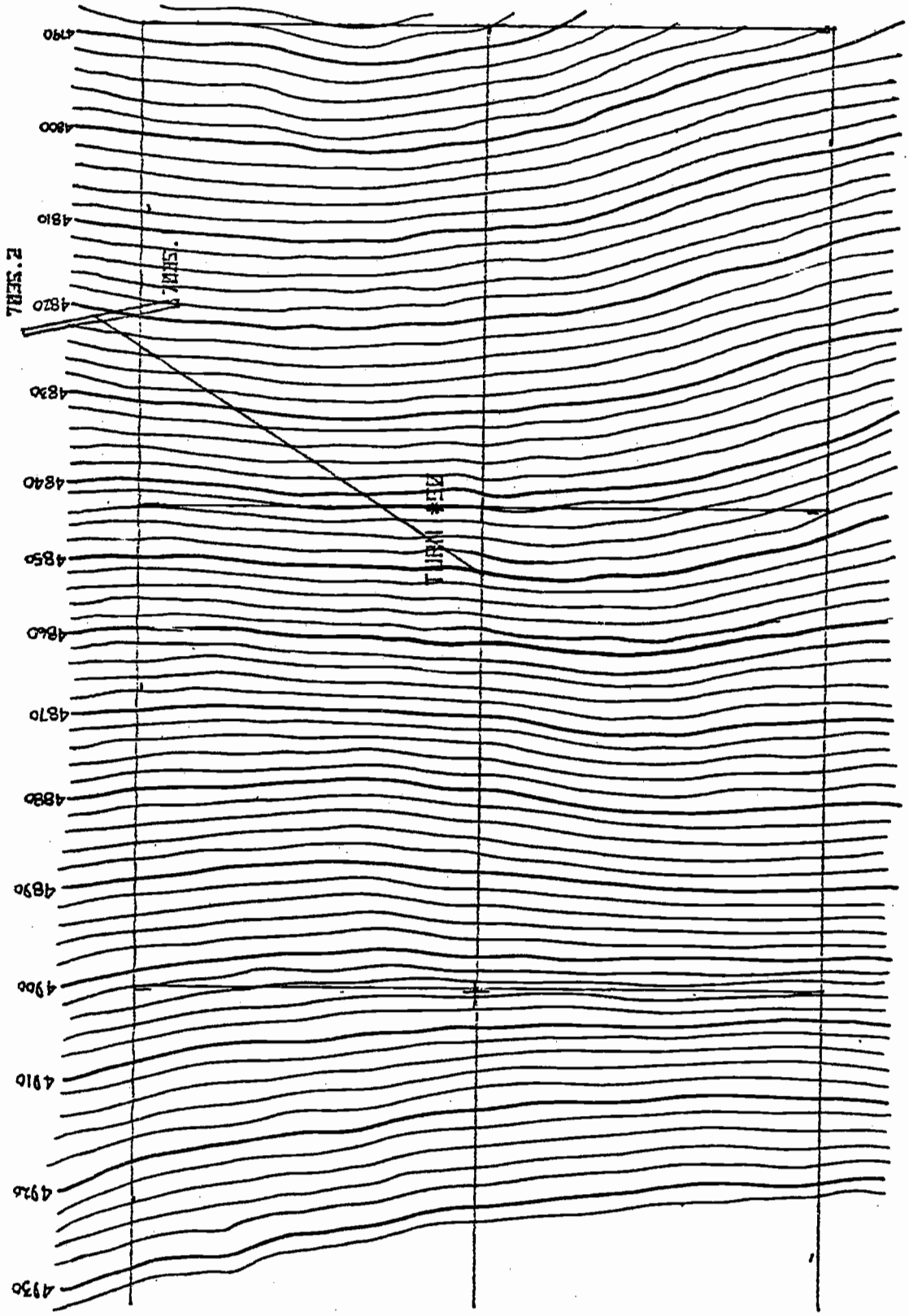

FIGURE 64. TURN LOCATION AND LOG TO MAINLINE LEAD ANGLE.

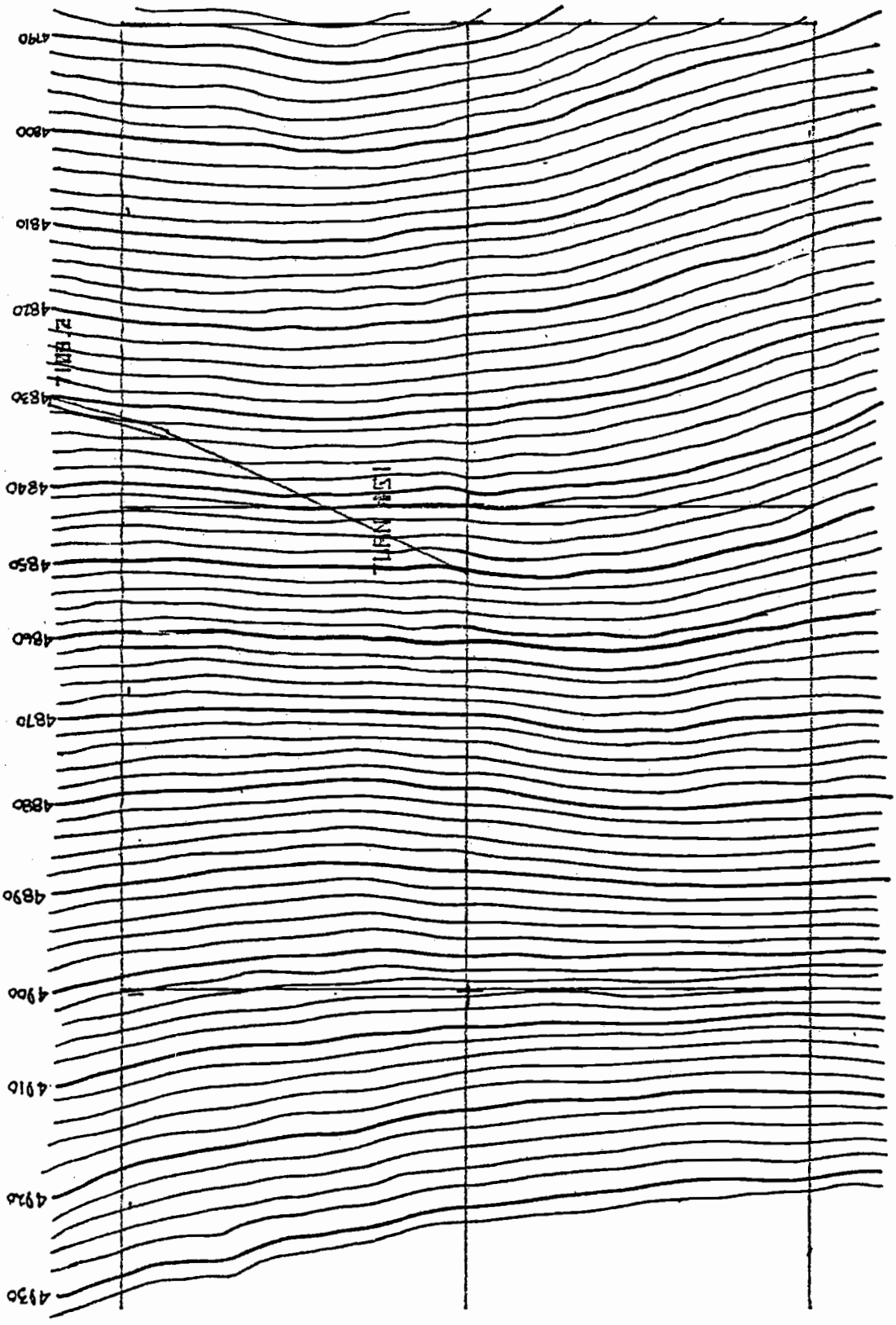

FIGURE 65. TURN LOCATION AND LOG TO MAINLINE LEAD ANGLE.

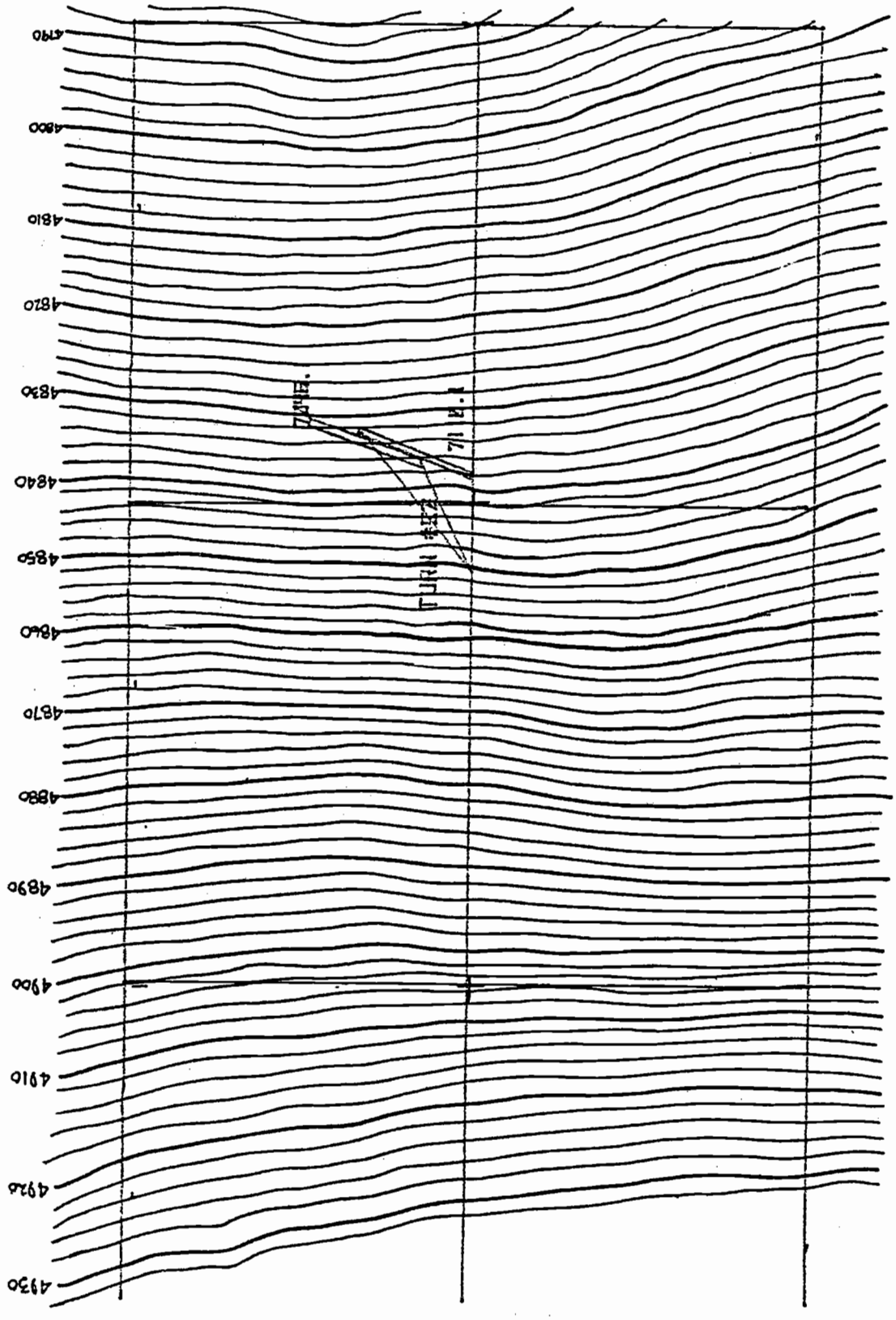

FIGURE 66. TURN LOCATION AND LOG TO MAINLINE LEAD ANGLE.